University of Venda

SCHOOL OF ENVIRONMENTAL SCIENCES

DEPARTMENT OF ECOLOGY AND RESOURCE MANAGEMENT

Fabrication of metal-oxide modified porous ceramic granules from aluminosilicate clay soils for defluoridation of groundwater

A master's research submitted to the University of Venda, School of Environmental Sciences, Department of Ecology and Resource Management

By

DENGA MASINDI ESTHER (11606933)

Signature…… Date……..

Supervisor: Professor W. M. Gitari

Signature…… Date……..

Co-supervisor: Dr S.A Akinyemi

Signature…… Date……

DECLARATION

I, Masindi Esther Denga hereby declare that **"Fabrication of metal-oxide modified porous ceramic granules from aluminosilicate clay soils for defluoridation of groundwater"** is my own work in design and execution and it has never been submitted for any degree or examination in any other university and that all sources of information herein have been duly, appropriately and acknowledged by means of comprehensive list of references.

Denga Masindi Esther

Signature: ……

Date: May 2017

ACKNOWLEDGMENTS

I would like to thank **God Almighty** for His overflowing grace that brought me this far. I thank Him for good health, strength, wisdom and courage to pursue this research. He had been my pillar of strength.

I would like to express my sincere gratitude and appreciation skillful supervisor and co-supervisors **Prof W.M Gitari, Dr S.A Akinyemi and Dr E.E Awokunmi** for their support, competent guidance, advice, mentorship, encouragement, constructive criticism during the trials and writing of the current dissertation and above all, their patience. Above all, I am grateful for their long hours of tuition and assistance that allowed me to complete a successful study.

I would like to acknowledge the financial support from **WRC Project No. K5/2363/3, NRF Project No. CSUR13092849176, Grant No. 90288,** and **THRIP Project No. TP12082610644 Research & Innovation Directorate, University of Venda and Sasol Inzalo Foundation.**

I would also like to express my sincere gratitude to **Environmental Remediation and Pollution Chemistry Research Group** members for their comments to my work during the presentations and stimulating discussions. Thanks for their assistance through this journey.

My profound gratitude to my mentor **Dr A.A Izuagie** for dedicating himself to helping me throughout my studies. I would also like to extend my gratitude to **Tholiso Ngulube**, **Rabelani Mudzielwana** and **Adivhaho Denga** for their consistent support during this study.

Special thanks to **Mr M.L Mphaphathi** for his immense support throughout my research.

DEDICATION

This study is dedicated to my late father **Mr. M.D. Denga**. May his soul rest in peace. I will always remember his words.

This study is also dedicated to my mother **Mrs. T.A. Denga,** my sister **Ms. Maanda Denga**, my brothers **Mr. Godfrey Denga, Lucky Denga, Shadrack Denga, Nndwakhulu Denga, Adivhaho Denga** and my daughter **Munaka Mphaphathi** for their love, endless support, motivation, understanding, courage and patience throughout my study.

ABSTRACT

Some boreholes in South Africa which serve as a source of drinking water for rural communities are reported to have high fluoride concentration, much above the WHO guideline of 1.5 mg/L. This study aimed at activating aluminosilicate clay soil mechanochemically, modifying aluminosilicate clay soil with Al-oxide and fabricating porous ceramic granules using Al-oxide modified mechanochemically activated aluminosilicate clay soil/ mechanochemically activated clay soil/ corn starch and evaluating their performances in defluoridation of groundwater.

The raw clay materials were mechanochemically activated for 5, 10, 15 and 30 minutes for physicochemical transformation of the solid aggregate. The morphology of the samples showed the honeycomb structure. The surface area analyses of samples using Brunauer–Emmett–Teller (BET) gave the highest surface area of 50.5228 m^2/g at 30 min activation time. Hence, the optimum activation time was 30 min. The Fourier Transform Infrared (FT-IR) analysis showed increase in the absorbance of FT-IR by Si-O-H groups at 510 cm^{-1} with increasing milling time. This is evidence that more surface Si-O-H groups were available at higher particle surface area that would be necessary to interact with fluoride. X-ray diffraction (XRD) analyses revealed that, at 30 minutes milling time, the peak broadening is intensified whereas the reflection peak intensities decreased. The X-ray fluorescence spectrometry (XRF) results for 30 minutes milling time showed that silica and alumina were the highest components in the clay soil.
Using the activated clay in batch defluoridation of fluoride-spiked water, a maximum fluoride removal of 41% was achieved at a pH_e of 2.41. The initial fluoride concentration was 9 mg/L while the sorbent dosage was 0.6 g/100 mL and the contact time being 30 minutes. The adsorption data fitted to both Langmuir and Freundlich isotherms. The adsorption data fitted only the pseudo-second-order kinetic, showing chemisorption.

Optimization of Al^{3+} concentration for modification was carried out by modifying the mechanochemical activated aluminosilicate clay soil with different concentrations of Al^{3+} from which the optimum modification was achieved with 1.5 M. Characterisation studies on the Al-oxide modified mechanochemically activated aluminosilicate clay soil by SEM, BET, FT-IR, XRD and XRF, analyses were carried out to determine the resultant changes in physicochemical properties of the adsorbent owing to modification. The SEM image of Al-oxide modified mechanochemically activated clay soil showed many small pores and honey-comb structure on the surface of different images. The BET surface area and the BDH adsorption cumulative area of the Al-oxide modified mechanochemically activated

aluminosilicate clay soil were more than double those for the raw clay soil. There was also an increase in pore volume of the Al-oxide modified mechanochemically activated aluminosilicate clay soil. The FT-IR spectra showed that there was increase in the absorbance by the Si-OH, H-O-H, Al-O-H and Si-O-Al. The equilibrium pH of solution was higher than the point-of-zero charge (pHpzc) implying that fluoride removal occurred at solution pH > pHpzc where the net surface charge of the mechanochemically activated clay aluminosilicate soil was negative.The efficiency of 1.5 M Al-oxide modified aluminosilicate clay soil to remove fluoride from water was studied and found to be 96.5 % at pH_e 6.86, contact time of 30 minutes and dosage of 0.3 g/100 mL for 10 mg/L fluoride solution at 200 rpm shaking speed. The result shows that Al-oxide modified mechanochemically activated aluminosilicate clay soil is effective for defluoridation. The adsorption data fitted to both Langmuir and Freundlich isotherms. The adsorption data fitted only the pseudo-second-order kinetic, showing chemisorption. Al-oxide modified mechanochemically activated aluminosilicate clay soil was tested for fluoride removal on field water and the percentage fluoride removal was 96.5 % at the dosage of 0.6 g/100 mL with the pH_e of 6.48.

The optimum Al-oxide modified mechanochemically activated aluminosilicate clay soil/ mechanochemically activated clay soil/ corn starch mixing ratio for fabrication of porous ceramic granules was determined by varying ratios and temperature. The optimum ratio found was 20:5:1.The porous ceramic granules were characterised using SEM, BET, FT-IR, XRD and XRF. SEM analysis showed that the porous ceramic granules have the porous structure of the organic foam template. The porous ceramic granule showed an increase in pore surface area and volume as compared to mechanochemically activated aluminosilicate clay soil. The FT-IR showed the presence of a strong broad bending and stretching vibrations band at about 993 cm^{-1} which shows the presence of Si–O–Si bonds. Mineralogical characterisation showed the presence of quartz, albite, horneblende and microcline as the main minerals of the calcined porous ceramic granules. The major oxides of the porous ceramic granules as shown by XRF analysis were SiO_2, Al_2O_3, MnO and Na_2O. The porous ceramic granules reduced the concentrations of fluoride in the water from 10 to 3.31 mg/L. The optimum adsorption capacity was 0.6648 mg/g at a pH_e of 6.32 and the percentage fluoride removal was 66.9 % at an adsorbent dosage of 1.0063 g/100 mL and a temperature of 600 ºC. The porous ceramic granules were tested for fluoride removal on field water and the percentage fluoride removal was 45.4 % at the dosage of 1.0009 g/100 mL with the pH_e of 7.87.

Mechanochemically activated aluminosilicate clay soil showed higher adsorption capacity at acidic pH, therefore it is recommended that future work should focus on improving their adsorption capacity at wider range of pH. The porous ceramic granules can also be evaluated in column dynamic flow experiments.

Keywords: Clay soil; groundwater; defluoridation; adsorption capacity; optimization; characterization, Al oxide, calcination.

TABLE OF CONTENT

Contents

List of Figures

List of Tables

ACRONYMS

BET- Brunauer Emmet Teller

BJH- Barret-Joyner Halenda

CEC- Cation Exchange Capacity

DWAF- Department of Water Affairs and Forestry

FTIR- Fourier Transform Infra-Red spectroscopy

ICP-Ms- Inductively Coupled Plasma-Mass Spectrometer

pHpzc -pH at point of zero charge

RGNDWM- Rajiv Gandhi National Drinking Water Mission

SEM- Scanning Electron Microscopy

WHO- World Health Organisation

XRD- X-ray Diffraction

XRF- X-ray Fluorescence

CHAPTER 1: Introduction

1.1 Background

Clay soil is a natural earthy material composed of very fine particles, usually silicates of aluminum, iron and magnesium. It impedes the flow of water; meaning it absorbs water slowly and then retains it for a long time. Wet clay soil tends to be heavy, sticky and swells from the added moisture. Dry clay soil shrinks and settles. The top layer can bake into a hard, concrete-like crust which cracks. Clay has a great range of applications, including oil absorbents, iron casting, animal feeds, pottery, pharmaceuticals, drilling fluids, waste water treatment, food preparation and paint.

Clay pots are used for transportation and storage of drinking water. Inexpensive, locally made ceramics may improve the quality of the water, apart from keeping water relatively cool; the clay pots may reduce the fluoride content of the water (Ndengwa, 1980). In Mukondeni, clay soil is used for clay pots, serving dishes, decorated ornaments flower pots and ceramic pots. These ceramic pots are used for removal of chemicals in water. During their preparation they are mixed with sawdust, which opens pores for water to pass through during filtration. Some ceramic pots are painted in silver whereas others are used without silver.

Groundwater contributes only 0.6% of the total water resources of the earth (Meenakshi & Mehshwari, 2006). It is the major and most preferred source of drinking water in rural as well as urban areas in developing countries. This is due to the fact that it does not require treatment. In some South African rural communities, scarcity of freshwater made groundwater an alternative source of drinking water. Unfortunately groundwater is sometimes contaminated with naturally occurring chemicals and one of such is fluoride.

Fluoride is a naturally occurring compound derived from fluorine, which is the 13th most abundant element in the earth's crust (Mandinic *et al.*, 2010; Ozbek & Akman, 2012). It exists in the form of fluorides in various minerals such as sellaite (MgF_2), fluorspar (CaF_2), cryolite (Na_3AlF_6) and fluorapatite ($Ca_5(PO_4)_3F$) (Tomar *et al.*, 2013). Due to higher stability of fluoroapatite (Kps = 3.16 x 10^{-60}) with respect to hydroxiapatite (Kps = 2.34 x 10^{-59}) and the same charge and similar ionic radii of fluoride and hydroxide anions, fluoride shows a great trend to isomorphically substitute hydroxide within the apatite network that conforms bones and teeth (Gómez-Hortigüela *et al.*, 2013).

Fluoride in drinking water could be beneficial or detrimental to human health depending on its concentration and total amount ingested. The presence of fluoride is beneficial to calcification of dental enamel, in particular for children under eight years old. However,

excess fluoride intake causes dental and skeletal fluorisis (Sorg, 1978). World Health Organisation (WHO) established that the maximum limit for the concentration of fluoride in drinking water is 1.5 mg/L, beyond which ingestion of water is harmful for human health (WHO, 2011). Moreover, it has been found that intelligent quotient (IQ) of the children living in the high fluoride areas was significantly lower (Lu *et al*., 2000).

People consuming water with high concentrations of fluoride may develop fluorosis condition. Fluorosis is one of the most frequently occurring endemic diseases and currently affecting millions of people worldwide (Zheng, 1994). It typically develops when the F^- concentration of drinking water is greater than 5 to 10 mg/L (Jinadasa *et al.,* 1988; Çengeloğlu *et al.,* 2002; Mahramanlioglu *et al.,* 2002). The symptoms of fluorosis are denser, harder and more fragile, provoking yellowish or brownish spots or mottling of the enamel of the teeth and crippling skeletal fluorosis.

Porous ceramic granular is a solid-phase medium that produces a stable Al–Fe surface complex for fluoride adsorption (Chen *et al*., 2010). It is widely used for a variety of applications, including burners, thermal barrier coatings and insulating layers (Rice, 1998; Scheffler & Colombo, 2005). Pore-forming agents are used frequently as a method to produce porous ceramics with restrained porosity and pore size. Starch is a frequently used pore-forming agent in ceramic technology; due to its chemical composition (consisting essentially of C, H and O), it is easily burnt out during firing without residues in the final ceramic body (Gregorova & Pabst, 2006). Porous ceramic granules could be the good candidate as a metal-support material; due to its large surface area and continuous porous structure (Chen *et al*., 2010). The study by Wang et al. (2014) revealed the synthesis and characterization of Mg-Fe-La trimetal composite as an adsorbent for fluoride removal with fluoride adsorption capacity was 112.17 mg/g. This was a very high adsorption capacity at near neutral pH. It was concluded that the Mg-Fe-La composite can be a very promising material for fluoride removal. Some of the studies were done using granular ferric hydroxide (Yulin *et al*., 2009) and polymer/alumina composites (Karthikeyan *et al*., 2009). The present study is focused on the development of a new adsorbent by the impregnation of porous granular ceramics with aluminum salt to remove fluoride from aqueous solution.

1.2 Problem statement

Due to scarcity of municipal piped water supply, residents in Vhembe district rely mostly on groundwater for their domestic use. Groundwater having higher fluoride content affects health status of dependents. Monitoring of fluoride concentrations in groundwater,

identification of sources, and monitoring of the impact of fluoride on human health was done by Odiyo & Makungo (2012) in Siloam Village, Vhembe district, Limpopo Province, South Africa. Through their study they observed that 87% of households that use groundwater, 85% have members with mottled teeth. Fifty percent of the people with mottled teeth are (school) learners between the ages of 11-14 years. The occurrence of high fluoride concentrations in groundwater and the risk of fluorosis associated with using such water for human consumption is a problem (Hassen, 2007). Fluorosis is a dangerous disease and it can be life threatening. The problem of fluorosis may result in death (Hassen, 2007).

In a previous study Denga, (2013) evaluated Mukondeni red clay soil. The study showed that Mukondeni-red clay soils was able to decrease fluoride concentrations from 8.87 mg/L to 5.10 mg/L. In this study, Mukondeni red clay soil which is aluminosilicate-rich, will be utilized for fabrication of porous ceramic granules that will then be coated with Al_2O_3 and evaluated for defluoridation of groundwater.

1.3 Motivation for the study

Groundwater is the most available, preferable and widely used source of drinking water in many rural communities in Sub-Saharan Africa (Gitari *et al*., 2013); as a result of this, it is of great importance to deal with excessive fluoride, which is prevalent in groundwater sources of some of these communities

Both dental and skeletal fluorosis is a significant public health problem and there are also social and economic problems associated with it. Mukondeni-red clay soil is valuable because it is a locally available, cheap and reliable adsorbent that can be effectively used and cheaply regenerated. These clay soil properties will support an aluminum oxide layer for defluoridation of groundwater. The clay soils will be used for fabrication of the ceramic granules.

1.4 Objectives of the study

1.4.1 Main objective

- Fabrication of Al-oxide coated porous ceramic granules from mechanochemically activated aluminosilicate clay soils and their application in defluoridation of groundwater.

1.4.2 Specific objectives

- Mechanochemical activation of the clay soil.
- Physicochemical and mineralogical characterization of the clay soils.

- Optimization of conditions for the modification of aluminosilicate clay soil with Al oxide.
- Evaluate fluoride adsorption capacity of the porous ceramic granules fabricated from clay soils.
- Evaluate fluoride adsorption capacity of the Al-oxide coated porous ceramic granules fabricated from the clay soils.
- Model the adsorption and kinetic data using various adsorption and kinetic models.

1.5 Hypothesis of the study

Al-oxide modified porous ceramic granules fabricated from aluminosilicate clay soils have high efficiency in removing fluoride from groundwater.

1.6 Delineation and limitation of the study

This study will focus on fluoride concentration rather than other negatively charged ions which can limit the fluoride adsorption capacity of clay soil. The climate also limits the collection of water samples as the fluoride concentration may be diluted if there is rainfall. Samples for this experiment will only be collected once.

Reference

Çengeloğlu, Y., Kir, E. & Ersoz, M., 2002. Removal of fluoride from aqueous solution by using red mud. *Separation and Purification Technology*, 28, pp. 81-86.

Chen, N., Zhang, Y.Z., Feng, C.P., Sugiura, N., Li, M. & Chen, R.Z., 2010. Fluoride removal from water by granular ceramic adsorption, *Journal of Colloid Interface Science*, 348, pp. 579-584.

Chen, N., Zhang, Y.Z., Feng, C.P., Li, M., Zhu, D., Chen, R. & Sugiura, N., 2010. Studies on fluoride adsorption of iron-impregnated granular ceramics from aqueous solution. *Material Chemistry and Physics*, 125, pp. 293-295.

Denga, M.E. 2014. Evaluation of the fluoride adsorption capacity of locally available clay soil in Vhembe district. School of Environmental Sciences, *BSc Thesis*, University of Venda.

Gitari W. M., Ngulube T, Masindi V., & Gumbo J. R., 2013. Defluoridation of groundwater using Fe^{3+} -modified bentonite clay: Optimization of adsorption condition. *Desalination & water treatment*, pp 1-13.

Gómez-Hortigüela, L., Pérez-Pariente, J., García, R. Chebude, Y., & Díaz, I., 2013. Natural zeolites from Ethiopia for elimination of fluoride from drinking Water. *Separation and Purification Technology*, 120, pp. 224-229.

Gregorová, E., Pabst, W. & Bohačenko, I., 2005. *Characterization of different starch types for their application in ceramic processing*. Prague, Czech Republic.

Hassen, A., 2007. *Selection of clay adsorbents and determination of the optimum condition for defluoridation of groundwater in Rift Valley region*. Ethiopia: Addis Ababa University.

Jinadasa, K.B., Weerasooriya, S.W.R. & Dissanayake, C.B., 1988. A rapid method for the defluoridation of fluoride-rich drinking waters at village level. *International Journal of Environmental Studies*, 31, pp. 305-312.

Lu, Y., Sun, Z.R., Wu, L.N., Wang, X., Lu, W., & Liu, S.S., 2000. Effect of high fluoride water on intelligence in children. *Fluoride*, 33 (2), pp. 74-78.

Mahramanlioglu, M., Kizilcikli, I., & Bicer, I.O., 2002. Adsorption of fluoride from aqueous solution by acid treated spent bleaching earth. *Journal of Fluorine Chemistry*, 115, pp. 41-47.

Mandinic, Z., Curcic, M., Antonijevic, B., Carevic, M., Mandic, J., Djukic-Cosic, D., & Lekic, C.P., 2010. Fluoride in drinking water and dental fluorosis. *Science of the Total Environment*, 408, pp. 3507-3512.

Meenakshi, M.R.C., 2006. Fluoride in drinking water and its removal. *Journal of Hazardous Materials*. B137, pp. 456-463.

Ndegwa, W.M., 1980. Investigations leading to defluoridation of waters in Kenya. Thesis, Nairobi: University of Nairobi.

Nemade, P.D., Alappat, B.J. & Rao, A.V., 2002. Removal of fluorides from water using low cost adsorbents. *Water Science and Technology Water Supply*, 2, pp. 311–317.

Odiyo, J.D & Makungo, R., 2012. Fluoride concentrations in groundwater and impact on human health in Siloam Village, Limpopo Province, South Africa. *Water SA*, 5, pp. 731-736.

Ozbek, N. & Akman, S., 2012. Method development for the determination of fluorine in tooth paste via molecular absorption of aluminium mono fluoride using a high-resolution continuum source nitrous oxide/acetylene flame atomic absorption spectrophotometer, *Talanta*, 94, pp. 246-250.
Rice, R. W., 1998. *Porosity of ceramics*. New York: Marcel Dekker.

Scheffler, M. & Colombo, P., 2005. Cellular ceramics—structure, manufacturing, properties and applications. *Wiley–VCH, Weinheim*. Pp. 342-360, pp. 401-620.

Sorg, T.J., 1978. Treatment technology to meet the interim primary drinking water requirement for in organic. *Journal of American Water Works Association*, 20 (2), pp. 105-111.

Tomar, V., Prasad, S., & Kumar, D., 2013. Adsorptive removal of fluoride from water samples using Zr–Mn composite material. *Journal of MicroChemical Engineering*, 111, pp. 116-124.

Wang, J., Kang, D., Yu, X., Ge, M. & Chen, Y., 2014. Synthesis and characterization of Mg-Fe-La trimetal composite as an adsorbent for fluoride removal. *Chemical Engineering Journal*, 264, 506-513.
World Health Organization (WHO), 2011. *Guidelines for drinking water quality*. 4: Geneva.

Zheng, B.S., 1994. *Research on endemic fluoride toxicosis and industrial fluoride pollution*. Beijing: Chinese Environmental Science Press.

CHAPTER 2: Literature review

2.1 Introduction

This section provides a literature on fluoride. It includes discussions in fluoride adsorption capacity of porous ceramic granules at various conditions of pH, fluoride content and adsorbent dosage, modified clays, utilization of clays in fabrication of ceramic granules for water treatment. It also includes advantages and disadvantages of these methods and techniques employed in defluoridation of groundwater.

2.2 Fluoride

Fluorine is a common element that does not naturally occur in elemental form due to its high reactivity. Fluorine occurs in natural water in a form of fluoride (F^-) ions and it is an important micronutrient in human beings for calcification of dental enamel and bone formation, when present in low concentration (Tomar *et al.*, 2013). Fluoride is a chemical which occurs naturally in the Earth's crust, from where they are leached into groundwater. Fluoride can be found in low concentrations below 10 ppm but in some critical situations concentrations of fluoride can exceed this value in groundwater. Freshwater supplies generally contain between 0.01-0.3 ppm, whereas the ocean contains between 1.2-1.5 ppm (WHO, 2002). Fluoride in rivers and lakes may be derived from precipitation while chemical weathering of fluoride-rich rocks in the drainage basin seem to provide for high-fluoride inland lakes (Kilham & Hecky, 1973). The acceptable limits of fluoride in drinking water according to WHO (2002) was prescribed to be less than 1.5 mg/L, so as to prevent dental decay in man.

Fluoridation is the controlled addition of fluoride in the public water supply with the aim of reducing tooth decay in the community in general. Children in areas with naturally fluoridated waters have shown a significantly lower incidence of tooth decay. The target range of fluoride concentration for public water systems that are fluoridating is 0.8 to 1.3 mg/L (Ohio Environmental Protection Agency, 2012).

Most of the fluoride found in groundwater occurs from the breakdown of rocks and soils, or weathering and deposition of atmospheric volcanic particles. Fluoride can also come from the run-off and infiltration of chemical fertilizers in agricultural areas, septic and sewage treatment system discharges in communities with fluoridated water supplies, liquid waste from industrial sources.

2.3 Problems of high F^- in groundwater in South Africa and other parts of the world

High fluoride concentrations are found to be prevalent in many parts of the developing world as millions of people depend on ground water with concentrations above the values prescribed by WHO (2002). Worst affected areas are arid parts of Northern China (Inner Mangolia), India, Sri Lanka, West Africa (Ghana, Ivory Coast and Senegal), North Africa (Algeria), South Africa, East African Rift (Kenya, Uganda, Tanzania and Ethiopia), Northern Mexico and Central Argentina (Smet, 1990). In the early 1980's, it was estimated that around 260 million people worldwide (30 countries) were drinking water with more than 1mg/L of fluoride (Smet, 1990).

South Africa is among countries having higher concentration of fluoride in their underground water on a regional scale (Ncube & Schutte, 2002). In South Africa, Western Cape, Limpopo, Kwa-Zulu Natal and North-West provinces are affected by this phenomenon. The current fluoride distribution in South Africa cannot show clear division since some areas have groundwater sources in which the fluoride ion concentrations are higher than the recommended limits for drinking water (Ncube & Schutte, 2005). Groundwater in Limpopo, North-West, Northern Cape, Western Cape and KwaZulu-Natal Provinces require partial defluoridation to the lower the levels of fluoride concentration safe for drinking water purposes because they contain high fluoride levels; beyond 3 mg/L. These provinces also contain a large population still living in rural areas and most of them use ground and surface water for drinking purposes (Ncube & Schutte, 2005).

The current status of fluoride ion distribution in South African groundwater is provided in Figure 2.1. The figure shows that the problems of high fluoride ion concentrations are currently concentrated in the Limpopo, Northern Cape, North-West and Kwa-Zulu-Natal Provinces (Ncube & Schutte, 2005).

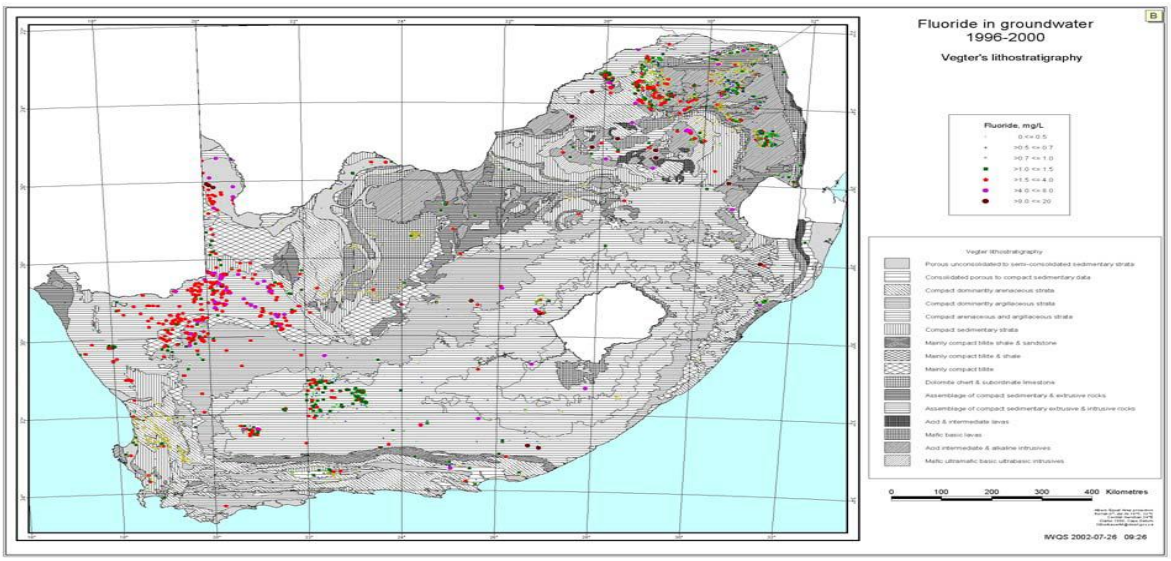

Figure 2.1: Fluoride in groundwater 1996 – 2000 (Ncube & Schutte, 2005)

In the North-West Province, Coetzee *et al.*, (2003) estimated a threshold fluoride concentration of 0.6 mg/L, a value much lower than the 1.5 mg/L of the South African Drinking Water Standard. High fluoride concentration of up to 30 mg/L was found in Bushveld and Pilanesberg regions (Ncube & Schutte, 2005). Fayazi (1994) suggested that the Karoo sediment strata contained fluoride derived from the surrounding Bushveld Granites during episodes of arid erosion. In South Africa, fluoride distribution maps show that the recommended level of 1.0 mg/L is situated in the Karoo sedimentary rocks (Ncube & Schutte 2002).

Table 2.1: Local number of people using ground water for domestic purposes (Ncube & Schutte, 2005).

Dependency of communities on groundwater for domestic purposes						
Province	**North-West**		**Free State**		**KwaZulu-Natal**	
Source	**Communities**	**People**	**Communities**	**People**	**Communities**	**People**
Groundwater	1063	1 411 707	72	122 161	807	2 416 721
Surface water	221	2 099 461	149	3097 252	75	212 698
Combined Source	13	108 593	30	139 452	48	149 685
None	-	-				
Unknown	-	-			1563	5 624 304
Total	1297	3 619 761	251	3340 865	2493	8 403 408
Supply potential						
Poor	160	48 733	-	-	-	-
Low	207	330 061	24	83 380	-	-
Moderate	341	1 220 101	99	905 112	996	2 590 125
High	266	1 620 011	124	2271 450	558	1 529 404
Very high	323	400 855	4	80 923	939	4 283 879
Total communities	**1297**	3 619 761	**251**	3340 865	**2493**	8 403 408
Total population		**3 619 761**		**3340 865**		**8 403 408**

Table 2.1 above shows the number of people depending on groundwater for domestic purposes. KwaZulu Natal has the highest number of people depending on groundwater as a source of drinking water and North-West province has the highest number of communities depending on groundwater for domestic purposes.

2.4 Factors that contribute to the occurrence of high fluoride in groundwater

In South Africa it has been confirmed that the general distribution of the fluoride ion in "problem areas" is controlled by the geochemistry of the rock in which the groundwater is encountered (Mc Caffrey, 1993; Fayazi, 1994; WRC, 2001). Lithological controls suggest that the cause of high fluoride concentrations in groundwater is due to the dissolution of fluoride bearing minerals in bedrock and soil (Mc Caffrey, 1993). The factors contributing to the occurrence can be classified into three major groups; climatic conditions, volcanic eruption and ion chemistry (Ncube & Schutte, 2002).

Climatic conditions

Comparatively temperatures and precipitation favour effective chemical weathering (Nanyaro *et al*., 1984). The composition of the waters therefore, reflects partly the lithology of the drainage basins. During arid episodes and the process of erosion, weathered products derived from granitic rocks containing fluorite in the groundwater at this point (Fayazi, 1994). Groundwater associated with dolerite dykes and silts, which have intruded sedimentary rocks often, have relatively high fluoride concentration. Industrial processes also contribute to the presence of fluoride in groundwater (Ncube & Schutte, 2002). Quantities of fluoride pour into the atmosphere each year from aluminum smelters, phosphate processing, coal burning, manufacturing of steel, fluoride compounds, bricks and glass products (Ncube & Schutte, 2002). This fluoride seeps to ground water or during combustion it is released to the atmosphere, mixed with water droplets, coming down in a form of precipitation. This contributes to high fluoride in groundwater.

Geology and Volcanic eruption

Volcanism is an important factor determining fluoride content of the natural waters (Gaciri & Davies, 1993). During volcanic eruption, four major geological systems namely metamorphic rocks of Precambrian age, sedimentary rocks of Carboniferous to Cretaceous age, Tertiary and Quaternary volcanic, and Unconsolidated Tertiary and Quaternary sediments, leach their chemicals or fluoride into groundwater. Groundwater obtained from these volcanic rocks had shown high fluoride content of up to 180 mg/L (Ncube & Schutte, 2002).

Ionic Chemistry

Other existing minerals in subsurface and other major and minor ionic constituents of groundwater may affect the dissolution characteristics of minerals for example, calcium fluoride (Rao, 1997). The correlation of Ca^{2+} and Na^{+} ions with fluoride concentrations was

evaluated by Ncube (2002). His study reported that high concentrations of Na^+ increases the solubility of fluoride in water and this leads to increasing concentrations of fluoride in water.

2.5 Health impacts of high F^- concentrations in drinking water

Health impacts

People consume fluoride through drinking water and this fluoride is easily absorbed by the human body. After absorption, fluoride ion is quickly distributed throughout the body, easily crossing the membranes and going into tissues. It accumulates in the body due to high reactivity of fluoride ion with calcium of teeth and bones. It forms calcium fluorophosphate (Fluorapatite) crystal and leaves unbound calcium in the same tissue, which gets calcified and in turn results in stiffness of tissues and joints (Tewari & Dubey, 2009). This finally leads to skeletal fluorosis in later stages. That is why fluoride is referred to as bone seeking mineral and bones act as sink for fluoride (Tewari & Dubey, 2009). About 90 % of the fluoride retrieved in body is associated with calcified tissues (Tewari & Dubey, 2009).

Dental fluorosis

The high F^- concentration of about 18 mg/L in the drinking water leads to destruction of teeth enamel and causes a number of conditions referred to collectively as dental fluorosis. Fluorosis has attained an alarming dimension all over the world. According to WHO (2002), drinking water of adequate quality should contain a maximum of 1.5 mg/L F^- concentration.

Dental fluorosis is a sign of excess consumption of fluoride in children under the age six to seven years. Incidences of mottled teeth have been observed even with a range of 0.7 – 1.5 mg F^-/L in drinking water. The minimal daily intake of fluoride that can cause very mild or mild fluorosis is estimated to be about 0.1 mg/kg body weight (Tewari & Dubey, 2009). Dental fluorosis is the loss of lustre and shine of the dental enamel. The discoloration starts from white yellow, brown to black. Enamel matrix is laid down on incremental lines before and after birth. Hence dental fluorosis is invariably seen on horizontal lines or on bands on the surface of the teeth. Fluorosis is seen as mild, moderate and severe depending on the amount of fluoride ingested during the stages of formation of the teeth.

Figure 2.2: Dental fluorosis (fluoridealert.org)

In South Africa dental fluorosis morbidity was assessed by Ncube & Schutte, (2005). In comparing the distribution of the percentage morbidity of fluorosis with that of fluoride concentration in groundwater sources, it is quite clear that high morbidity of fluorosis is observed in areas where fluoride concentrations are extremely high and in most cases the concentration exceeds the limits for drinking water (Ncube & Schutte, 2005).The distribution of dental fluorosis in selected provinces is shown in Figures 2.3, 2.4, 2.5 and 2.6. The results were based on the degree of mottling of the teeth as observed during the dental examinations. The maps show the spatial distribution of the current percentage morbidity of dental fluorosis for the Western Cape, North-West and KwaZulu-Natal Provinces (Ncube & Schutte, 2005).

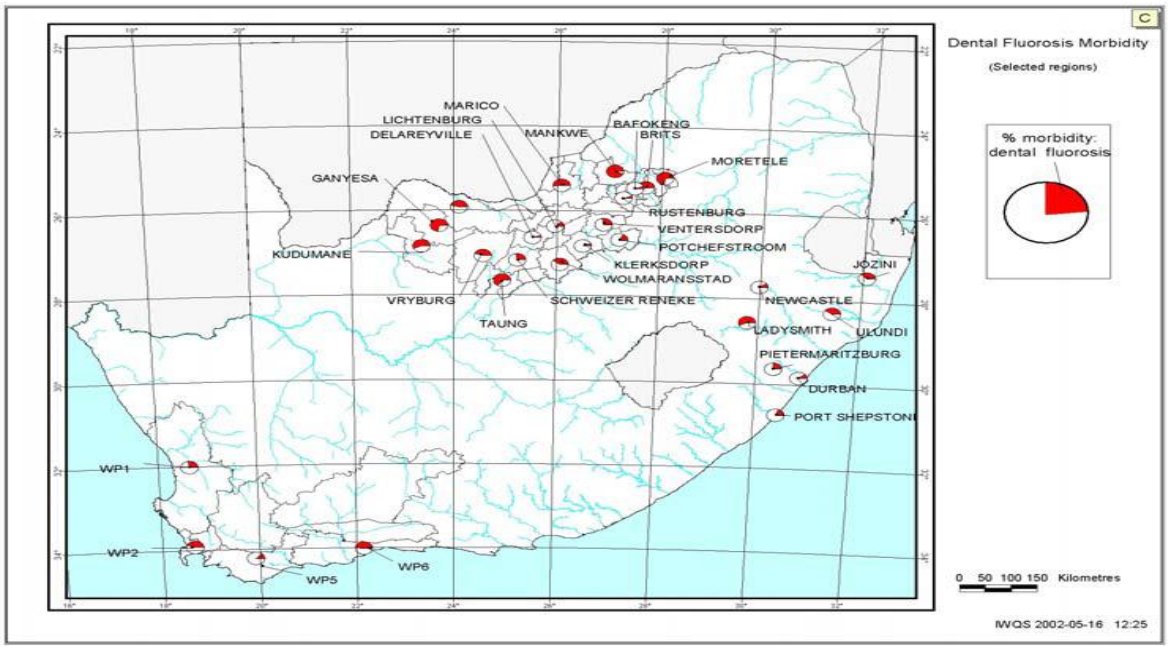

Figure 2.3: The distribution of percentage morbidity of dental fluorosis (Ncube & Schutte, 2005).

The size of the red shaded part (% morbidity of dental fluorosis) in each area gives the idea of the overall quality of drinking water consumed. This provides evidence on the maps that the occurrence of dental fluorosis and its morbidity correspond to the levels of fluoride ion concentrations in drinking water.

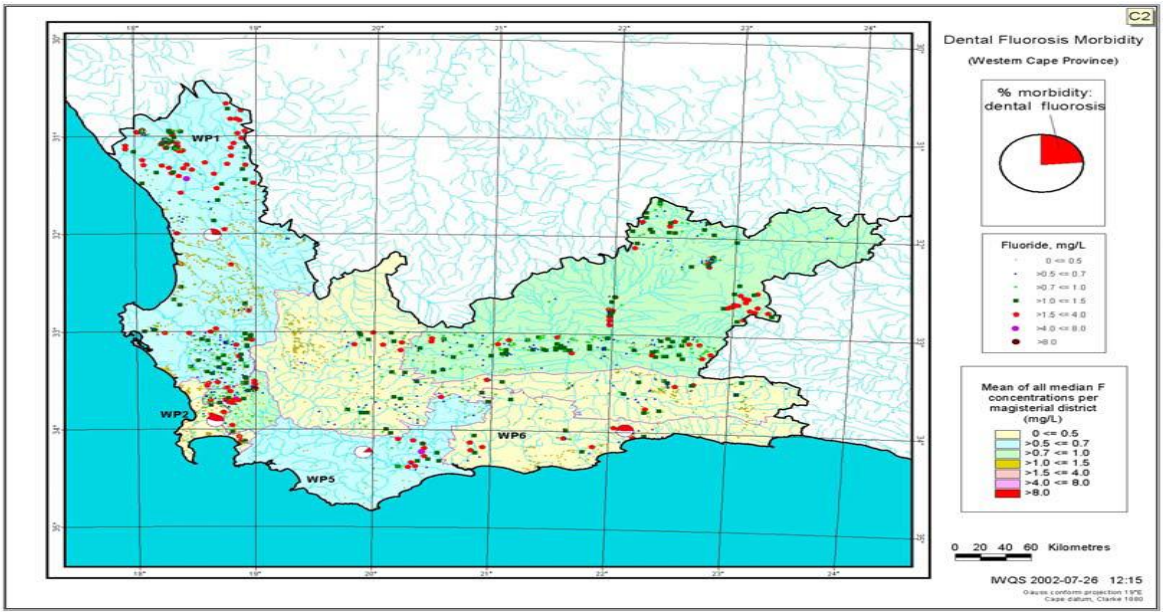

Figure 2.4: Dental fluorosis morbidity in Western Cape Province (Ncube & Schutte, 2005)

In Western Cape, the groundwater usage showed inconsistent results although it was confirmed that the Mitchell's Plain data are mostly for private boreholes, this is due to the migratory nature of the South African population post 1994 some provinces like the Western

Cape might show (Ncube & Schutte, 2005). These boreholes are not necessarily used for drinking water purposes but for other domestic uses such as general cleaning and irrigation purposes.

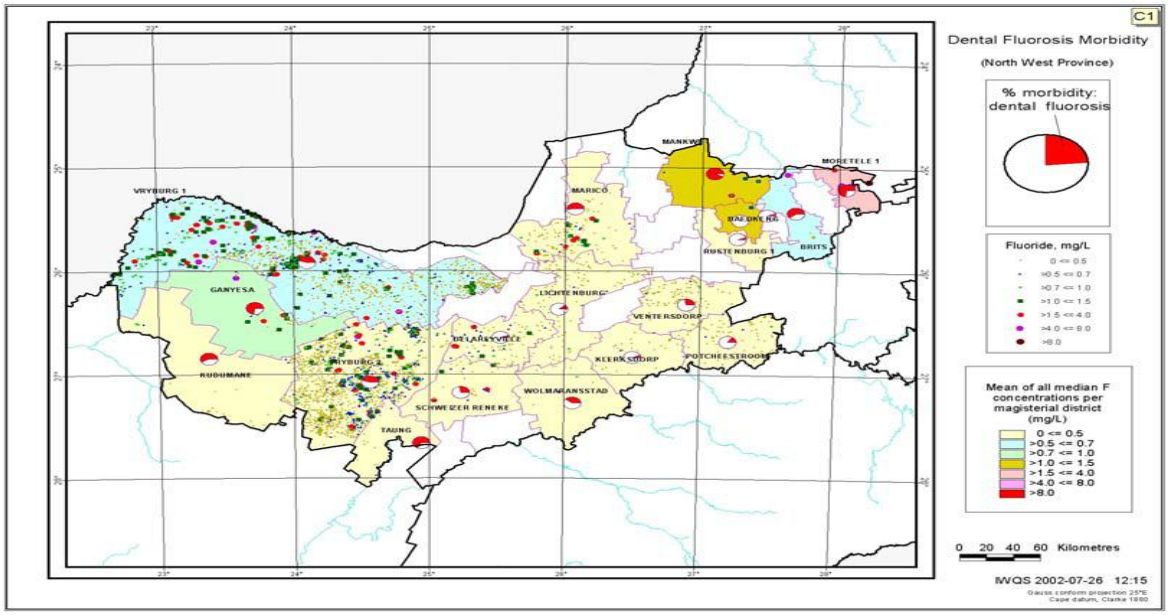

Figure 2.5: Dental fluorosis morbidity in North-West Province (Ncube & Schutte, 2005)

The province where the communities depend largely on groundwater for drinking water purposes has high fluorosis morbidity, for example, the North-West Province, the morbidity of dental fluorosis is high. A percentage of ninety seven morbidity of dental fluorosis was recorded in the North-West Province.

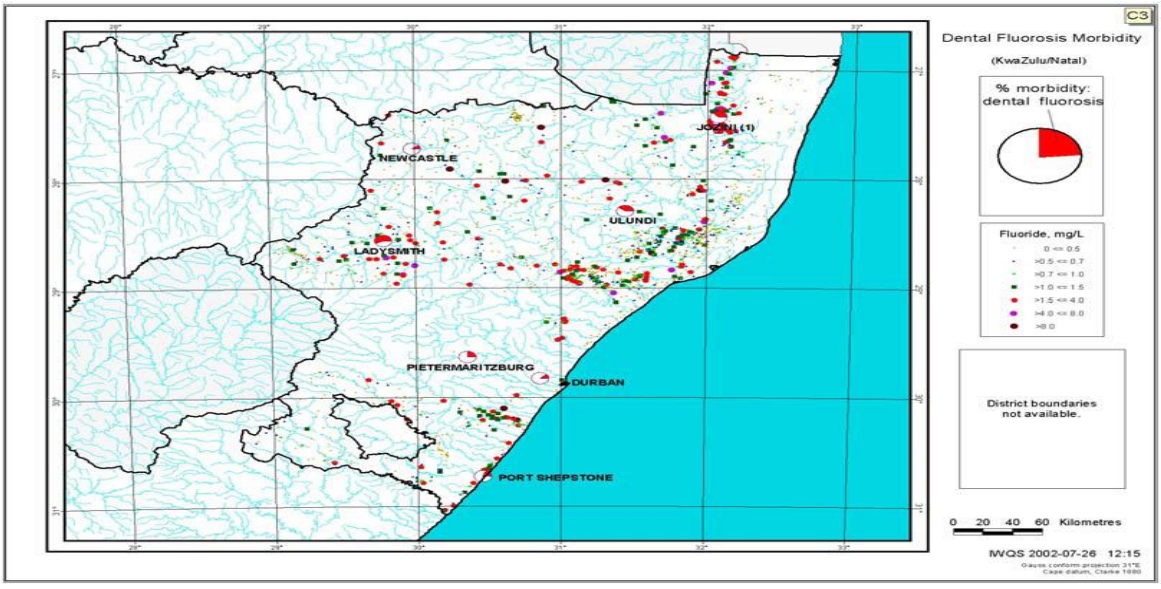

Figure 2.6: Dental fluorosis morbidity in Kwa-Zulu Natal Province (Ncube & Schutte, 2005).

The map on Figure 2.6 confirms the link between high fluoride levels in groundwater, the consumption of this fluoride contaminated water and also the occurrence of dental fluorosis in KwaZulu Natal (Ncube & Schutte, 2005). It has been observed by Ncube & Schutte, (2005) that in towns and villages where the water quality problem in terms of fluoride concentration is low, the morbidity of fluorosis is very low.

Skeletal fluorosis

The F^- ion substitutes the OH^- ion, leading to a build-up of F^- in bone tissue which eventually leads to skeletal fluorosis. Fluoride poisoning leads to severe pain associated with rigidity and restricted movements of cervical and lumbar spine, knee and pelvic joints as well as shoulder joints. In severe cases of fluorosis, there is complete rigidity of the joints resulting in stiff spine described as "bamboo spine", and immobile knee, pelvic and shoulder joints. Crippling deformity is associated with rigidity of joints and includes kyphosis, scoliosis, and flexion deformity of knee joints, paraplegia and quadriplegia (Tewari & Dubey, 2009).

2.6 Methods used for defluoridation

The process of removal of fluoride is generally termed defluoridation. Numerous commercial methods have been described, employing various materials for the fluoride removal since 1930 (Nemade *et al*., 2002). Defluoridation methods have been developed employing both organic and inorganic substances. The various methods are summarized below.

2.6.1 Adsorption method

There is a natural tendency for components of a liquid or a gas to collect often as a monolayer but sometimes as a multilayer at the surface of a solid material. This phenomenon is called adsorption (Humphrey *et al.*, 1997). Adsorption is a mass transfer process in which a constituent in the liquid or gas phase is accumulated on solid or liquid phase and separated from its original environment (Crittenden *et al.*, 2005). In adsorption method, different types of adsorbents are used for defluoridation and for adsorption of other components, dyes and heavy metals. Examples of adsorbents include activated alumina, coconut shell carbon, bagasse, chemically activated carbon, bone charcoal, natural zeolites, hydroxyapatite, clay pots and crushed clay pots. Membrane technologies such as donnan dialysis and other low cost bioadsorbents like saw dust, used tea leaves and cow dung have been found to be highly

effective, cheap and eco-friendly (Arulanantham *et al.*, 1989; Killedar & Bhargava, 1993; Hauge, 1994; Kumar, 1995; Muthukumaran *et al.*,1995; Raghuvanshi *et al.*, 2004).

2.6.1.1 Activated Alumina (AA)

Alumina (Al_2O_3) is practically insoluble in water. The solubility in acid and alkali depends upon previous heat treatment. Strong reagents do not easily attack it and alumina needs to be activated for the defluoridation process (Hassen, 2007). There are different grades of activated alumina (AA). The suitability of the grade for defluoridation depends upon the porosity and surface area of the alumina. Other considerations, which are also of importance, include the life of the AA for defluoridation purposes (Rajchagool, 1998).

The defluoridation capacity of AA is independent of temperature. The adsorption of F^- by activated alumina obeys Langmuir's adsorption isotherm indicating that the force of adsorption is governed by chemisorptions (Hassen, 2007). However, fluoride removal by AA may also take place with decreasing pH and the extent of chemisorption increases at a much higher rate. The AA also adsorbs bicarbonate ions. Thus, the defluoridation capacity of AA decreases at increased concentration of bicarbonate, but chloride and sulphate ions have no effect on fluoride removal capacity. It can be regenerated by 2 % hydrochloric acid, 2 % sodium hydroxide and 1 % sulphuric acid. Fluoride removal efficiency is typically above 95 % (Rajchagool, 1998; Johnston & Heijnen, 2002; Coetzee *et al.*, 2003; Hassen, 2007).

The equation below shows the treatment of alumina with HCl to make it acidic

$$Al_2O_3H_2O + HCl \rightarrow Al_2O_3HCl + H_2O \quad (2.1)$$

The acidity of alumina occurs when contacted with fluoride ions. This can be expressed by the following equation:

$$Al_2O_3.HCl + NaF \rightarrow Al_2O_3.HF + NaCl \quad (2.2)$$

A disadvantage of this process is that the regeneration steps result in an aqueous solution rich in fluoride which is difficult to dispose (Hassen, 2007). Apart from that, spent alumina may leach out fluoride ions when it comes in contact with alkali media (Johnston & Heijnen, 2002).

2.6.1.2 Bone Char

Bone char is produced by carbonizing bone at a high temperature ranging from 1100-1600 ° C (Rao, 2003). The bone exposed to that kind of temperature has superior qualities than those which are unprocessed and they replace bone as defluoridation agent. Bone char consist of a skeleton of calcium phosphate and carbonates; it is also cellular in structure with a great number of tubes and channels (Patil & Ingole, 2012). The process of defluoridation using bone

char is ion exchange wherein carbonate radical of the apatite comprising bone, Ca $(PO_4)_6.CaCO_3$ is replaced by the fluoride to form an insoluble fluorapatite (Rao, 2003). This can be shown by the following equation:

$$Ca_9 (PO_4)_6.CaCO_3 + 2F^- \rightarrow Ca_9 (PO_4)_6.CaF_2 + CO_3^{2-} \quad (2.3)$$

The phosphate ion in the bone char is exchanged for fluoride ion. Tan *et al.* (2003) gave details of the F^- uptake on hydroxyapatite:

$$Ca_{10}(PO_4)_6.(OH_2) + {}_nF^- \rightarrow Ca_{10}(PO_4)_6.(OH)_{2-n}F + nOH^- \quad (2.4)$$

2.6.1.3 Fly ash

Fly ash has been used for fluoride retention. This can be done by using two methods which are precipitation and adsorption. The precipitation method is based on addition of chemicals to water and adsorption method is based on ion exchange reaction on some suitable substance, capable of regeneration and reuse (Reardon & Wang, 2000; Ahmaruzzaman, 2009). Various studies have been conducted concerning defluoridation using fly ash. Nemade *et al.* (2002) investigated the removal efficiency of fluoride by fly ash. The results showed that fly ash was efficient in the removal of fluoride. Piekos & Paslawsk (1999) studied fluoride uptake characteristics of fly ash. In their study, the fluoride removal was done using columns packed with fly ash. The advantage of using fly ash as an adsorbent is that fly ash is effective adsorbent especially at high concentration (Rao, 2003).

2.6.1.4 Activated carbon

Activated carbon (AC) is an important carbon material which is commonly used as an adsorbent for the removal of fluoride (Loganathan *et al.*, 2013). Most of the carbons prepared from different carbonaceous sources showed fluoride removal capacity after alum impregnation (Rao, 2003). Abe *et al.* (2004) reported that F^- adsorption capacity increases with the specific surface area in 11 out of 12 carbonaceous materials studied by them. The amount of adsorption onto activated carbon depends on the pore size distribution (Loganathan *et al.*, 2013). This is due to that adsorption occurs where there are pores. Raw carbon is found to have low adsorption capacity. Srimurali *et al*. (1998), reported that raw carbon could adsorb only 7.9 and 19 % of fluoride. Ramos *et al.* (1991) investigated the fluoride adsorption behaviour of aluminum impregnated Activated Carbon (AlAC) manufactured from coconut shells which are calcined at temperature of 300 ° C. The AlAC was reported to have adsorption capacity

which is more than four times higher than the plain carbon at a concentration of 2-8 mgF/L (Loganathan *et al.*, 2013).

2.6.1.5 Clays and soils

The potential of clay- and soil-based systems for defluoridation is under investigation in many fluoride-endemic regions of the world, especially in developing countries. The first comprehensive study of fluoride adsorption onto minerals and soils was published by Bower and Hatcher in 1967, suggesting that excess fluoride in water could be removed to different degrees by adsorption onto a variety of soil and mineral types. Thereafter, fluoride adsorption onto soils and clays both in natural and modified activated forms has been studied extensively. Research in clays and soils includes Illinois soils in the United States (Omueti & Jones, 1977), Sodic soils in India clay pottery (Chhabra *et al.*, 1980; Hauge *et al.*, 1994), Alberta soil (Luther *et al.*, 1996), Ando soils in Kenya (Zevenbergen *et al.*, 1996), soils and fired clay chips in Africa and Sri Lanka (Padmasiri and Dissanayake, 1995; Moges *et al.*, 1996), activated clay (Bjorvatn and Bardsen, 1995), bentonite and kaolinite (Kau *et al.*, 1997; Kau *et al.*, 1998; Srimurali *et al.*, 2002; Kamble *et al.*, 2009), illite-goethite soils in China (Wang & Reardon, 2001), Red mud (Cengeloğlu *et al.*, 2002), trivalent-cation exchange zeolites (Onyango *et al.*, 2004), activated zeolite (Onyango *et al.*, 2006), laterite (Sarkar *et al.*, 2006) and montmorillonite (Tor, 2006).

2.6.2 Ion exchange treatments

Ion exchange treatment uses charged anion resins to remove fluoride ions in the water. The products most widely used are tricalcic phosphates (bone char, bone ash or animal black, bone powder, synthetic apatite) and synthetic resins (Sobsey, 2002).

Ion exchange on tricalcic phosphate takes place between a hydroxyl, a carbonate ion from apatite and a fluoride ion, thus forming insoluble fluoroapatite that can be easily decanted. Tricalcic phosphate is marketed in the form of a powder but may also be formed *in situ* through a reaction between phosphoric acid and calcium chloride or lime (Rajchagool, 1998; Sobsey, 2002).

Ion exchange treatments are at present not very successful and difficult to carry out (Hassen, 2007). The use of tricalcic phosphates is limited by the relatively low adsorption capacity and average mechanical properties (friability). At present, there are few fluoride exchange resins in the market and they still have limited exchange capacity.

An ion exchange mechanism whereby F^- is exchanged with OH groups in the mineral structure; is generally assumed to be the rate determining steps in the adsorption process (Gitari *et al*., 2013). The mechanism can be expressed as follows:

$$MOH_2 + F^- \leftrightarrow MF + H_2O \quad (2.5)$$

$$MOH + F^- \leftrightarrow MF + OH^- \quad (2.6)$$

2.6.3 Membrane process

Membrane processes such as reverse osmosis (RO), nanofiltration (NF) and electrodialysis are recently developed methods for F^- removal from water. All elements in water can be removed by membrane processes. Thus this method is said to be the best water purification process available, but 30 % of the raw water is lost in the process as brine (Sobsey, 2002). Reverse osmosis is well-known in the industrialized world like the U.S.A and Europe for the removal of ions and soluble materials from sea and brackish water. The study by Lhassani *et al., (*2001) indicates that F^- can be removed using nanofiltration. The performance of different RO and NF membrane for fluoride removal has previously been investigated (Hassen, 2007). However, the technology is not affordable by the rural community (Hassen, 2007) and moreover requires highly competent personnel to manage.

2.6.4 Precipitation Methods

These processes are based on the formation of insoluble fluorides following the action of suitable reagents, which precipitate and can then be separated from the water by decantation. The reagents used in such treatments are calcium or aluminium salts (decarbonation with lime, flocculation with sulphates of alumina) (Mariappan and Vasudevan, 1997).

The treatment requires relatively large quantities of chemical reagents, and generates sludge which is often difficult to remove and dispose. Hence, the quality and original mineral content of the water will not be preserved (Sobsey, 2002).

2.6.4.1 Precipitation using Lime and Alum

Since the early 1960s, the National Environmental Engineering Research Institute (NEER) in India, has been involved in research and development activities on the defluoridation of water (Hassen, 2007). One of the technologies, which have been successfully transferred from the laboratory to the field, is the Nalgonda Technology. The first community defluoridation plant for removal of fluoride from drinking water was constructed in the district of Nalgonda in Andhra Pradesh, in the town of Kathri, thus, the name of the technology. In this technology, raw water is mixed with adequate lime and alum. The amount of lime depends on

the alkalinity of the raw water. If the raw water has adequate alkalinity, the addition of lime is not required. Alum solution is added after the addition of lime, stirred gently for 10 minutes and the flocs formed are allowed to settle (Hassen, 2007).

This process of floc formation and settling requires an hour. In rural areas where people practice domestic defluoridation, the advice given is to mix water with lime and alum and leave it overnight so that the next morning the clean supernatant is decanted for use and is safe for consumption. In the Nalgonda technique, besides fluoride, turbidity, colour, odour, pesticides and organic substances, if any, are also removed. Bacterial contamination is also reduced significantly (Rajchagool, 1998).

The addition of lime or sodium carbonate ensures adequate alkalinity for effective hydrolysis of aluminium phosphate to aluminium hydroxide (that is, floc formation) and as a result, aluminium does not remain in the treated water (Rajchagool, 1998).

Precipitation reaction using lime can be written as indicated in equation 2.7:

$$Ca(OH)_2 + 2F^- \rightarrow CaF_2 + 2OH^- \quad (2.7)$$

2.6.4.2 Precipitation with calcium compounds

Many methods of precipitation of fluorides with salts of calcium, aluminium and iron are reported in literature (Llawler & Williams, 1984; Llarsen *et al.*, 1993). Precipitation processes are governed by the solubility of a forming salt. The most common method of treatment is the precipitation of calcium fluoride using calcium from either lime or calcium chloride (Parthasarathy, 1986).

The fundamental problem that exists when using lime arises from the low solubility of the calcium hydroxide. It therefore requires excess of reagent to complete precipitation (Hassen, 2007). The relatively high solubility of the calcium fluoride does not allow complete removal of F^-. An additional difficulty with lime precipitation is the poor settling characteristics of the precipitate (Coetzee *et al.*, 2003).

2.7 Adsorption studies using clay

Many studies report on the fluoride adsorption capacities of clays, clay soils and their potential use as sorbents. Chaturvedi *et al.* (1990) studied fluoride removal using China clay. The results showed that low F^- concentration, high temperature and acidic pH are factors favoring the adsorption of F^-. It was concluded that the alumina constituent of the China clay is responsible for F^- adsorption. This study further assessed the fluoride adsorption characteristics of clays collected from different areas, where a high fluoride concentration in

groundwater was a problem. Bauxitic clays were found to have the best overall potential as fluoride adsorbents. Simple chemical activation using 1 % Na_2CO_3 solutions and dilute hydrochloric acid could enhance adsorption capacity of certain clay types (Coetzee *et al.*, 2003).

Several researchers have studied the removal of F^- using fired clays. Hauge *et al.*, (1994) studied the defluoridation of drinking water using pottery. The study investigated the effect of firing on F^- adsorption. The results showed that clays fired at temperatures of up to 600 °C gave higher F adsorption (Hauge *et al.*, 1994). Moges *et al.*, (1996) studied the defluoridation of water using fired clay chips in Ethiopia. Their findings indicated that F^- adsorption is affected by factors such as initial concentration, mass of adsorbent and the pH of the solution. Natural clays present a major advantage due to their abundance in nature (locally available). Since these clay minerals are widely available in Ethiopia, they can be used as alternative defluoridating materials.

2.8 Porous ceramic granules and their application in water treatment

Tomar *et al.*, (2013) investigated the removal of fluoride from water samples using Zr-Mn composite material and the excellent removal of up to 90 % was achieved. The results obtained showed that the removal of fluoride using Zr-Mn composite material could be effective. Fluoride removal from water by granular ceramic adsorption was studied by Chen (2010). The adsorption capacity was found to be 0.4432 mg/g and was found to be pH dependent and the maximum removal occurred at pH 5.0- 0.8. It was evident that the granular ceramic used as adsorbent for fluoride removal procedures maintained water quality. This granular ceramic is a promising material for fluoride removal from aqueous solution.

The effectiveness of iron-impregnated granular ceramic in removing fluoride from aqueous solution was evaluated by Chen *et al.* (2010). Two fluoride adsorption capacities were obtained which are 2.157 ($FeSO_4.7H_2O$) and 1.699 (Fe_2O_3). This made $FeSO_4.7H_2O$ granular ceramic to be more effective compared to Fe_2O_3 granular ceramic. Based on the results, the iron impregnated granular ceramic had a potential of removing fluoride in aqueous solution. The study done by Wang *et al.* (2014) investigated the synthesis and characterization of Mg-Fe-La trimetal composite as an adsorbent for fluoride removal. The fluoride adsorption capacity was 112.17 mg/g. This was a very high adsorption capacity at near neutral pH. It was concluded that the Mg-Fe-La composite can be a very promising material for fluoride removal from aqueous solution.

Fluoride removal using granular ferric hydroxide was investigated by Tang *et al.* (2009). The fluoride adsorption capacity was obtained to be 3.521 mg/g at pH range of 3-6.5. The results showed the effectiveness of using granular ferric hydroxide in the removal of fluoride in water. Defluoridation of water via Light Weight Expanded Clay Aggregate (LECA) was studied by Sepehr *et al.* (2014). The highest adsorption capacity was 23.86 mg/g at a pH of 6. The results demonstrated the potential utility of LECA that could be developed into a useful technology for the removal of fluoride from drinking water.

2.9 Mukondeni red clay soil

Mukondeni red clay soil falls under the aluminosilicate group with the characteristics such as high swelling and shrinking potential. This aluminosilicate is said to be tenacious with high plasticity and strength in both wet and dry conditions. It is also characterized by hornblende, plagioclase and quartz. Silica (SiO_2) is found to be the highest component of the Mukondeni red clay soils. According to Johari *et al*. (2011), silica in clay soil exists as free form silica and as compound silica such as in kaolinite ($Al_2Si_2O_5(OH)_4$). The red colour of clay can be attributed to the presence of a slightly high iron oxide (±6.12%). Mukondeni red clay is grittier and has low plastic index (PI). This low PI helps the clay not to crack when drying (Amponsah-Dacosta *et al*., 2013).

2.10 Starch chemistry and its application in fabrication of porous ceramic granules

Starch is one of the frequently used pore-forming agents in ceramic technology (Dìaz & Hampshire, 2004; Reynaud *et al*., 2005). It is a natural biopolymer and easily burnt out during firing without residues in the final ceramic body (Gregorova *et al*., 2005). After burn-out of the starch and sintering of the ceramic matrix a material is obtained with a porosity corresponding to the original amount, shape and size of the starch particles including the allowed swelling during the consolidation (Lyckfeldt *et al*., 1995). The important properties of starches which make them to be widely used, are their thickening, gelling, adhesive and film-forming abilities and besides the favourable gelling properties, they are environmentally friendly, easy to burn out and, not least important, they are very cheap (Lyckfeldt and Ferreira, 1997).

Most starches consist of mixtures of two polysaccharide types, a linear one, amylose, and a highly branched one, amylopectin (Lyckfeldt *et al*., 1995) Amylose gives the starch its gelling property in aqueous suspensions. The glucose units that build up the polymeric chains

in starch expose a large amount of hydroxyl groups and therefore, give a strong hydrophilic character to starch granules (Lyckfeldt *et al*., 1995). This is illustrated in Figure 2.7.

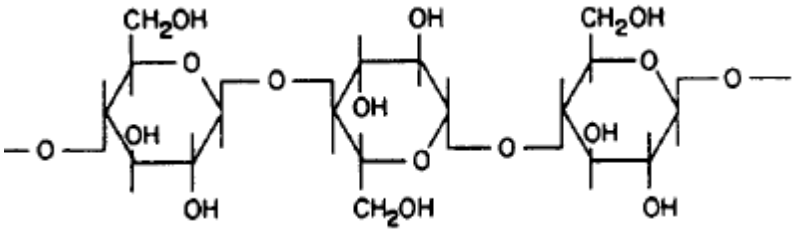

Figure 2.7: Starch as a polymer consisting of condensed glucose units (Lyckfeldt & Ferreira, 1997)

The study done by Chen *et al.* (2010), investigated the preparation and characteristics of porous granular ceramic containing dispersed aluminum and iron oxides as adsorbent for fluoride removal from aqueous solution. Wheat starch was added in order to create pores so as to allow percolation of water during fluoride removal. The adsorption capacity of the adsorbent was 1.79 mg/g. The study showed that the Al/Fe porous granular ceramic has the potential of being used to develop an important technology for fluoride removal from aqueous solution.

Conclusion

The literature review revealed the occurrence of high fluoride content in different countries of the world, with South Africa being one of the countries having higher prevalence of fluoride in their groundwater. Some of the provinces which were assessed were Western Cape, North-West, Kwazulu Natal and Limpopo Provinces. It is shown that the higher the dependencies of the communities on groundwater as a source of drinking water the higher the possibility of dental fluorosis morbidity. In order to prevent the continuous spread of fluorosis several technologies can be used. These technologies are adsorption, ion exchange, membrane process and precipitation method. Fluorosis can also be controlled by using an alternative source of drinking water which contains a low concentration of fluoride. Of all the technologies, adsorption is the most used as it is suitable for household and community defluoridation plant.

Studies done using clay and soils as adsorbents were also reviewed; they are good adsorbents because they are locally available and not costly.

References

Abe, I., Iwasaki, S., Tokimoto, T., Kawasaki, N., T. Nakamura, T. & Tanada, S., 2004. Adsorption of fluoride ions onto carbonaceous materials. *Journal of Colloid Interface Science*, 275, pp. 35–39.

Ahmaruzzaman, M., 2009. A review on the utilization of fly ash. *Progress in Energy and Combustion Science*. 36, pp. 372-363.

Amponsah-Dacosta, F., Muzerengi, C., Mhlongo, S.E., & Mukwevho, G.F., 2013. Characterization of clays for making ceramic pots and water filters at Mukondeni village, Limpopo Province, South Africa. *Journal of Engineering and Applied Sciences*, 8 (11) pp. 927-932.

Arulanantham, A.J., Krishna, T.R. & Balasubramaniam, N., 1989. *Indian Journal of Environmental Health*, 13, p. 531.

Bjorvatn, K., & Bardsen, A., 1995. Use of activated clay for defluoridation of water. In: Proceedings of the First International Workshop on Fluorosis and Defluoridation of Water, Dahi, E., and Bregnhoj, H., Eds., *International Society for Fluoride Research, Auckland*, 40-45.

Bower, C.A. & Hatcher, J.T., 1967. Adsorption of fluoride by soils and minerals. *Soil Science*, 103, pp. 151-154.

Çengeloğlu, Y., Kir, E. & Ersoz, M., 2002. Removal of fluoride from aqueous solution by using red mud. *Separation and Purification Technology*, 28, pp. 81-86.
Chaturvedi, A.K., Yadava, K.P., Pathak, K.I.C.K. & Singh, V.N., 1990. Defluoridation of water by adsorption of fly ash. *Water Air and Soil Pollution*, 49, pp. 51–61.

Chen, N., Zhang, Y.Z., Feng, C.P., Sugiura, N., Li, M. & Chen, R.Z., 2010. Fluoride removal from water by granular ceramic adsorption, *Journal of Colloid Interface Science*, 348, pp. 579-584.

Chen, N., Zhang, Y.Z., Feng, C.P., Li, M., Zhu, D., Chen, R. & Sugiura, N., 2010. Studies on fluoride adsorption of iron-impregnated granular ceramics from aqueous solution. *Material Chemistry and Physics*, 125, pp. 293-295.

Chen, N., Zhang, Z., Feng, C., Zhu, D., Yang, Y. & Sugiura, N., 2011. Preparation and characterization of porous granular ceramic containing dispersed aluminum and iron oxides as adsorbents for fluoride removal from aqueous solution. *Journal of Hazardous Materials*, 186, pp. 863-868.

Chhabra, R., Singh, A., & Abrol, I.P., 1980. Fluorine in sodic soils. *Soil Science Society of American Journal*, 44, pp. 33-36.

Coetzee, P.P., Coetzee, L.L., Puka, R., & Mubenga1, S., 2003. Characterisation of selected South African clays for defluoridation of natural waters. *Water SA*, 29, pp. 331-338.

Crittenden, J., Trussell, R., Hand, D., Howe, K. & Tchobanoglous, G., 2005. *Water treatment: principles and design*. New York: John Wiley and Sons.

Díaz, A. & Hampshire, S., 2004. Characterization of porous silicon nitride materials produced with starch. *Journal of European Ceramics Society*, 24, pp. 413-419.

Fayazi, M., 1994. Regional groundwater investigation on the Northern Springbok flats. Department of Water Affairs and Forestry. *Geohydrology*, *GH Report No. 3684*, 108-155.
Freundlich, H.M.F., 1906. Over the adsorption in solution, *Journal of Physical Chemistry*, 57, pp. 385-470.

Gregorová, E., Pabst, W. & Bohačenko, I., 2005. *Characterization of different starch types for their application in ceramic processing*. Prague, Czech Republic.

Hassen, A., 2007. *Selection of clay adsorbents and determination of the optimum condition for defluoridation of groundwater in Rift Valley region*. Ethiopia: Addis Ababa University.

Hauge, S., Østerberg, R., Bjorvatn, K., and Selvig, K., 1994. Defluoridation of drinking water with pottery: effect of firing temperature. *Scandinavian Journal of Dental Research*, 102, pp. 329-33.

Humphrey, J.L., George, E. & Keller, I.I., 1997. Separation process technology. United Kingdom: Mc Graw-Hill Professional Publishing.

Johari, I., Said, S., Jaya, R.P., Bakar, B.H.A. & Ahmad, Z.A., 2010. Chemical and physical properties of fired-clay brick at different type of rice husk ash. *International Conference on Environmental Science and Engineering IPCBEE*. Singapore: IACSIT Press, 8, pp. 171-174.

Johnston, R. & Heijnen, H., 2002. Safe water technology for arsenic removal. *Report*. World Health Organization.

Kamble, S.P, Dixit P., Rayalu, S.S. & Labhsetwar, N.K., 2009. Defluoridation of drinking water using chemically modified bentonite clay. *Desalination*, 249, pp. 687-693.

Kau, P.M.H., Smith, D.W., & Binning, P., 1998. Experimental sorption of fluoride by kaolinite and bentonite. *Geoderma*, 84, pp. 89-108.

Kau, P.M.H., Smith, D.W., & Binning, P.J., 1997. Fluoride retention by kaolin, *Journal of Contaminant Hydrology*, 28, pp. 267-288.

Kilham, P. & Hecky, R.E., 1973. Fluoride: geochemical and ecological significance in East African waters and sediments. *Limnology and Oceanography*, 18 (6), pp. 44-52.

Killedar, D.J. & Bhargava, D.S., 1993. *Indian Journal of Environmental Health*, 35, p. 81.

Kumar, S., 1995. Compressive myelophathy in fluorosis. *Indian Journal of Environmental Protection*, 16, pp. 50-72.

Lhassani A., Rumeau M., Benjelloun D. & Pontie, M., 2001. Selective demineralisation of water by nanofiltration application to the defluoridation of brackish water. *Water Resources*, 35, pp. 3260-3264.

Llarsen, M.J., Pearce, E.I. & Jensen, S.J., 1993. Defluoridation of water at high pH with use of brushite, calcium hydroxite, and bone char. *Journal of Dental Research,* 72 (11), pp. 1519-1525.

Llawler, D.F & Williams, D.H., 1984. Equalization/neutralization modeling: an application to fluoride removal. *Water Resources*, 11, pp. 25-32.

Loganathan, P., Vigneswaran, S., Kandasamy, J. & Naidu, R., 2013. Defluoridation of drinking water using adsorption process. *Journal of Hazardous Materials*, pp. 248-249.

Lunge, S., Biniwale, R., Labhsetwar, N. & Rayalu, S.S., 2011. User perception study for performance evaluation of domestic technique for its application in rural areas. *Journal of Hazardous Materials*, 191, pp. 325-332.

Luther, S.M., Poulsen, L., Dudas, M.J., & Rutherford, P.M., 1996. Fluoride sorption and mineral stability in an Alberta soil interacting with phosphogypsum leachate. *Canadian Journal of Soil Science*, 76, pp. 83-91.

Lyckfeldt, O. & Ferreira, J.M.F., 1997. Processing of porous ceramics by 'starch consolidation'. *Department of Engineering Ceramics and Glass*, Aveiro: University of Aveiro.

Lyckfeldt, O., Liden, E. & Carlsson, R., 1995. Processing of thermal insulation materials with controlled porosity. In: D.P. Stinton and S.Y. Limaye, eds. *Ceramic Transactions, Low-Expansion Materials*. Westerville: The American Ceramic Society. 52, pp. 217-228.

Mariappan, P. & Vasudevan, T., 1997. Domestic defluoridation techniques and sector approach for fluorosis mitigation. *Department of Industrial Chemistry*, Karakudi: Alagappa University.

McCaffrey, L.P. & Willis, J.P., 1993. Distribution of fluoride-rich groundwater in the eastern parts of Bophuthatswana, relationship to bedrock and soils and constraints on drinking water supplies: a preliminary report. *Africa Needs Ground Water*. *An International Ground Water Convention*. 1, pp. 1-8.

Moges, G., Zewge, F., & Socher, M., 1996. Preliminary investigations on the defluoridation of water using fired clay chips. *Journal of African Earth Science*, 21, pp. 479-482.

Muthukumaran, K.J., Balasubramaniam, N. & Ramkrishna, T.V., 1995. *Indian Journal of Environmental Protection*, 15 (7), pp. 514-517.

Nanyaro, J.T., Aswathanarayana, U. & Mungure, J.S., 1984. A geochemical model for the abnormal fluoride concentration in parts of Northern Tanzania. *Journal of African Earth Science*, (2), pp. 129-140.

Ncube, E.J. & Schutte, C.F., 2002. *The distribution of fluoride in South African groundwater and the impact thereof on dental health*. M. Sc. Pretoria: University of Pretoria.

Ncube, E. J., & Schutte, C. F., 2005. The occurrence of fluoride in South African groundwater: A water quality and health problem. *Water S.A*, 31 (1), pp. 35-40.

Nemade, P.D., Alappat, B.J. & Rao, A.V., 2002. Removal of fluorides from water using low cost adsorbents. *Water Science and Technology Water Supply*, 2, pp. 311–317.

Ohio Environmental Protection Agency, 2012. Ohio's groundwater quality. *Ohio Department of Health.*

Omueti, J., & Jones, R.L., 1977. Fluoride adsorption by Illinois soils. *Journal of Soil Science*, 28, pp. 546-572.

Padmasiri, J.P. & Attanayake, M.A.S.L., 1991. Reduction of iron in groundwater using a low cost filter unit. *Journal of Geological Society, Sri Lanka,* 3**,** pp. 68-77.

Parthasarathy, N., Buffle, J. & Haerdi, W., 1986. Combined Use of Calcium Salts and Polymeric Aluminium Hydroxide for Defluoridation of Waste Waters. *Water Resources*, 20 (4), pp. 443-448.

Patil, S.S. & Ingole, N.W., 2012. Studies on defluoridation - a critical review. *Journal of Engineering Research and Studies*, 3, pp. 111-119.

Piekos, R. & Paslawska, S., 1999. Fluoride uptake characteristics of fly ash. *Fluoride*, 32, pp. 14–19.

Raghuvanshi, S.P., Singh, R. & Kaushik, C.P., 2004. *International Journal of Applied Ecology and Environmental Resources*, 2, p. 35.

Rajchagool, S., Puangpinyo, W., & Rujanawisan, N., 1998. Fluorosis and the solution by technical means.

Ramos, R.L., Ovalle-Turrubiartes, J. & Sanchez-Castillo, M.A., 1999. Adsorption of fluoride from aqueous solution on aluminium-impregnated carbon. *Carbon 37*, pp. 609–617.

Rao, C.R.N., 2003. Fluoride and environment—a review. In: Proceedings of the Third International Conference on Environment and Health, Chennai, India, 15–17 December 2003; pp. 386–399.

Rao, N.R., 1997. Phosphate pollution in the groundwater of lower Vamsadha river basin, India. *Environmental Geology*, 31, pp. 117-122.

Reardon, E.J. & Wang, Y.X., 2000. A limestone reactor for fluoride removal from wastewaters.

Reynaud, C., Thévenot, F., Chartier, T. & Besson, J.L., 2005. Mechanical properties and mechanical behaviour of SiC dense-porous laminates. *Journal of European Ceramics Society*, 25, pp. 589–597.

RGNDWM, 1993. *Prevention and control of fluorosis in India. Health aspects*, Ministry of Rural Development, CGO Complex**.**

Sarkar, M., Banerjee, A. & Pramanik, P.P., 2004. *Science Reporter*, 86 (1), pp. 28-29.

Sepehr, M.N., Kazemian, H., Ghahramani, E., Amrane, A., Sirasankar, V. & Zarrabi, M., 2014. Defluoridation of water via light weight expanded clay aggregate (LECA): adsorbent characterization, competing ions, chemical regeneration, equilibrium and kinetic modeling. *Journal of the Taiwan Institute of Chemical Engineers*, 45, pp. 1821-1834.

Sobsey, M.D. 2002. Managing water in the home: accelerated health gains from improved water supply.

Srimurali, M., Pragathi, A., & Karthikeyan, J., 1998. A study on removal of fluorides from drinking water by adsorption onto low-cost materials. *Environmental Pollution*, 99, pp. 285-289.

Tan, I.A.W., Ahmad, A.L. & Hameed, B.H., 2003. Biosorption isotherms, kinetics, thermodynamics and desorption studies of 2,4,6-trichlorophenol on oil palm empty fruit bunch-based activated carbon. *Journal of Hazardous Materials*, 164, pp. 473-482.

Tang, Y., Guan, X., Wang, J., Gao, N., McPhail, M.R. & Chusuei, C.C., 2009. Fluoride adsorption onto granular ferric hydroxide: effects of ionic strength, pH, surface loading, and major co-existing anions. *Journal of Hazardous Materials*, 171, pp. 774-779.

Tewari, A. & Dubey, A., 2009. Defluoridation of drinking water: efficacy and need. *Department of Chemistry*. Kampur: Pranveer Singh Academy of Technology.

Tomar, V., Prasad, S., & Kumar, D., 2013. Adsorptive removal of fluoride from water samples using Zr–Mn composite material. *Journal of MicroChemical Engineering*, 111, pp. 116-124.

Tor, A. 2009. Removal of fluoride from aqueous solution by using montmorillonite. *Desalination*, 201, pp. 267-276.

Tor, A., Danaoglu, N., Arslan, G. & Cengeloglu, Y., 2009. Removal of fluoride from water by using granular red mud: Batch and column studies. J*ournal of Hazardous Materials*, 164, pp. 271-278.

Wang, J., Kang, D., Yu, X., Ge, M. & Chen, Y., 2014. Synthesis and characterization of Mg-Fe-La trimetal composite as an adsorbent for fluoride removal. *Chemical Engineering Journal*, 264, 506-513.

Wang, Y., & Reardon, E.J., 2001. Activation and regeneration of a soil sorbent for defluoridation of drinking water. *Applied Geochemistry*, 16, pp. 531-539.

Water Resource Commission (WRC), 2001. Distribution of fluoride-rich groundwater in the Eastern and Mogwase Regions of the Northern and North-West Province. Pretoria: *WRC Report No. 526/1/01 1.1 - 9.85*.

World Health Organization, (WHO), 2002 Geneva, Fluorides, Environmental Health Criteria, 227.

Zevenbergen, C., Van Reeuwijk, L.P., Frapporti, G., Louws, R.J., & Schuiling, A., 1996. Simple method for defluoridation of drinking water at village level by adsorption on Ando soil in Kenya. *Science of the Total Environment*, 188, pp. 225-232.

CHAPTER 3: Mechanochemical activation of aluminosilicate clay soil and its evaluation of defluoridation potential

Abstract

Fluoride occurs naturally in water systems as a result of run-off from weathering of fluoride-containing rocks and soils and leaching from soil into ground water. There is a substantial shortfall in the availability of potable water in less developed or developing countries, therefore communities are forced to use groundwater for drinking. The purpose of the present study was to (1) mechanochemically activate aluminosilicate clay soil, (2) assess the physicochemical characteristics of the mechanochemically activated aluminosilicate clay soil, (3) assess the efficiency of fluoride removal from groundwater using mechanochemically activated aluminosilicate clay soil and (4) model the adsorption data. The raw clay materials were mechanochemically activated for 5, 10, 15 and 30 minutes for physicochemical transformation of the solid aggregate. The morphology of the samples showed the honeycomb structure. The surface area analyses of samples using Brunauer–Emmett–Teller (BET) gave the highest surface area of 50.5228 m^2/g at 30 min activation time. Hence, the optimum activation time was 30 min. The Fourier Transform Infrared (FT-IR) analysis showed increase in the absorbance of FT-IR by Si-O-H groups at 510 cm^{-1} with increasing milling time. This is evidence that more surface Si-O-H groups were available at higher particle surface area that would be necessary to interact with fluoride. X-ray diffraction (XRD) analyses revealed that, at 30 minutes milling time, the peak broadening is intensified whereas the reflection peak intensities decreased. The X-ray fluorescence spectrometry (XRF) results for 30 minutes milling time showed that silica and alumina were the highest components in the clay soil. Using the activated clay in batch defluoridation of fluoride-spiked water, a maximum fluoride removal of 41% was achieved at a pH_e of 2.41. The initial fluoride concentration was 9 mg/L while the sorbent dosage was 0.6 g/100 mL and the contact time being 30 minutes. The adsorption data fitted to both Langmuir and Freundlich isotherms. The adsorption data fitted only the pseudo-second-order kinetic, showing chemisorption. However, further investigations are required to improve its adsorption capacity which is the next topic of the next chapter.

Keywords: *Clay soil; groundwater; defluoridation; adsorption capacity; optimization; characterization.*

3.1 Introduction

Groundwater is considered to be the most preferred drinking water especially in rural communities of South Africa. The Department of Health in South Africa has legislated regulations in respect of fluoridation of potable water supplies in September 2000 (Department of Health, 2000; Noh and Cotzee, 2006). The final regulations were approved by Parliament in September 2001, stating that fluoridation of municipal water up to a level of 0.7mg/L was recommended. World Health Organisation (WHO) established that the maximum limit for the concentration of fluoride in drinking water is 1.5 mg/L, beyond which ingestion of water is harmful for human health (WHO, 2011).

Prolonged ingestion of fluoride rich water may lead to dental and skeletal fluorosis. The reason being that groundwater is usually free from water borne diseases associated with surface water. Occurrence of high fluoride concentrations in groundwater and the risk of fluorosis associated with using such water for human consumption is a problem faced by many countries (Coetzee *et al.*, 2003) including parts of South Africa.

Mechanochemistry is the study of chemical and physicochemical transformations of substances in all states of aggregation induced by mechanical energy (Wieczorek-Ciurowa & Gamrat, 2007). Mechanochemical activation is one of such methods, which involve simple grinding of an inorganic material and this would lead to physical disintegration along with the formation of active surfaces as well as changes in the physicochemical behaviour of materials (Meenakshi *et al.*, 2007)

In this study, the effectiveness of mechanochemically activated aluminosilicate-rich clay for fluoride removal was examined. Defluoridation experiments were performed in batch mode under different experimental conditions, such as pH, contact time, adsorbent dosage, initial fluoride concentration, temperature, leached metals and co-existing ions. The characterization studies of the adsorbent by XRD, XRF, SEM, BET, pH at point-of-zero charge and Cation Exchange Capacity analyses were carried out to determine the properties of the clay material. Adsorption mechanisms and adsorption kinetics were evaluated for the better understanding of the defluoridation mechanism of mechanochemically activated aluminosilicate-rich clay soil.

3.2 Materials and methods

3.2.1 Collection and preparation of aluminosilicate clay

The aluminosilicate-rich clay soil for this study was obtained from Mukondeni Village, Vhembe district in South Africa. Field water was collected from a community borehole in Siloam, Vhembe district in South Africa. All reagents including TISAB-III were obtained from Monitoring and Control Laboratories (Pty) Ltd and Sigma-Aldrich Co. LLC. Pieces of plant material and pebbles were removed by hand. Two hundred grams of the clay soil were washed with Milli-Q water at ratio of 1:10. The mixture was stirred and allowed to settle for 5 minutes; the water was decanted and the procedure was repeated twice. The residue obtained was rinsed with deionized water at the ratio of 1:5. The process was repeated until aluminosilicate-rich clay was free of dirt. The mixture was scooped into a plastic bottle and made-up to 100 mL mark with Milli-Q water, after which it was shaken thoroughly for 30 minutes on a reciprocating shaker at 250 rpm. Aluminosilicate-rich clay was decanted into plastic bottles and centrifuged for 5 minutes at 40 rpm. After centrifugation, the water was poured out and the residue was were filled into the petri-dish. The residue was oven-dried for 12 hours at temperature of 105^0 C, after which it was milled to fine powdery materials, sieved and then stored in plastic bags for future experiments.

3.2.2 Preparation of NaF solution

A litre of 1 000 mg/L F^- stock solution was prepared by dissolving 2.21 g of NaF (analytical grade) in some Milli-Q water in a litre volumetric flask. The volume of solution was be raised to the etched mark by adding more Milli-Q water. Lower fluoride solutions were prepared from the stock solution by serial dilution.

3.2.3 Physicochemical and mineralogical characterization of mechanochemically activated aluminosilicate clay soil and raw clay soil

The physicochemical and mineralogy of mechanochemically activated aluminosilicate clay soil was carried out using steps described in section 3.2.3.1- 3.2.3.10.

3.2.3.1 Determination of geological fluoride

One gram of clay soil was dispersed in 100 ml of Milli-Q water. The mixture was agitated on the reciprocating shaker for 1 hour at 250 rpm. After shaking, the mixture was centrifuged and the obtained supernatant was analysed for residual fluoride. The four-standard calibrated ORION fluoride ion-selective electrode was used after addition of TISAB III to both

standards and sample at a ratio of 1:10. The fluoride content of the clay was determined to be 0.0616 mg/L, which is very low as compared to the WHO (2011) guideline of 1.5 mg/L. Therefore there was no need to subject the clay to further treatment for fluoride removal.

3.2.3.2 Mechanochemical activation

The RETSCH R5 200 ball mill was used for mechanical treatment of solids samples, which were milled for 5, 10, 15 and 30 minutes at 700 rpm. Each milling was carried out with a 10 g air-dried sample put in a 150 cm^3 capacity steel pot with weight of 121.1 g and 7 mm diameter steel balls. The intensive cooling of pots with cold running water increased the efficiency of mechanical treatment (Juhfisz and Opoczky, 1990).

3.2.3.3 Morphology of raw and mechanochemically treated clay

The morphology of the clay soil sample was determined for 5, 10, 15 and 30 minutes mechanochemically activated aluminosilicate clay soil using Hitachi X-650 scanning electron micro analyser equipped with CDU lead detector at 25 kV. The samples were sprinkled onto aluminum scanning electron microscope (SEM) stubs covered in carbon glue. The excess sample was blown-off with compressed air and the stubs evaporation coated with carbon. The stubs were then examined with a FEI Nova NanoSEM 230 using the high resolution in-lens secondary detector. Elemental analysis was carried out using an Oxford X-Max detector and INCA software.

3.2.3.4 Surface area and pore volume of raw and mechanochemically activated aluminosilicate clay soil

The surface area was carried out by BET analysis and micropore volume were determined using the nitrogen adsorption/desorption isotherms collected at liquid nitrogen temperature (77K). Micromeritics TriStar II surface area and porosity analyser (USA) were used. Prior to analysis, the samples were degassed at desired temperature for particular time under a vacuum of more than 2 μm Hg. Nitrogen gas flow was used in the experiment to ensure no moisture in the sample. The desorption branch of the isotherm is used to determine the Barret-Joyner-Halenda (BJH) pore size distributions of the material. This procedure was done for 5, 10, 15 and 30 minutes for the mechanochemically activated aluminosilicate clay soil.

3.2.3.5 Fourier Transform Infra-Red (FTIR) spectroscopic determination

The functional groups of the mechanochemically activated aluminosilicate clay soil was analysed using Bruker Tensor 27 FT-IR & OPUS Data Collection Program. Prior to any solid sample deposition, the surface of the diamond ATR waveguide was cleaned by soaking with acetone and wiped using lens-cleaning tissues. Before recording background spectra, acetone was allowed to evaporate for at least 15 minutes. For each measurement, approx. 100 mg of solid dry sample was firmly pressed against the waveguide surface. Each sample spectrum was independently recorded three times to ensure reproducibility of the measurement procedure.

3.2.3.6 Analysis of mineralogy using XRD technique

The mineralogical characteristics of the 30 minutes mechanochemically activated aluminosilicate clay soil samples were evaluated using XRD technique. After representative sampling using a riffle splitter, the samples were milled in a tungsten carbide vessel and prepared according to the standardized Panalytical back loading system, which provided nearly random distribution of the particles. The sample was analysed using a PANalytical X'Pert Pro powder diffractometer in θ–θ configuration with an X'Celerator detector and variable divergence- and fixed receiving slits with Fe filtered Co-Kα radiation (λ=1.789Å). The phases were identified using X'Pert Highscore plus software. The relative phase amounts (weight %) was estimated using the Rietveld method (Autoquan Program). Errors are on the 3 sigma level in the column to the right of the amount.

3.2.3.7 Analysis of chemical composition using XRF technique

The elemental composition of the clay in form of their oxides of the 30 minutes mechanochemically activated aluminosilicate clay soil was done using PANanalytical Axios instrument. The sample preparation involved milling of clay samples to less than 75 μ fraction. The milled sample was then roasted at 1000 °C for at least 3 hours to oxidize iron (Fe^{2+}) and Sulphur (S), and to determine the Loss on Ignition (L.O.I) percentage. The analysis of major oxides required that the glass disks are prepared through fusing 1 g roasted sample, 8 g (12-22) flux consisting of 35% alkali borate ($LiBO_2$) and 64.71% lithium tetraborate ($Li_2B_4O_7$) at 1050 °C. The glass disks were then analysed by XRF instrument equipped with a 4 kW Rhodium (Rh) tube. Trace element analysis was achieved by mixing 12 g milled sample and 3 g Hoechst wax. The mixture was then pressed into a powder briquette by a hydraulic press with an applied pressure of 25 ton.

3.2.3.8 pH at point-of- zero charge (pHpzc) of mechanochemically activated clay soil

The pH at point-of-zero charge was determined using 0.01, 0.1 and 1 M KCl solutions. The respective solutions of 60 mL were measured into plastic containers and the pH adjusted to a desired value using 0.1 M HCl and 0.1 M NaOH. The adjusted pH constituted the initial pH (pH_0). From 60 mL, 50 mL of solutions with known pH were then measured into clean and dry 100 mL plastic bottles. A mass of 0.6 g of adsorbent was weighed into each bottle. The mixtures were shaken in a water bath shaker at 200 rpm for 24 h. The equilibrium pH (pHe) of each mixture was measured after the equilibration time. The change in pH (ΔpH = pHe - pH0) was plotted against the initial pH of KCl solution. In the ΔpH-pH0 profiles, the pHpzc is the abscissa for ΔpH = 0. This is the point where the curve crosses the horizontal axis.

3.2.3.9 Cationic Exchange Capacity (CEC)

The cationic exchange capacity of the mechanochemically activated aluminosilicate clay soil was determined by extracting the exchangeable cations such as Ca^{2+}, K^{+} , Mg^{2+} and Na^{+} with 1 M ammonium acetate (NH_4OAc). A solution of 1000 mg/L of 1 M ammonium acetate was prepared by dissolving 77.0825 g of the salt in Milli-Q water in 1 L volumetric flask. The pH of solution was measured to be 7. A solution of 50 mL was measured into a 250 mL plastic bottle and 10 g of clay soil was added into the solution. The mixture was shaken along with a blank on the water bath shaker at temperature of 298 K for 30 minutes at a speed of 200 rpm. After shaking, the mixture was filtered through a membrane filter. A volume of 175 mL of ammonium acetate in 25 mL portions was passed through the solid on membrane filter so as to wash the solid and remove the exchangeable cations. The total volume of solution that passed through the membrane filter was 225 mL.

After filtration the supernatant was diluted by a factor of 10 using 3 M nitric acid and thereafter the supernatant was analysed for exchangeable cations using Inductively Coupled Plasma-Mass Spectrometer (ICP-MS)

3.3 Fluoride adsorption experiments

Batch experiments were carried out at specific values of experimental parameters to optimize adsorption conditions. The following experimental parameters were considered:

3.3.1 Effect of pH

The effect of pH on fluoride adsorption onto mechanochemically activated aluminosilicate clay soil was evaluated. A mass of 0.6 g of adsorbent was dispersed into 90 mL

of 10 mg/L fluoride solution contained in six 250 mL plastic bottles. The pH values of the mixtures were adjusted using 0.1 M HCl and 0.1 NaOH to the desired values. The initial fluoride concentration of 9 mg/L was employed in this study. The bottles were tightly closed and shaken at 200 rpm for 30 minutes. After shaking, the equilibrium pH was measured and recorded. The mixtures were then centrifuged for 5 minutes at 40 rpm and the supernatants obtained were analysed for residual fluoride using a four-standard calibrated ORION fluoride ion-selective electrode having added TISAB III to both standards and samples at volume ratio of 1:10 for 30 minutes.

3.3.2 Effect of contact time

Masses of 0.1, 0.3 and 0.4 g of the adsorbent soil were weighed into 100 mL of 9 mg/L fluoride solution in twenty four 250 mL plastic bottles. The initial pH of each mixture was adjusted to 2. The mixtures were shaken at 200 rpm for 1, 5, 10, 20, 30, 50, 70 and 90 minutes at 299 K. After shaking, the equilibrium pH was measured and recorded. The mixtures were then centrifuged for 5 minutes at 40 rpm and the supernatants obtained were analyzed for residual fluoride using a four-standard calibrated ORION fluoride ion-selective electrode having added TISAB III to both standards and samples at volume ratio of 1:10 for 30 minutes.

3.3.3 Effect of adsorbent dosage

The effect of adsorbent dosage on fluoride removal was evaluated. Masses of 0.1, 0.2, 0.5, 0.6, 0.8, 0.9 and 1 g of mechanochemically activated aluminosilicate clay soil samples were weighed into 100 mL of 9 mg/L fluoride solution in seven 250 mL plastic bottles. The initial pH of each mixture was adjusted to 2. The mixtures were shaken at 200 rpm for 30 minutes at 297 K. After shaking, the equilibrium pH was measured and recorded. The mixtures were then centrifuged for 5 minutes at 40 rpm and the supernatants obtained were analysed for residual fluoride using a four-standard calibrated ORION fluoride ion-selective electrode having added TISAB III to both standards and samples at volume ratio of 1:10.

3.3.4 Effect of F^- concentrations

The effect of adsorbate concentration was evaluated at temperatures of 298, 309 and 318 K. For each temperature, 0.6 g of the adsorbent was weighed into 100 mL of 4.5, 9, 18, 36, 45, 54, 72 and 90 mg/L fluoride solutions in eight 250 mL plastic bottles. The initial pH of each mixture was adjusted to 2. The mixtures were shaken at 200 rpm for 30 minutes. After shaking, the equilibrium pH was measured and recorded. The mixtures were then centrifuged

for 5 minutes at 40 rpm and the supernatants obtained were analysed for residual fluoride using a four-standard calibrated ORION fluoride ion-selective electrode having added TISAB III to both standards and samples at volume ratio of 1:10.

3.3.5 Effect of temperature

The effect of temperature was evaluated at temperatures of 298, 309 and 318 K. For each temperature, 0.6 g of the adsorbent was weighed into 100 mL of 4.5, 9, 18, 36, 45, 54, 72 and 90 mg/L fluoride solution in eight 250 mL plastic bottles. The initial pH of each mixture was adjusted to 2. The mixtures were shaken at 200 rpm for 30 minutes. After shaking, the equilibrium pH was measured and recorded. The mixtures were then centrifuged for 5 minutes at 40 rpm and the supernatants obtained were analysed for residual fluoride using a four-standard calibrated ORION fluoride ion-selective electrode having added TISAB III to both standards and samples at volume ratio of 1:10.

3.3.6 Effect of medium pH on the chemical stability of the adsorbent

The effect of pH on fluoride onto mechanochemically activated aluminosilicate clay soil was evaluated. A mass of 0.6 g of adsorbent was dispersed into 100 mL of 9 mg/L fluoride solution contained in six 250 mL plastic bottles. The pH of the mixture was adjusted using 0.1 M HCl and 0.1 NaOH to the pH of 2-12. The initial fluoride concentration of 9 mg/L was employed in the study. The bottles were tightly closed and shaken at 200 rpm for 30 minutes. After shaking, the equilibrium pH was measured and recorded. The mixtures from were then centrifuged for 5 min at 40 rpm and the supernatants obtained were analysed for leached metals using Inductively Coupled Plasma-Mass Spectrometer (ICP-MS).

3.3.7 Determination of adsorption percentages and capacities

The fluoride adsorption percentage and capacity from the equilibrium fluoride concentration was calculated using the following equations:

$$\% \text{ Adsorption} = \frac{C_o - C_e}{C_o} \times 100 \quad (3.1)$$

$$\text{Adsorption capacity } (q_e) = \frac{C_o - C_e}{m} \times V \quad (3.2)$$

Where C_o= initial fluoride concentration (mg/L)

C_e = equilibrium fluoride concentration (mg/L)

m = mass of adsorbent (g)

v = volume of the solution used in the batch (L), and
q_e = the amount of adsorbed fluoride at equilibrium (mg/g)

3.4 Results and discussion

3.4.1 Morphology of mechanochemically activated aluminosilicate clay soil

The SEM images of raw (Figure 3.1) and mechanochemically activated aluminosilicate clay soil treated at 5, 10 15, and 30 minutes are depicted in Figures 3.2, 3.3, 3.4 and 3.5, respectively. SEM images indicated honeycomb, spongy, and porous morphology with irregular structure in the surface morphology. The images showed presence of very high amount of patches which could be as a result of change in milling time.

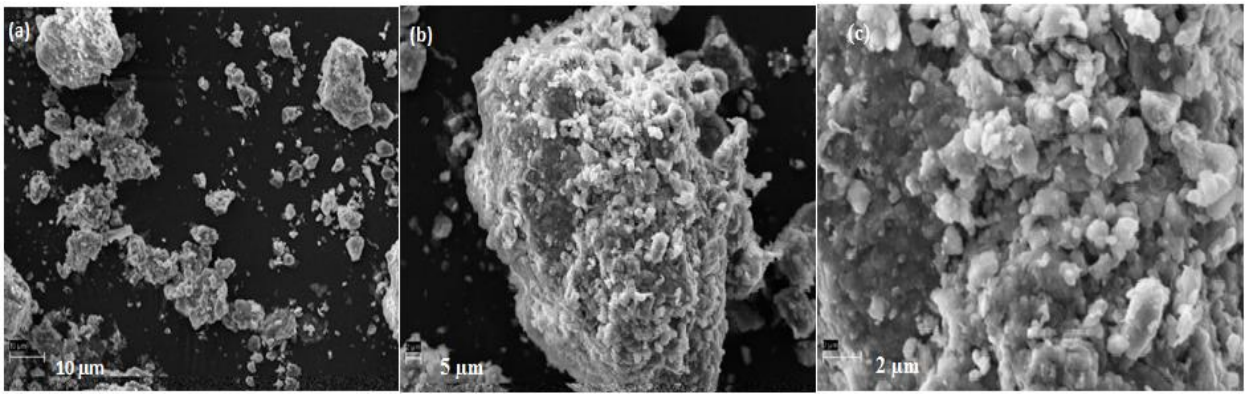

Figure 3.1: SEM images of raw aluminosilicate clay soil after milling for 3 minutes at magnification of 5 000x (a), SEM image at magnification of 10 000x (b), SEM image at magnification of 20 000x (c).

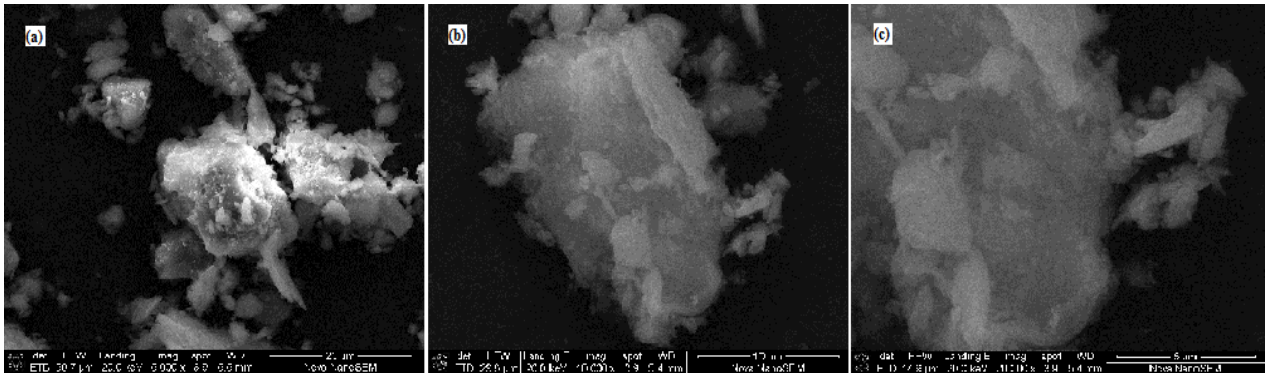

Figure 3.2: SEM images of mechanochemically activated aluminosilicate clay soil after milling for 5 minutes at magnification of 5 000x (a), SEM image at magnification of 10 000x (b), SEM image at magnification of 20 000x (c).

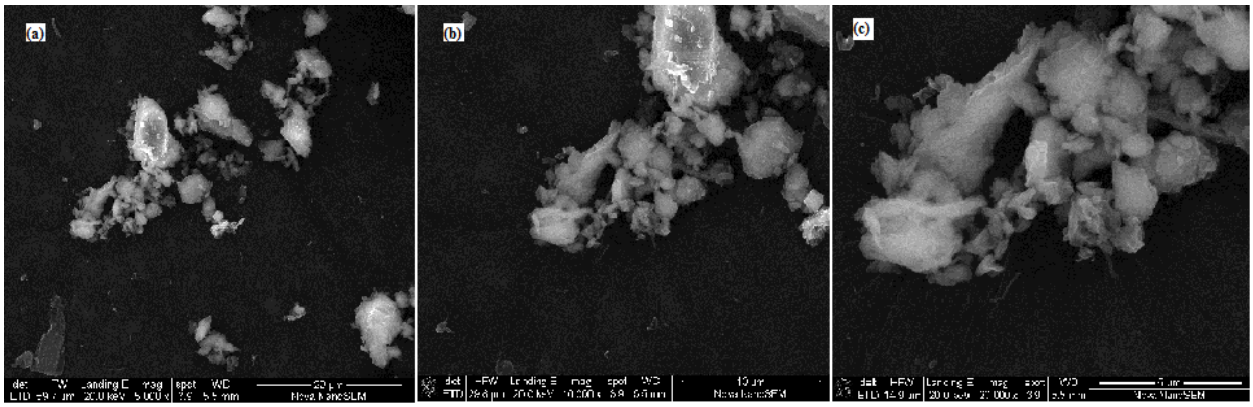

Figure 3.3: SEM images of mechanochemically activated aluminosilicate clay soil after milling for 15 minutes at magnification of 5 000x (a), SEM image at magnification of 10 000x (b), SEM image at magnification of 20 000x (c).

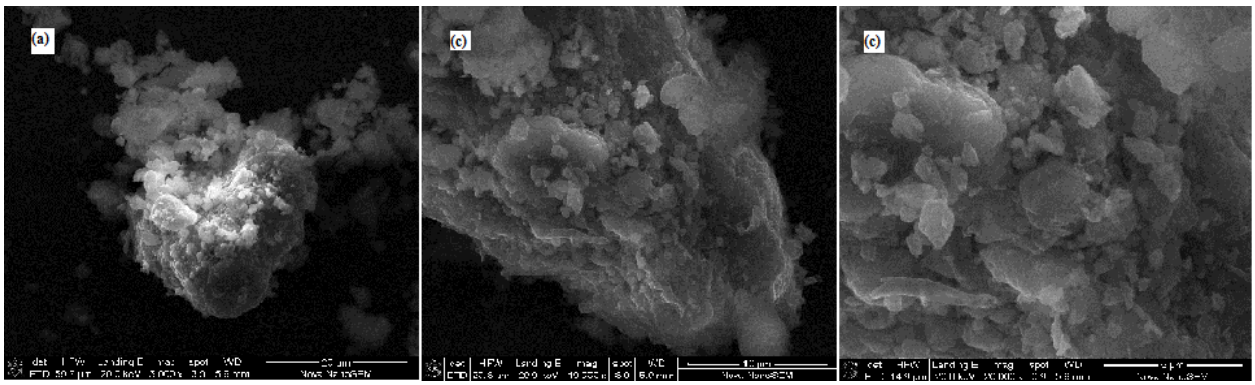

Figure 3.4: SEM images of mechanochemically activated aluminosilicate clay soil after milling for 20 minutes at magnification of 5 000x (a), SEM image at magnification of 10 000x (b), SEM image at magnification of 20 000x (c).

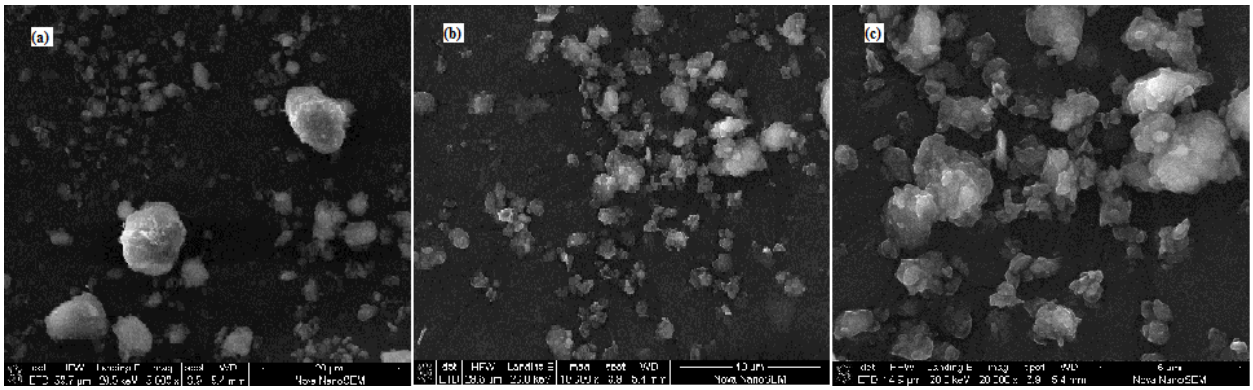

Figure 3.5: SEM images of mechanochemically activated aluminosilicate clay soil after milling for 30 minutes at magnification of 5 000x (a), SEM image at magnification of 10 000x (b), SEM image at magnification of 20 000x (c).

The image appears to be porous in nature and shows large agglomerates of very fine particles of clay soil. The pores and voids generated could be due to the swelling of clay soil

during washing. The importance of porosity in this study is for the percolation of water. The particle size of the SEM images differs from 5 minutes to 30 minutes milling time. At 5 minutes milling time, the particle size was bigger whereas at 30 minutes milling time the particle size was smaller. Small particle sizes promotes sintering when subjecting the clay soil to high temperatures for long periods of time with almost no destruction of the highly crystalline honeycomb structure. Neto & Moreno (2008) in their studies observed high aspect ratio particles leading to higher sphericity which is the same trend observed in this study. SEM is not a confirmatory test for particle size, hence the need for surface area and pore volume determination.

3.4.2 Surface area and pore volume of raw and mechanochemically activated aluminosilicate clay soil

The BET results are presented in Table 3.1. The raw clay as indicated in Table 3.1 has a relatively low surface area and pore volume. The surface area and pore volume of the mechanochemically activated clay samples increased with corresponding increase in the milling time. On the other hand, the pore size of the mechanochemically activated aluminosilicate clay soil decreased with increase in the milling time.

Table 3.1: Surface area, pore volume and size of raw and mechanochemically activated aluminosilicate clay soil

Milling time (min)	Surface area (m^2/g)	Pore volume (cm^3/g)	Pore size (nm)
Before treatment	43.4311	0.066401	6.11553
5	11.8551	0.026845	9.05772
10	25.1441	0.048960	7.99035
15	40.3591	0.100597	7.78870
30	50.5228	0.089755	7.67081

Previous studies have employed mechanochemical activation to enhance the surface area (Meenakshi *et al.*, 2007) together with the increase in surface energy and surface reactivity of the material and consequently in chemical activity (Thompson *et al.*, 1993) which in turn would definitely increase the sorption capacity of the absorbent.

3.4.3 Fourier Transform-Infrared Spectroscopic (FT-IR) Analysis of mechanochemically activated aluminosilicate clay soil

The FT-IR spectra of mechanochemically treated aluminosilicate clay soil was done to identify the possible changes in the functional groups associated with aluminosilicate clay due to activation at an different times (Figures 3.6). The stretching vibrations of Si-O-H bands were noticed at absorbance bands of 998 cm^{-1} for activation at 5 minutes; 910 cm^{-1}, for activation at 10 minutes while the same absorbance value of 996 $cm^{-1}$was noticed at activation time 15 and 30 minutes. However, changes in the Si-O-H stretching at different activation time may be due to changes in the release of functional groups necessary for interaction with fluoride. Similar trend of results were noticed for Si-O-Si stretching and bending vibrations. The peaks observed in the range of 1200-400 cm^{-1} were the characteristic vibrations of mixed metals. The highest peak was observed at 30 minutes milling time (Figure 3.6). It was observed that the increase in milling time also resulted in increased peak heights.

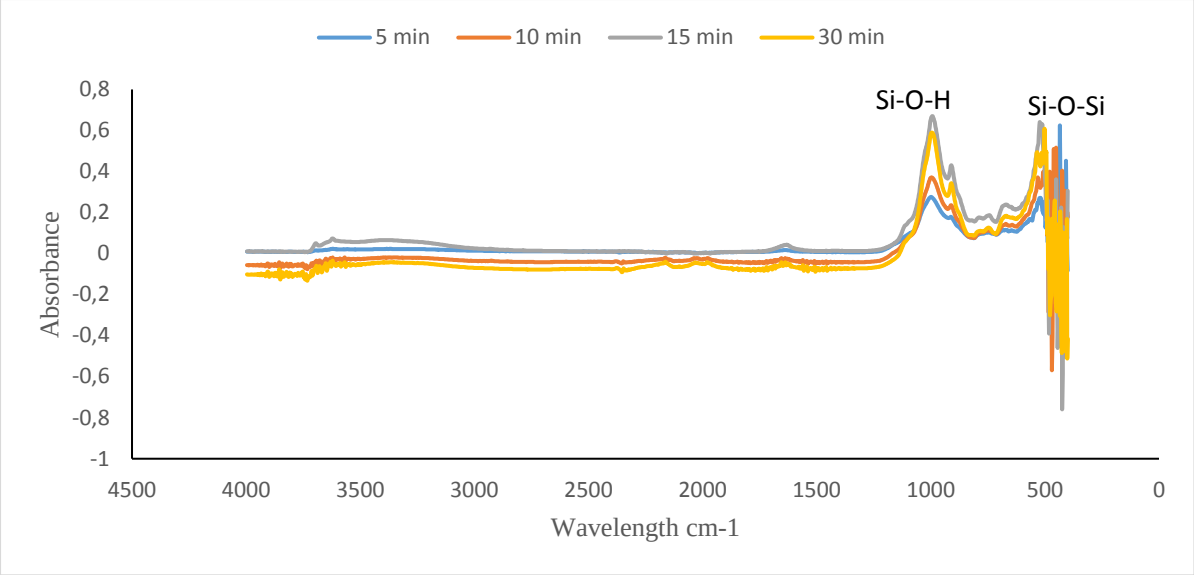

Figure 3.6: FT-IR spectra of 5, 10, 15 and 30 minutes mechanochemically activated aluminosilicate clay soil.

The experiments did not go beyond 30 minutes milling time. The optimum milling time of 30 minutes was also confirmed by BET results, which showed that the increase in milling time also increased the surface area of the adsorbent. The increase in adsorbent surface area supports adsorption since there will be more binding sites for fluoride. FT-IR images also confirm that 30 minutes milling time is the optimum mechanochemical activation.

3.4.4 X-ray diffraction analysis of mechanochemically activated aluminosilicate clay soil

The qualitative X-ray diffraction spectra are shown in Figure 3.7 and the quantitative X-ray diffraction results are indicated in Table 3.2. Figure 3.7 shows the major mineral components are quartz and plagioclase feldspar. Other minerals occurring in minor quantities are vermiculite, talc, muscovite and actinolite.

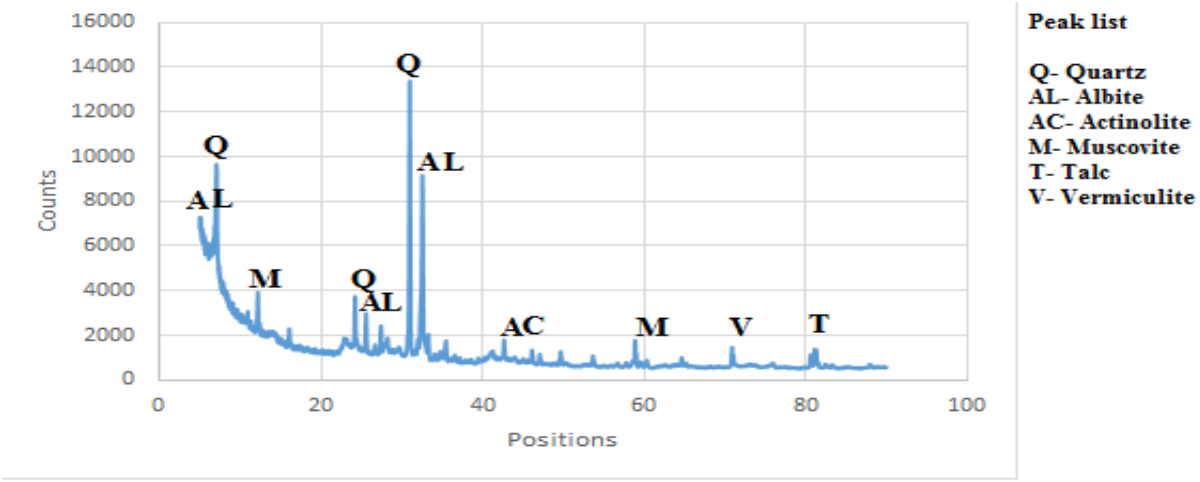

Figure 3.7: Diffraction traces with the identified phases

Table 3.2: The results of mineral phases found in mechanochemically activated aluminosilicate clay soil

Mineral phases	weight%	3 σ error
Actinolite	5.23	0.75
Muscovite	8.77	0.96
Plagioclase	29.12	1.44
Quartz	31.37	1.20
Talc	12.01	1.20
Vermiculite	13.50	1.47

Table 3.2 shows the abundance of the mineral phases in the clay soil. Quartz is the most abundant mineral phase with 31.37 weight %, followed by plagioclase (29.12 weight %); feldspar and actinolite had the lowest weight % of 5.23. The vermiculite is a net negative charge due to substitution for Si, Al and Mg in the phyllosilicate structure of the clay. Vermiculite clay is formed from the alteration/weathering of biotite which suggests that the provenance of the clay is granitic in composition.

3.4.5 X-ray fluorescence analysis of mechanochemically activated aluminosilicate clay soil

The results of XRF analysis of major oxides for 30 minutes mechanochemically activated aluminosilicate clay soil (Table 3.3) showed that silica (SiO_2) has the highest composition followed by alumina (Al_2O_3). The ratio of silicate to alumina was calculated to be

3.87, confirming that the clay is aluminosilicate by composition. The minor components are MnO, Cr_2O_3 and P_2O_5.

Table 3.3: Physical and chemical parameters of mechanochemically activated aluminosilicate clay soil

Oxide	Composition (wt. %)
SiO_2	62.63
Al_2O_3	16.19
Fe_2O_3	6.75
Na_2O	2.78
K_2O	1.02
MgO	3.14
CaO	1.78
Cr_2O_3	0.09
TiO_2	0.66
MnO	0.04
P_2O_5	0.05
LOI[a]	4.73
SiO_2/Al_2O_3	3.87
K_2O/Na_2O	0.37
$Fe_2O_3 + MnO + TiO_2$	7.45

LOI[a] = Loss on ignition

The results of trace elemental analysis (Table 3.3) showed that chromium had the highest concentration directly followed by barium and strontium. The trace elements with the lowest concentration were thulium and lutetium with the concentration of 0.23 mg/kg. The analyses of trace elements assist with the confirmation of the adsorbent elemental composition.

Table 3.4: Concentration of trace metals in mechanochemically activated aluminosilicate clay soil

Trace element	Concentration (mg/kg)	Trace element	Concentration (mg/kg)
Sc	22.60	Pr	4.57
V	139.48	Nd	15.62
Cr	618.17	Sm	3.18
Co	28.17	Eu	1.08
Ni	310.63	Gd	2.73
Cu	42.98	Tb	0.47
Zn	64.75	Dy	2.30
Rb	57.34	Ho	0.51
Sr	336.85	Er	1.33
Y	13.23	Tm	0.23
Zr	135.64	Yb	1.24
Nb	6.57	Lu	0.23
Mo	0.81	Hf	3.89
Cs	3.75	Ta	0.40
Ba	448.67	Pb	16.76
La	19.47	Th	3.29
Ce	41.32	U	0.87

3.4.6 pH at point-of-zero charge

The pH at point-of-zero charge (pHpzc) of an adsorbent has a significant role in the process of adsorption. The pHpzc represents the pH at which the net surface charge on the adsorbent is zero (Valdivieso *et al.*, 2006). The Mukondeni red clay soil has high pHpzc characteristic of clay materials dominated by aluminosilicate materials (Gitari *et al.*, 2013). The mean pHpzc is 6.4 ± 0.3. The change in pH was determined and plotted against the initial pH of KCl solution. Figure 4.8 showed the patterns of the plots for the adsorbent in the solutions of KCl concentrations. The plots showed the point where the curve crosses the horizontal axis. Due to this the pHpzc is the abscissa for ΔpH equals zero (Izuagie *et al*., 2015).

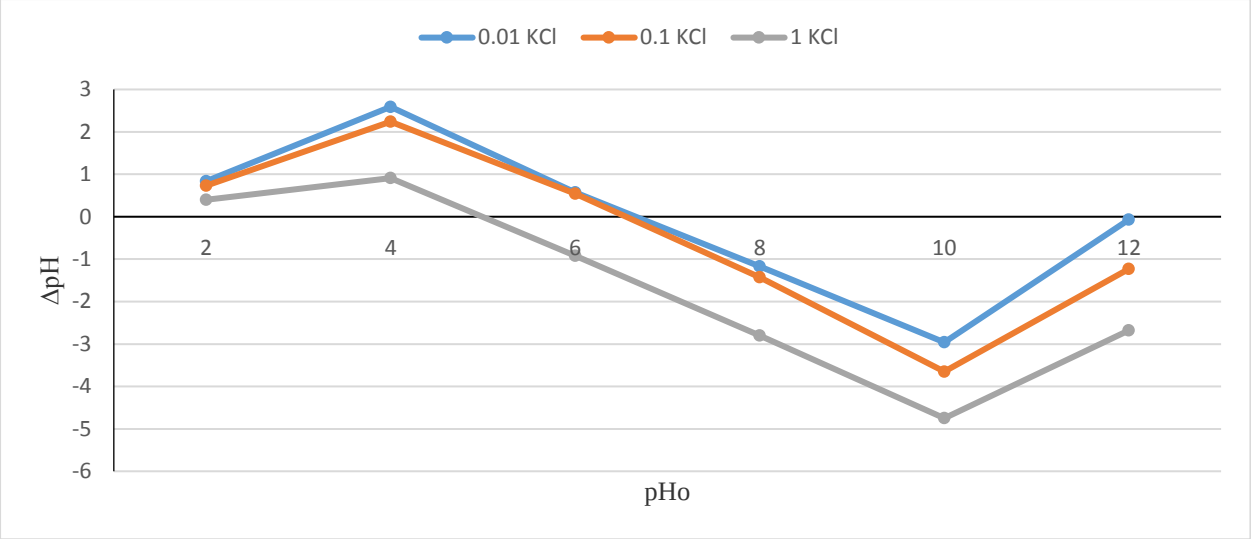

Figure 3.8: Effect of pH at point-of-zero charge of mechanochemically activated clay soil for 0.01, 0.1 and 1 M KCl (volume of solution: 50 mL, adsorbent dosage: 0.6 g, contact time: 24 h and shaking speed: 200 rpm).

3.4.7 Cation Exchange Capacity

Cation Exchange Capacity is the total number of exchangeable cations that the soil is capable of holding at a given pH. The Cation Exchange Capacity for mechanochemically activated aluminosilicate clay soil was evaluated by measuring the concentrations of Ca^{2+}, K^{+}, Mg^{2+} and Na^{+} as exchangeable cations on the surface of 30 minutes mechanochemically activated aluminosilicate clay soil (Figure 3.9). The trend of exchangeable cations concentrations were observed in the following order Mg^{2+}> Ca^{2+}> K^{+} >Na^{+} (Figure 3.9). The results were in agreement with those reported by Mudzielwana (2016) who observed the same trend at a pH of 7. However, there is possibility of surface exchange of fluoride with these cations during defluoridation experiments.

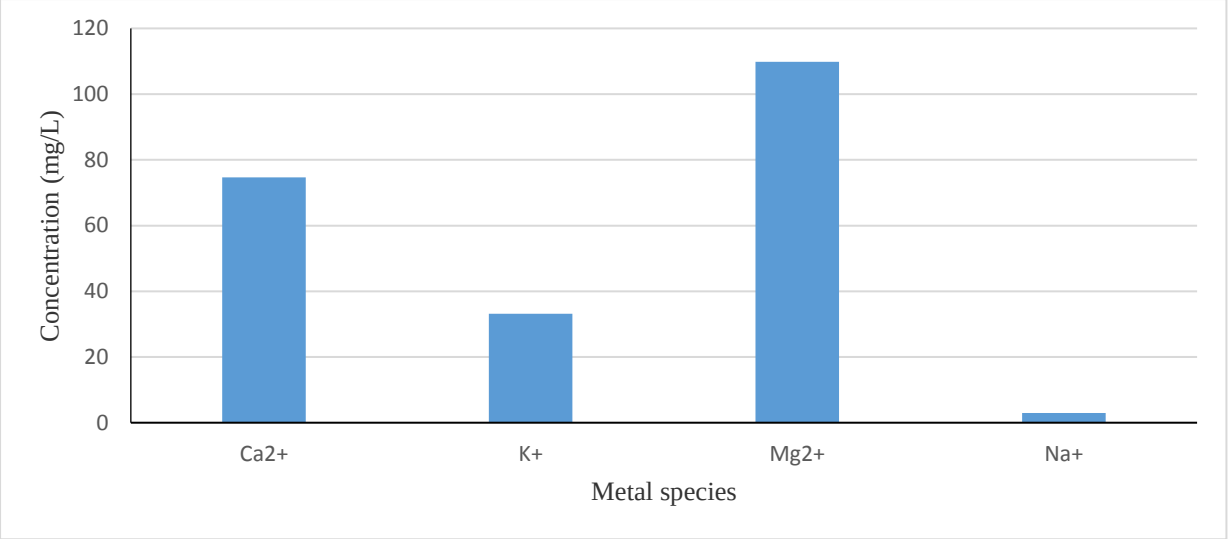

Figure 3.9: Cation exchange capacity of mechanochemically activated aluminosilicate clay soil (solution volume: 50 mL, adsorbent dosage: 0.6 g, contact time: 24 hours and shaking speed: 200 rpm).

3.5 Optimization of adsorption conditions

3.5.1 Effect of pH

The pH of aqueous solutions is a primary parameter that affects and controls the sorption capacity of a sorbent for ions isolating from the solution due to its influence on the surface properties of the sorbent and the ionic forms of the pollutants in the solutions. Figure 3.10 shows the effect of pH on percent fluoride removal and adsorption capacity. At lower pH, there was higher percent fluoride removal. This might be due to the increase in the electropositivity of the adsorbent surface which enhanced attraction for the negatively charged fluoride ions (Izuagie *et al*., 2016). Above pH_e 2.41, the percent fluoride removal decreases. The decrease of percent fluoride removal might be attributed to the formation of hydroxyl groups that compete with fluoride ions for uptake by clay soil materials and co-precipitate (Izuagie *et al*., 2016). The optimum pH for fluoride removal from solution was at the lowest pH_e of 2.41.

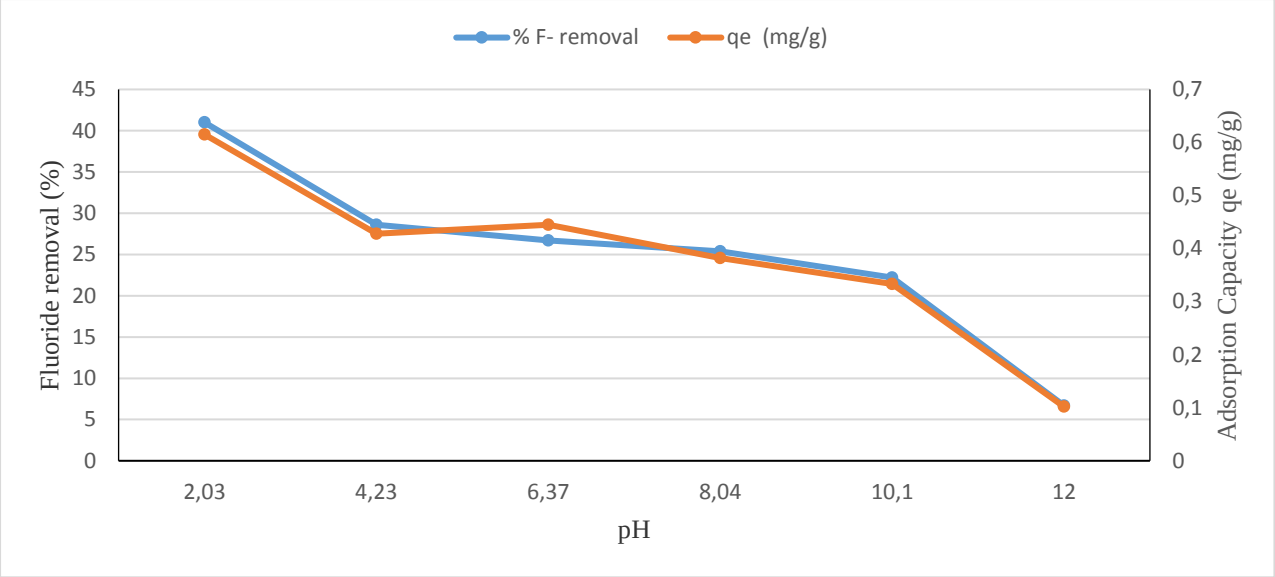

Figure 3.10: Variation of % fluoride removal and adsorption capacity with equilibrium pH (initial fluoride concentration: 9 mg/L, volume of solution: 100 mL, temperature: 297 K, shaking speed: 200 rpm, dosage: 0.6 g).

3.5.2 Effect of contact time

The effect of contact time on the percent fluoride removal and adsorption capacity of adsorbent were studied. It was observed that the adsorption capacity decreased with the increase in contact time. The adsorption pattern (Figure 3.11) revealed that initially, during the first 30 minutes of the contact time the adsorption was much faster where maximum fluoride removal took place. The saturation observed after 30 minutes could be due to the unavailability of the active sites on the sorbent surface (Christina & Viswanathan, 2015). Thereafter the adsorption phase was slow until 90 minutes probably moving toward reaching the equilibrium. There were no subsequent experiments which were conducted beyond 90 minutes. The optimum contact time for fluoride removal from solution was 30 minutes.

a)

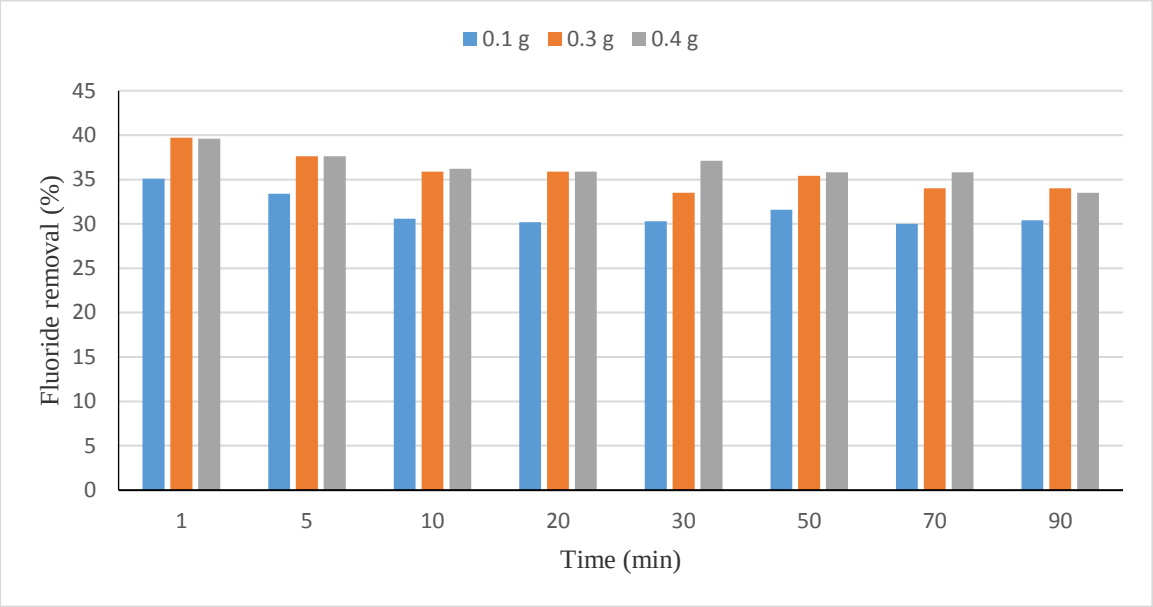

b)

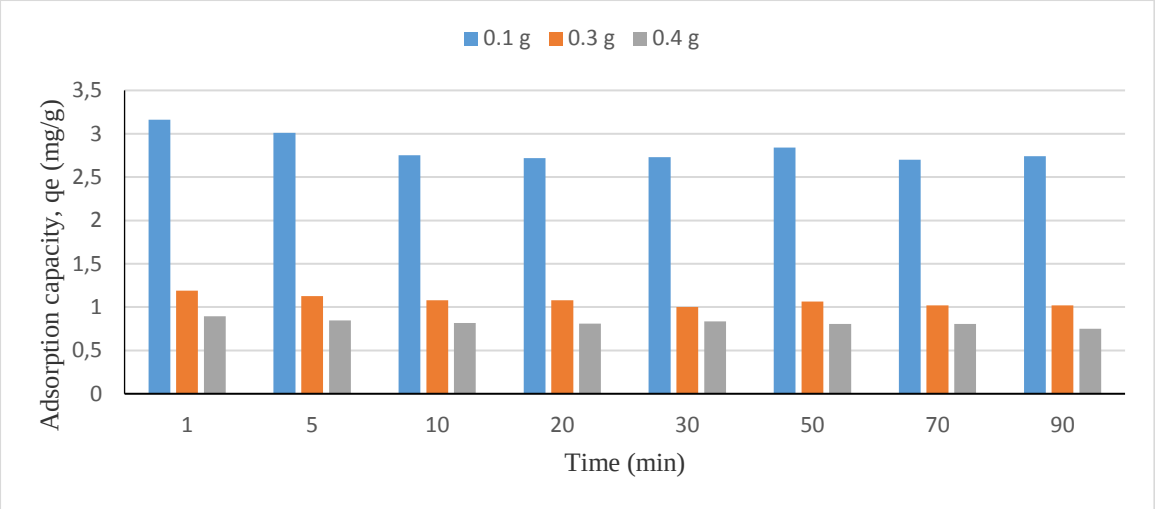

Figure 3.11: Variation of **(a)** % fluoride removal and **(b)** adsorption capacity with contact time at adsorbent doses of 0.1, 0.3 and 0.4 g (initial fluoride concentration: 9 mg/L, solution volume: 100 mL, and temperature: 296 K and shaking speed: 200 rpm).

3.5.3 Effect of adsorbent dosage

The effect of the adsorbent dosage on the percent fluoride removal and adsorption capacity were studied. The amount of adsorbent dosage significantly influenced the extent of fluoride adsorption. An increase in the mass of the adsorbent at constant fluoride concentration led to a decrease in adsorption capacity; this was due to abundance of adsorption surface without a corresponding in fluoride ion concentration. Percent fluoride removal increased with increase in adsorbent dosage owing to availability of more active adsorption sites on the adsorbent surface (Kamble *et al.*, 2010).

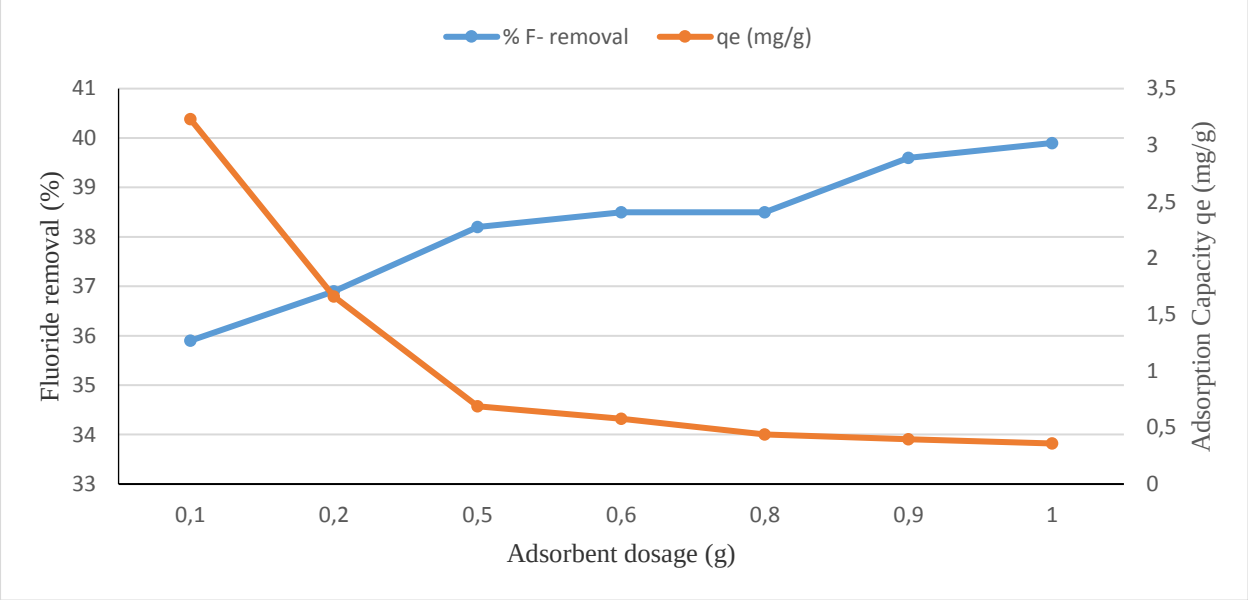

Figure 3.12: Variation of % fluoride removal and adsorption capacity with adsorbent dosage (initial fluoride concentration: 9 mg/L, solution volume: 100 mL, contact time: 30 min, shaking speed: 200 rpm and temperature: 298 K).

3.5.4 Effect of adsorbate concentration

Effect of adsorbate concentration on the percentage removal of fluoride was studied at various adsorbate concentrations with other parameters remaining constant. Figure 3.13 showed the effect of adsorbate concentration on percent fluoride removal and adsorption capacity. It was observed that when initial fluoride concentration increased, the fluoride adsorption capacity also increased. This might be due to the fact that at higher concentration gradient between the bulk of aqueous solution and the adsorbent material, the driving forces increased. The percent fluoride removal decreased with increase the in the initial fluoride

concentration removal. This might be due to limited space for adsorption on the adsorbent surface at higher concentration of fluoride.

a)

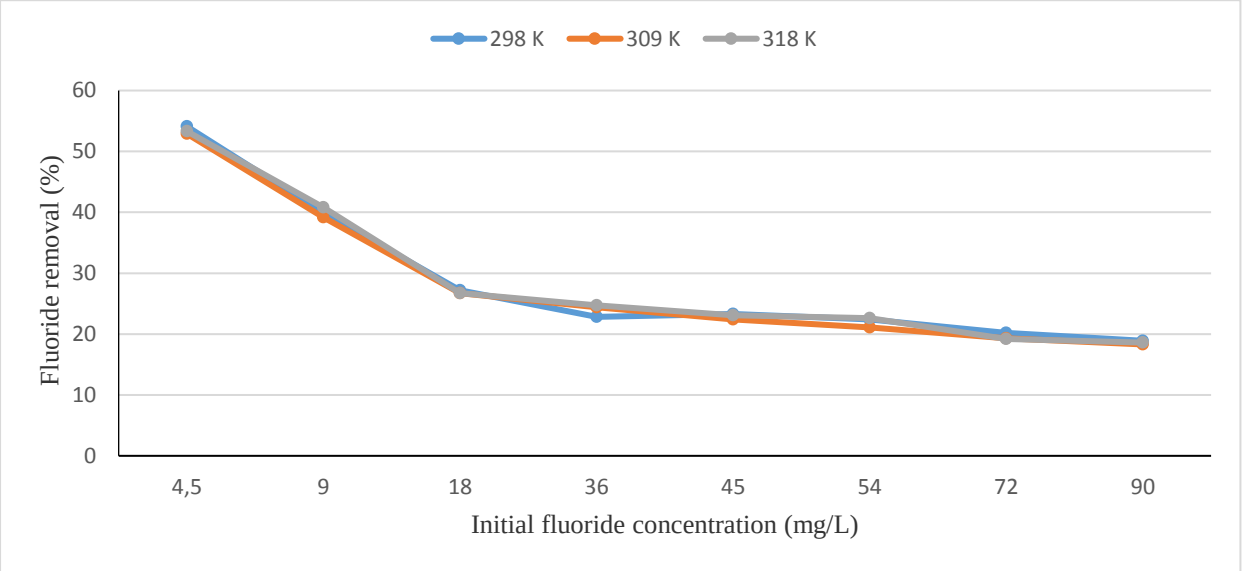

b)

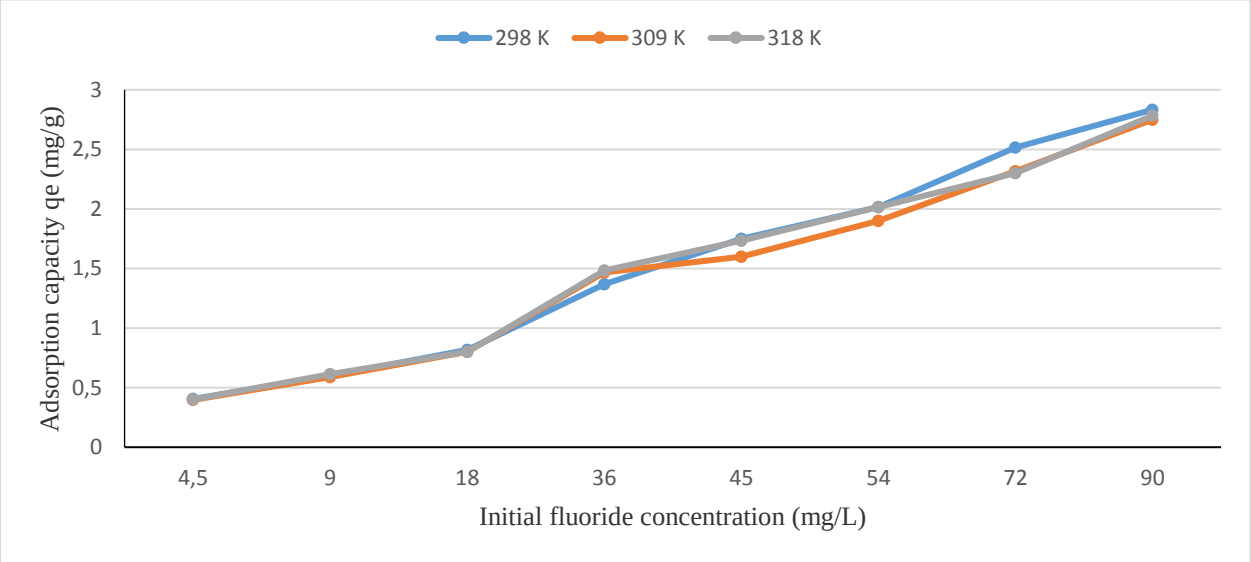

Figure 3.13: Variation of **(a)** % fluoride removal and **(b)** adsorption capacity with adsorbate concentration at 298, 309, and 318 K (contact time: 30 min, solution volume: 100 mL, shaking speed: 200 rpm and dosage: 0.6 g).

3.5.5 Effect of temperature

The effect of temperature on the percent fluoride removal and adsorption capacity of adsorbent were studied. Figure 3.14 showed the effect of temperature on percent fluoride removal and adsorption capacity. It was observed that there was no significant effect of temperature on the

amount of fluoride removed. Therefore the minimum temperature of 298 K may be suitable for adsorption process.

a)

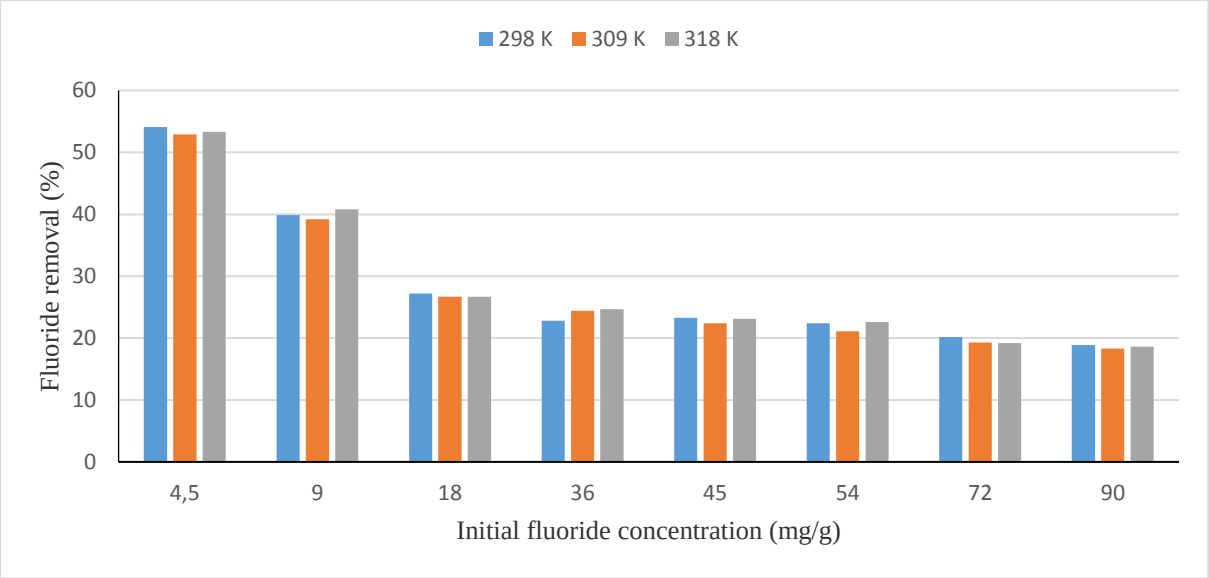

b)

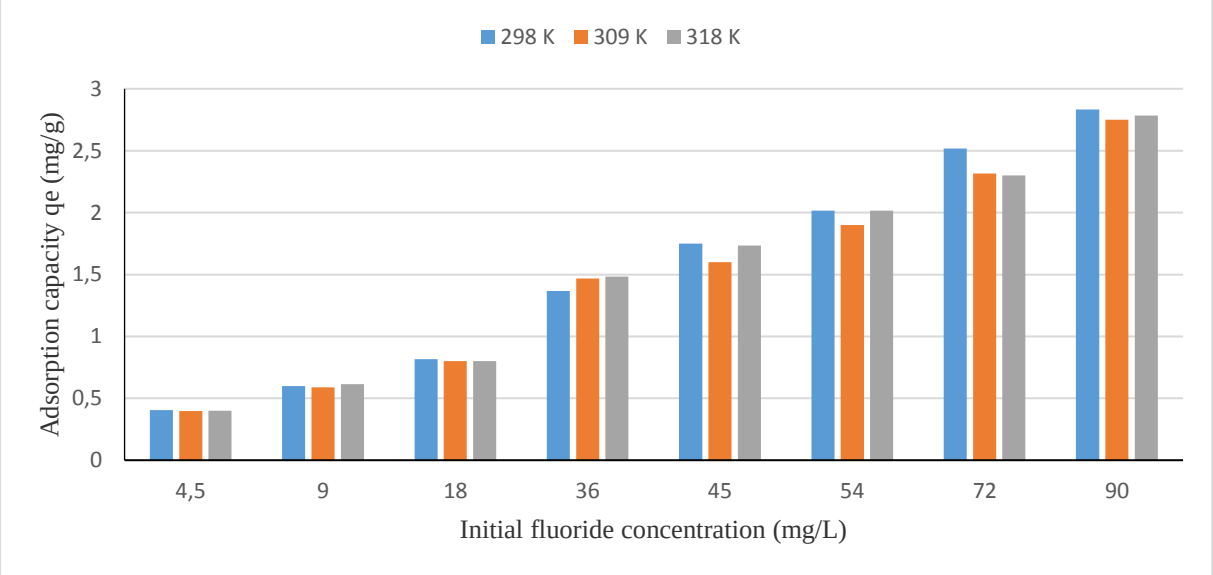

Figure 3.14: Variation of **(a)** % fluoride removal and **(b)** adsorption capacity with temperature at 298, 309, and 318 K (contact time: 30 min, solution volume: 100 mL, shaking speed: 200 rpm and dosage: 0.6 g).

3.6 Effect of medium pH with chemical stability of the adsorbent

The possibility of metal oxides to leach into water at various pH values was evaluated by analysing the supernatants obtained during batch experiment involving different initial pH

solutions while keeping other parameters constant. The analysis was done using Inductively Coupled Plasma-Mass Spectrometer (ICP-MS). The results are presented in Table 3.6 (refer to Appendix A). In Figure 3.15 it was observed that the concentration of Na was very high at all pH levels. This was due to the addition of NaOH during pH adjustment. High concentration of Si, Al and Fe was observed at higher pH levels.

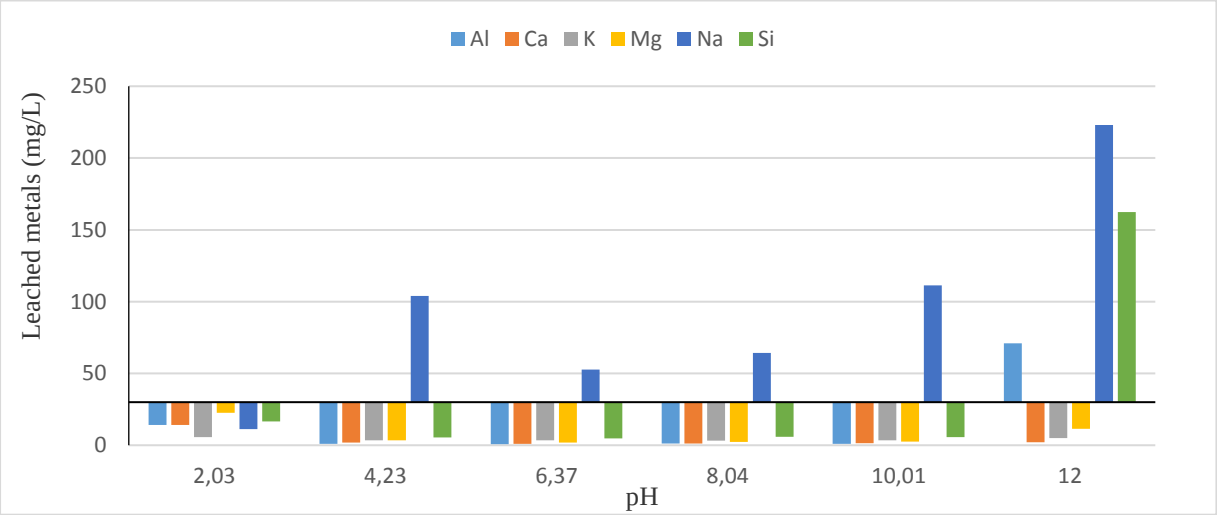

Figure 3.15: Leached metals as a function pH (initial fluoride concentration: 9 mg/L, solution volume: 100 mL, temperature: 298 K, shaking speed: 200 rpm).

3.7 Adsorption models

The equilibrium models are very important for understanding the adsorption systems. Adsorption models reflect the relationship between the amount of a solute adsorbed at constant temperature and its concentration in the equilibrium solution (Yousef *et al*., 2011).

There are several isotherm equations available for analysing experimental adsorption equilibrium data. In this study, two adsorption isotherms Langmuir and Freundlich were applied to the equilibrium data of adsorption of fluoride onto mechanochemically activated aluminosilicate clay soil.

3.7.1 Langmuir model

The Langmuir model assumes that adsorption is monolayer and is dependent on the assumption that the adsorbent surface consists of active sites having a uniform energy and therefore, the adsorption energy is constant (Weber & Chakkravorti, 1974). The Langmuir adsorption isotherm expression is shown in Equation 3.3 (Langmuir, 1918).

$$q_e = \frac{q_{max} K_L C_e}{1 + K_L C_e} \quad (3.3)$$

The linear form of Langmuir equation is represented by equation 3.4.

$$\frac{C_e}{q_e} = \frac{1}{q_m} C_e + \frac{1}{K_L q_m} \quad (3.4)$$

where q_e is amount of adsorbed fluoride at equilibrium (mg/g)

q_{max} is measurement of the adsorption capacity (mg/g) based on Langmuir isotherm

K_L is rate of adsorption Langmuir constant (mg/L)

C_e is equilibrium fluoride concentration (mg/L)

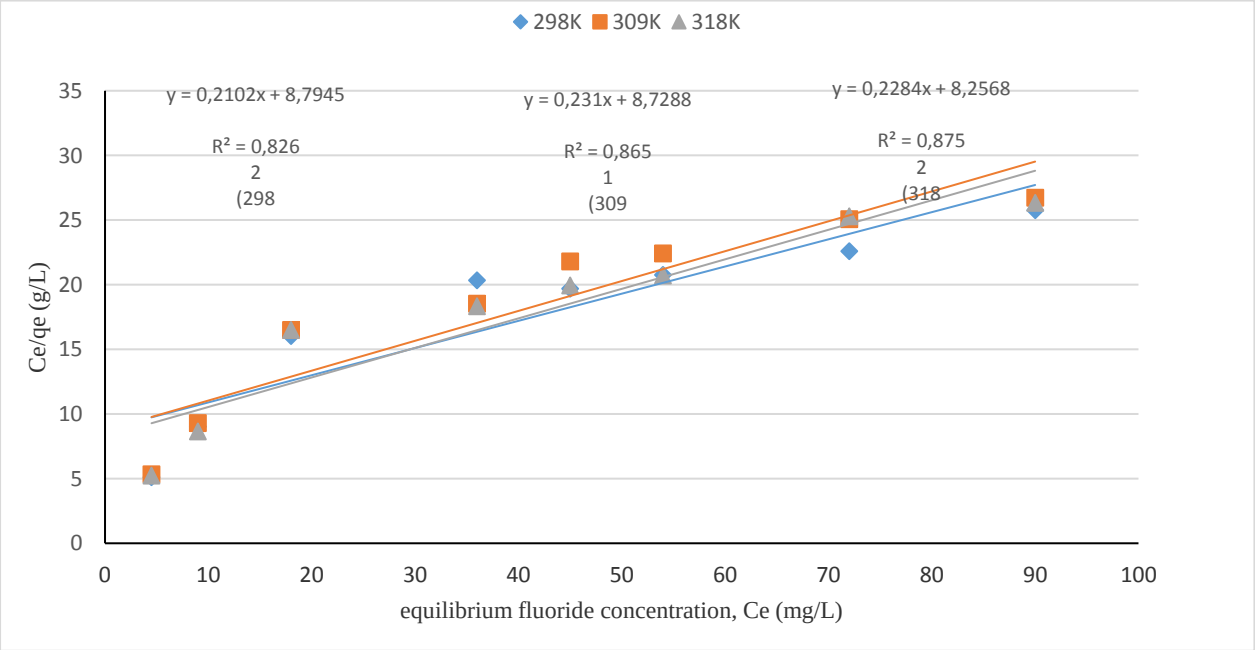

Figure 3.16: Langmuir model graph at temperatures of 298, 309 and 318 K (contact time: 30 min, solution volume: 100 mL, adsorbent dosage: 0.6 g and shaking speed: 200 rpm).

3.7.2 Freundlich model

The Freundlich model assumes that the adsorbent surface energy is heterogeneous. It is assumed that the stronger binding sites are occupied first and that the binding strength decreases with the increasing degree of site occupation (Yousef *et al*., 2011). The Freundlich adsorption model expression is shown in Equation 3.5 (Freundlich, 1906).

$$q_e = K_F \ C_e^{1/n} \quad (3.5)$$

The linear form is represented by Equation

$$\log q_e = \log K_F + \frac{1}{n} \log C_e \quad (3.6)$$

Where q_e is amount of adsorbed fluoride at equilibrium (mg/g)

K_F is adsorption capacity of the adsorbent (mg/g (L/mg)$^{1/n}$)

C_e is equilibrium fluoride concentration (mg/L)

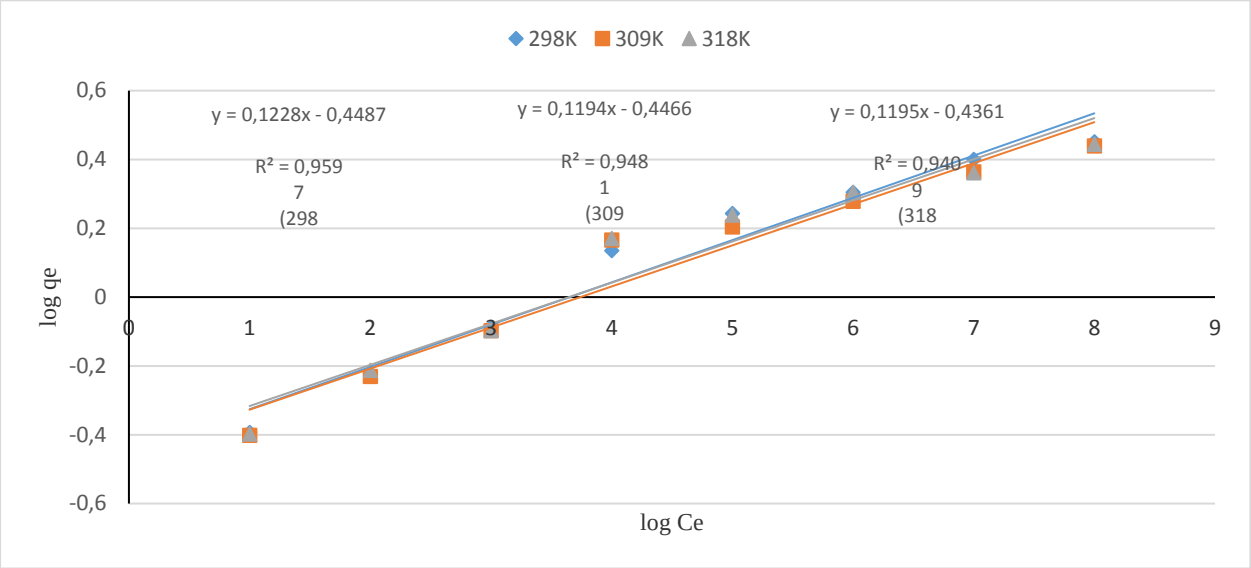

Figure 3.17: Freundlich model graph at temperatures of 298, 309 and 318 K (contact time: 30 min, volume: 100 mL, adsorbent dosage: 0.6 g and shaking speed: 200 rpm).

Table 3.15: Calculated Langmuir and Freundlich models parameters

Temperature (K)	Langmuir model constants			Freundlich model constants		
	q_m (mg/g)	K_L (L/mg)	R^2	1/n	K_F	R^2
298	4.7573	0.0239	0.826	0.123	2.810	0.960
309	4.3290	0.0265	0.856	0.119	2.796	0.948
318	4.3783	0.0277	0.875	0.120	2.730	0.941

The experimental data were found to fit well into Freundlich model. This was due to the R^2 which was closer to 1. Freundlich model is applicable on multi-site adsorption onto the rough or smooth surface of an adsorbent. Since the value of 1/n and K_L is less than 1, the adsorption was favourable to both Langmuir and Freundlich models. This showed that the adsorbent is partly homogeneous and heterogeneous.

3.8 Adsorption kinetics

The kinetics of adsorption describes the rate of adsorbate uptake on adsorbent and it controls the equilibrium time (Tan *et al.*, 2009). The kinetics of the adsorption data was analysed using two different kinetic models: the pseudo-first-order and pseudo-second-order models, which are extensively used in kinetics studies.

3.8.1 Pseudo-first-order model

The adsorption kinetics of fluoride onto mechanochemically activated clay aluminosilicate soil described by pseudo-first-order model is given in Equation 3.7 (Ho & McKay, 1998; Tutem *et al*., 1998).

The Lagergren pseudo-first-order model is given as:

$$\frac{dq_t}{dt} = k_1(q_e - q_t) \quad (3.7)$$

q_t(mg/g) is the fluoride concentration at any time *t*,

q_e(mg/g) is the maximum sorption capacity of the pseudo-first-order

k_1(min^{-1}) is the pseudo-first-order rate constant.

After integration, Equation (3.7) becomes:

$$\log(q_e - q_t) = -\frac{k_1}{2.303}t + \log q_e \quad (3.8)$$

The pseudo-first-order model was tested by fitting the adsorption data into it using the data presented in Table 3.9(refer to Appendix A).

Table 3.16: Parameters of pseudo-first-order of mechanochemically activated aluminosilicate clay soil

Adsorbent dosage (g)	Time (min)	log ($q_e - q_t$)	log ($q_e - q_t$)	log ($q_e - q_t$)	q_t (mg/g)	q_t (mg/g)	q_t (mg/L)
		0.1	0.3	0.4	0.1	0.3	0.4
	1	-	-	-	3.160	1.190	0.895
	5	-0.8239	-1.2007	-1.3010	3.010	1.127	0.845
	10	-0.3872	-0.9469	-1.0969	2.750	1.077	0.815
	20	-0.3565	-0.9469	-1.0604	2.720	1.077	0.808
	30	-0.4815	-0.9212	-1.2218	2.830	1.000	0.835
	50	-0.4949	-0.8962	-1.0458	2.840	1.063	0.805
	70	-0.3372	-0.7696	-1.0458	2.700	1.020	0.805
	90	-0.3768	-0.7696	-0.8386	2.740	1.020	0.750

The plot of $\log(q_e - q_t)$ values against *t* did not give straight lines. Hence, the model was not applicable to the sorption process as shown in Figure 3.18.

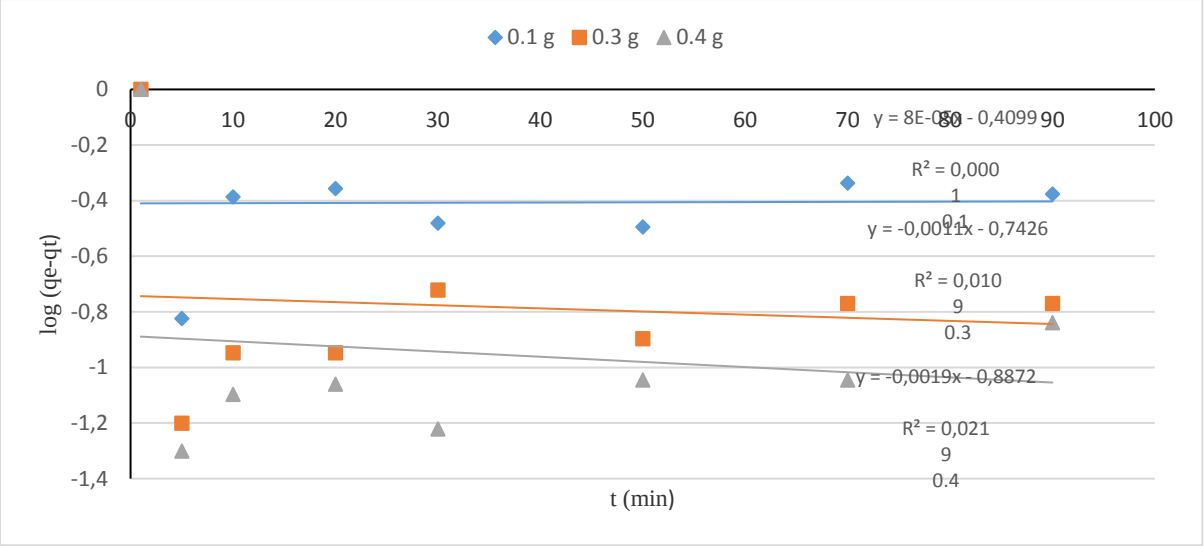

Figure 3.18: Pseudo-first-order profiles at different adsorbent dosages of **a.** 0.1 g, **b.** 0.3 g and **c.** 0.4 g of mechanochemically activated aluminosilicate clay soil (initial fluoride concentration: 9 mg/L, solution volume: 100 mL, temperature: 298 K and shaking speed: 200 rpm).

3.8.2 Pseudo-second-order kinetic model

The adsorption kinetics of fluoride onto described by pseudo-second-order kinetic model is given in Equation 3.9 (Yang & Al-Duri, 2005).

$$\frac{dq_t}{dt} = k_2(q_e - q_t)^2 \quad (3.9)$$

q_t(mg/g) is the fluoride concentration at any time *t*,

q_e (mg/g) is the maximum sorption capacity of the pseudo-second-order

k_2(g/(mg min)) is the rate constant for the pseudo-second-order process.

After integration, Equation (3.9) gives the linear form of the pseudo-second-order:

$$\frac{t}{q_t} = \frac{1}{k_2\, q_e^2} + \frac{t}{q_e} \quad (3.10)$$

which can simply written as:

$$\frac{t}{q_t} = \frac{1}{h} + \frac{t}{q_e} \quad (3.11)$$

h (mg/(g min)) is the initial sorption rate defined as:

$$h = k_2 q_e^2 \quad (3.12)$$

The $^{t}/_{q_t}$was plotted against time *t* for adsorbent dosages of 0.1, 0.3 and 0.4 g. This gave almost perfect straight lines as shown in Figure 3.19. The data fitted well to a pseudo-second-order. It can be concluded that the fluoride adsorption was by chemisorption.

Table 3.17: Parameters of pseudo-second-order kinetics

Adsorbent dosage (g)	Time (min)	C_t (mg/L) 0.1	C_t (mg/L) 0.3	C_t (mg/L) 0.4	q_t (mg/g) 0.1	q_t (mg/g) 0.3	q_t (mg/g) 0.4	t/q_t (g/L) 0.1	t/q_t (g/L) 0.3	t/q_t (g/L) 0.4
1		5.84	5.43	5.42	3.160	1.190	0.895	0.3164	0.8403	1.1193
5		5.99	5.62	5.62	3.010	1.127	0.845	1.6611	4.4366	5.9172
10		6.25	5.77	5.74	2.750	1.077	0.815	3.6364	9.2851	12.270
20		6.28	5.77	5.77	2.720	1.077	0.808	7.3529	18.570	24.752
30		5.37	6.00	5.66	2.830	1.000	0.835	10.601	30.000	35.928
50		6.16	5.81	5.78	2.840	1.063	0.805	17.606	47.067	62.112
70		6.30	5.94	5.78	2.700	1.020	0.805	25.926	68.627	86.957
90		6.26	5.94	6.00	2.740	1.020	0.750	32.847	88.235	120.00

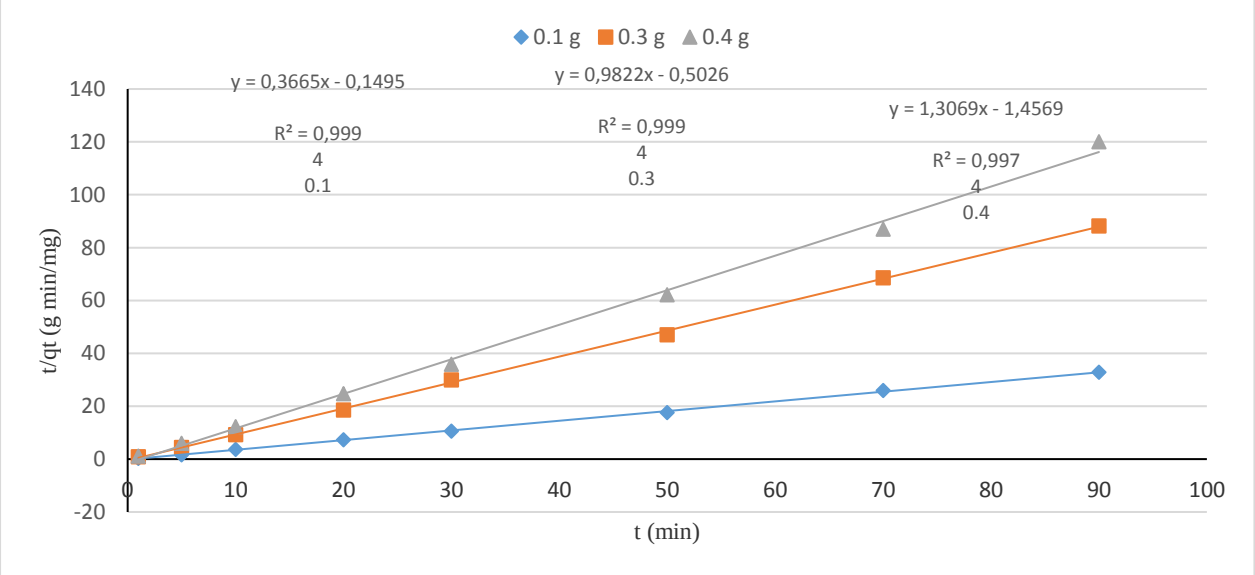

Figure 3.19: Pseudo-second-order profile at different adsorbent dosages (initial fluoride concentration: 9 mg/L, solution volume: 100 mL, temperature: 298 K and shaking speed: 200 rpm).

The calculated q_e and the experimental q_e were compared. The results indicate that the adsorption data fitted well on pseudo-second-order kinetic model.

Table 3.18: Pseudo-second-order parameters at different adsorbent dosages

Adsorbent dosage (g)	Equation	Experimental q_e (mg/g)	Calculated q_e (mg/g)	k_2 (L mg^{-1} min^{-1})
0.1	y = 0.3665x - 0.1495	2.729	3.160	0.8985
0.3	y = 0.9822x - 0.5026	1.018	1.190	1.9195
0.4	y = 1.3069x -1.4569	0.765	0.895	1.1723

3.9 Adsorption mechanism onto mechanochemically activated aluminosilicate clay soil

The mechanism of fluoride adsorption onto mechanochemically activated aluminosilicate clay was evaluated. The pHpzc values at 1 M, 0.1 M, and 0.01 M KCl were 6.00, 6.55, and 6.64 respectively. The mean pHpzc is 6.4 ± 0.3. The pHpzc determination showed that at pH 6.4 ±0.3 the surface has neutral charge, below 6.4 ±0.3 the surface is positively charged and above that it is negatively charged.

The mechanism involved in the fluoride adsorption process using aluminosilicate clay soil can be described by the following equations:

$$\equiv \mathrm{SiOH} + \ \mathrm{H^+} \ \rightarrow \ \equiv \mathrm{SiOH_2^+} \qquad (3.13)$$

$$\equiv \mathrm{SiOH_2^+} + \ \mathrm{F^-} \ \rightarrow \ \equiv \mathrm{SiOH_2F} \qquad (3.14)$$

The fluoride removal only occurred at low pH. That means fluoride removal was by attraction of fluoride ions to the positively charged surface of the clay as illustrated by equation (3.14).

3.10 Fluoride adsorption capacity of mechanochemically activated aluminosilicate clay soil compared to other adsorbents

Comparison of adsorption capacity of mechanochemically activated aluminosilicate clay soil with adsorption capacities of other developed adsorbents is presented in Table 3.19. It was observed that mechanochemically activated aluminosilicate clay soil had lower adsorption capacity as compared to montmorillonite, bentonite and mechanochemically activated kaolinites. It was also observed that mechanochemically activated aluminosilicate clay soil had slightly high adsorption capacity as compared to red mud.

Table 3.19: Comparison of different adsorption capacities of different adsorbents for fluoride

Adsorbent	Adsorption capacity (mg/g)	Experimental conditions	Reference
Red mud	0.60	pH 3-4; 20 mg/L F^-	Lv *et al.*, (2012)
Montmorillonite	3.37	pH 6.2; 120 mg/L F^-	Tor (2006)
Bentonite	2.31	pH 5; 10 mg/L F^-	Yi *et al.*, (2014)
Mechanochemically activated kaolinites	0.78	pH 3-11; 3 mg/L F^-	Meenakshi et al.,(2008)
Mechanochemically activated aluminosilicate clay soil	0.62	pH 2;10 mg/L F^-	Present study

3.11 Conclusions

The SEM images revealed the effect of milling on the shape. The images also demonstrated that milling tend to breakdown elongated, high aspect ratio particles. The morphological analysis reveals smaller particle size at 30 minutes milling time which promoted adsorption of fluoride.

The surface area and pore volume of the mechanochemically activated clay samples increased with corresponding increase in the milling time. Conversely, the pore size decrease with the increase in the milling time.

For FT-IR of mechanochemically activated aluminosilicate clay soil, the stretching vibrations of Si-O-H bands were noticed at absorbance 998 cm^{-1} for activation at 5 minutes; 910 cm^{-1}, for activation at 10 minutes while the same absorbance value of 996 $cm^{-1}$was noticed at activation time of 15 and 30 minutes. However, changes in the Si-O-H stretching at different activation time may be due to changes in the release of functional groups necessary for interaction with fluoride.

The XRD major mineral components are quartz and plagioclase feldspar. Other minerals occurred in minor quantities are vermiculite, talc, muscovite and actinolite. Quartz is the most abundant mineral phase with 31.37 weight %, followed by plagioclase (29.12 weight %); feldspar and actinolite had the lowest weight % of 5.23.

The XRF analysis of results showed that silica (SiO_2) has the highest concentration followed by alumina (Al_2O_3). The ratio of silicate to alumina was calculated to be 3.87, confirming that the clay is aluminosilicate by composition. The minor components are MnO, Cr_2O_3 and P_2O_5.

The mean pHpzc is 6.4 ± 0.3. The plots showed the point where the curve crosses the horizontal axis due to this the pHpzc is the abscissa for ΔpH equals zero. The trend of CEC concentrations were observed in the following order Mg^{2+}> Ca^{2+}> K^+ >Na^+.

The mechanochemical activation had tremendous impact on the efficiency of adsorption. The study reveals that the fluoride absorption capacity depends on the contact time, absorbent dosage, concentration of fluoride, the pH and temperature. Maximum fluoride uptake was achieved within 30 minutes of agitation for S/L of 0.6 g/100 mL at 200 rpm. At constant agitation time within 30 minutes, the pH was observed to decrease with adsorbent dosage. Maximum adsorption capacity was achieved at 0.6 g absorbent dosage thereafter there was no significant removal. The percentage of fluoride removal decreased with an increase in initial F^- concentration. Adsorption capacity of the synthesized material increased with the corresponding decrease in pH. The maximum % fluoride removal (i.e. 41.0 %) was obtained at the pH_e of 2.41.

The adsorption data fitted well into the Freundlich model when compared to Langmuir model. Pseudo-first-order and pseudo-second-order models when tested Pseudo-second-order model was determined to be the appropriate kinetic model for the fluoride sorption. The mechanism involved in the fluoride adsorption process using aluminosilicate clay soil was also evaluated. Considering the fact that optimum adsorption was achieved at pH value of 2.41 as reported, there is a need to further the studies on the modifications of the material for effectiveness of adsorption in a wide pH range.

References

Christina, E. & Viswanathan, P. 2015. Development of a novel nano-biosorbent for the removal of fluoride from water, *Chin. J. Chem. Eng*, 23, pp. 924-933

Coetzee, P.P., Coetzee, L.L., Puka, R., & Mubenga1, S., 2003. Characterisation of selected South African clays for defluoridation of natural waters. *Water SA*, 29, pp. 331-338.

DEPARTMENT OF HEALTH .2000. Regulation No. 873 Regulations under the Health Act, 1977 (Act No. 63 of 1977) Regulations on Fluoridating Water Supplies. Government Gazette No. 21533 (Vol. 423) 8 Sep (Regulation Gazette No. 6874). Pretoria, South Africa.

Department of Water Affairs and Forestry (DWAF), South African Water Quality Guidelines for Domestic Use, 1st ed., Department of Water Affairs and Forestry, Pretoria, 1996. Available from: www.dwaf.gov.za

Gitari W. M., Ngulube T, Masindi V., & Gumbo J. R., 2013. Defluoridation of groundwater using Fe^{3+} -modified bentonite clay: Optimization of adsorption condition. *Desalination & water treatment*, pp 1-13.

Izuagie, A.A., Gitari, W.M. & Gumbo, J.R. (2016). Synthesis and performance evaluation of Al/Fe oxide coated diatomaceous earth in groundwater defluoridation: towards fluorosis mitigation. *J. Environ. Sci. Health, Part A: Toxic/Hazard. Subs. Environ. Eng.*, pp. 1-15. DOI: 10.1080/10934529.2016.1181445.

Freundlich, H.M.F., 1906. Over the adsorption in solution, *Journal of Physical Chemistry*, 57, pp. 385-470.

Ho, Y.S. & McKay, G., 1998. Sorption of dye from aqueous solution by peat. *Chemical Engineering Journal*, 70, pp. 115-124.

Juhász, A. Z. & Opoczky, L. 1990. Mechanical Activation of Minerals by Grinding. Pulverizing and Morphology of Particles: *Academic Press*, Budapest.

Kamble, S.P, Dixit P., Rayalu, S.S. & Labhsetwar, N.K., 2009. Defluoridation of drinking water using chemically modified bentonite clay. *Desalination*, 249, pp. 687-693.

Langmuir, I., 1918. The adsorption of gases on plane surfaces of glass, mica and platinum, Journal of *American Chemical Society*, 40, pp. 1361-1368.

Loganathan, P., Vigneswaran, S., Kandasamy, J., & Naidu, R., 2013. Review: Defluoridation of drinking water using adsorption processes. *Journal of Hazardous Materials*, 248 (249), pp.1–19.

Lv, G., Wu, L., Liao, L., Zhang, Y. & Zhaohui, Y., 2012. Preparation and characterization of red mud sintered porous materials for water defluoridation. *Journal of Applied Clay Science*, pp.1 -7

Meenakshi, S., Sairam Sundaram, C. & Sukumar, R. 2008. Enhanced fluoride sorption by mechanochemically activated kaolinites. *J. Hazardous Materials*. 153, pp. 164-172

Mudzielwana, R. 2016. Synthesis, characterization and performance evaluation of groundwater defluoridation capacity of smectite rich clay soils and Mn-modified bentonite clay composites School of Environmental Sciences, *MSc Thesis*, University of Venda.

Neto, J.B. & Moreno, R. 2008. Effect of mechanical activation on the rheology and casting performance of kaolin/talc/alumina suspensions for manufacturing dense cordierite bodies, *Applied Clay Science*, 38, pp. 209-218.

Noh, J. & Coetzee, P. 2006. An inter-laboratory comparative study of fluoride determination in water. *Department of Chemistry*, University of Johannesburg.

Thompson, J.G., Gabbitas, N. & Uwins, P.J.R. 1993. The intercalation of alkalihalides in the solid state: a systematic studies of the intercalates and their derivates, *Clays Clay Mine*r, 6, pp. 279-291

Tor, A. 2009. Removal of fluoride from aqueous solution by using montmorillonite. *Desalination*, 201, pp. 267-276.

Tutem, E., Apak, R. & Unal, C.F., 1998. Adsorption removal of chlorophenols from water by bituminous shale, *Water Resources*, 32, pp. 2315-2324.

Valdivieso, A.L., Bahena, J.L.R., Song, S. & Urbina, R.H. 2006. Temperature effect on the zeta potential and fluoride adsorption at the a-Al_2O_3 /aqueous solution interface, *J. Colloid Interface Sci*, 298, 1-5.

Wieczorek-Ciurowa, K. & Gamrat, K. 2007. Some aspects of mechanochemical reactions. *Material Science*, 25, pp. 1.

Weber, T.W. & Chakkravorti, R.K., 1974. Pore and solid diffusion models for fixed-bed adsorbers. *AlChE Journal*, 20, p. 228.

World Health Organization, 2011. *Guideline for drinking water, world health organization*. Geneva.

Yang, X. & Al-Duri, B., 2005. Kinetic modeling of liquid-phase adsorption of reactive dyes on activated carbon. *Journal of Colloid and Interface Science*, 287, pp. 25-34.

Yi, Z., Ying, X., Hao, C., Bingjie, L., Xiang, G., Dongfeng, W. & Peng L. 2014. La(III)-loaded bentonite/chitosan beads for defluoridation from aqueous solution. *Journal of rare earths, vol. 32(5)*, pp. 458-466.

Yousef, R.I., El-Eswed, B. & Al-Muhtaseb, A., 2011. Adsorption characteristics of natural zeolites as solid adsorbents for phenol removal from aqueous solutions: kinetics, mechanism, and thermodynamics studies. *Chemical Engineering Journal*, 171, pp. 1143-1149.

CHAPTER 4: Synthesis of Al-oxide modified mechanochemically activated aluminosilicate clay soil and its application for defluoridation of groundwater

ABSTRACT

Portable drinking water is scarce in rural areas of South Africa, therefore people are forced to drink groundwater. Excess of fluoride (>1.5 mg/L) in drinking water is harmful to human health. The objectives of the present study are: (1) synthesis of Al oxide-modified mechanochemically activated aluminosilicate clay soil, (2) physicochemical characterization of Al-oxide modified mechanochemically activated aluminosilicate clay, (3) to evaluate the effect of various operating parameters (contact time, adsorbent dosage, adsorbate concentration and pH), (4) to model the adsorption data and (5) to evaluate the efficiency of Al-oxide modified mechanochemically activated aluminosilicate clay soil on fluoride removal from field water. Optimization of Al^{3+} concentration for modification was carried out by modifying the mechanochemical activated aluminosilicate clay soil with different concentrations of Al^{3+} from which the optimum modification was achieved with 1.5 M. Characterisation studies on the Al-oxide modified mechanochemically activated aluminosilicate clay soil by SEM, BET, FT-IR, XRD and XRF, analyses were carried out to determine the resultant changes in physicochemical properties of the adsorbent owing to modification. The SEM image of Al-oxide modified mechanochemically activated clay soil showed many small pores and honey-comb structure on the surface of different images. The BET surface area and the BDH adsorption cumulative area of the Al-oxide modified mechanochemically activated aluminosilicate clay soil were more than double those for the raw clay soil. There was also an increase in pore volume of the Al-oxide modified mechanochemically activated aluminosilicate clay soil. The FT-IR spectra showed that there was increase in the absorbance by the Si-OH, H-O-H, Al-O-H and Si-O-Al. The equilibrium pH of solution was higher than the point-of-zero charge (pHpzc) implying that fluoride removal occurred at solution pH > pHpzc where the net surface charge of the mechanochemically activated clay aluminosilicate soil was negative.The efficiency of 1.5 M Al-oxide modified aluminosilicate clay soil to remove fluoride from water was studied and found to be 96.5 % at pH_e 6.86, contact time of 30 minutes and dosage of 0.3 g/100 mL for 10 mg/L fluoride solution at 200 rpm shaking speed. The result shows that Al-oxide modified mechanochemically activated aluminosilicate clay soil is effective for defluoridation. The adsorption data fitted to both Langmuir and Freundlich isotherms. The adsorption data fitted only the pseudo-second-order kinetic,

showing chemisorption. Al-oxide modified mechanochemically activated aluminosilicate clay soil was tested for fluoride removal on field water and the percentage fluoride removal was 96.5 % at the dosage of 0.6 g/100 mL with the pH_e of 6.48.

Keywords: Clay soil; groundwater; defluoridation; adsorption capacity; optimization; characterization.

4.1 Introduction

Fluoride in drinking water may have beneficial or harmful effects on human health depending on its concentration and duration of ingestion. The optimum fluoride in drinking according to WHO (2011) is 1.5 mg/L, concentration above that requires defluoridation. The previous chapter discussed the application of mechanochemically activated aluminosilicate clay soils. The adsorbent showed low fluoride removal capacity obtained at low pH, this limit its application for defluoridation of groundwater for drinking purpose. There is therefore need to develop high adsorption capacity fluoride adsorbent based on locally available clay materials and that can operate at a wide range of pH. In this study, the effectiveness of Al oxide-modified mechanochemically activated aluminosilicate clay soil for fluoride removal was examined. The modification of the mechanochemically activated aluminosilicate clay soil by Al-oxide is expected to enhance the fluoride removal in water.

4.2. Materials and method

4.2.1 Characterization of Al-oxide modified mechanochemically activated aluminosilicate clay soil

4.2.1.1 Morphology of Al-oxide modified mechanochemically activated aluminosilicate clay soil

The morphology of the Al-oxide modified mechanochemically activated aluminosilicate clay soil sample was determined using Hitachi X-650 scanning electron micro analyser equipped with CDU lead detector at 25 kV. The samples were sprinkled onto aluminum scanning electron microscope (SEM) stubs covered in carbon glue. The excess sample was blown-off with compressed air and the stubs evaporation coated with carbon. The stubs were then examined with a FEI Nova NanoSEM 230 using the high resolution in-lens secondary detector. Element analysis was carried out using and Oxford X-Max detector and INCA software.

4.2.1.2 Surface area and pore volume of Al-oxide modified mechanochemically activated aluminosilicate clay soil

The Surface area was carried out by BET analysis and micropore volume were determined using the nitrogen adsorption/desorption isotherms collected at liquid nitrogen temperature (77K). Micromeritics TriStar II surface area and porosity analyser (USA) were used. Prior to analysis, the samples were degassed at desired temperature for particular time under a vacuum of more than 2 μm Hg. Nitrogen gas flow was used in the experiment to ensure no moisture in the sample. The desorption branch of the isotherm was used to determine the Barret-Joyner-Halenda (BJH) pore size distributions of the material. This procedure was done for 5, 10, 15 and 30 minutes mechanochemically activated aluminosilicate-rich clay soil.

4.2.1.3 Fourier Transform Infra-Red (FT-IR) spectroscopic determination

The functional groups of the Al-oxide modified mechanochemically activated aluminosilicate clay soil was analysed using Bruker Tensor 27 FT-IR & OPUS Data Collection Program. Prior to any solid sample deposition, the surface of the diamond ATR waveguide was cleaned by soaking with acetone and wiped using lens-cleaning tissues. Before recording background spectra, acetone was allowed to evaporate for at least 15 min. For each measurement, approximately 100 mg of solid dry sample was firmly pressed against the waveguide surface. Each sample spectrum was independently recorded three times to ensure reproducibility of the measurement procedure.

4.2.1.4 Analysis of mineralogy using XRD technique

The mineralogical characteristics of the Al-oxide modified mechanochemically activated aluminosilicate clay soil were evaluated using XRD technique respectively. After representative sampling using a riffle splitter, the samples were milled in a tungsten carbide vessel and prepared according to the standardized Panalytical back loading system, which provided nearly random distribution of the particles. The sample was analysed using a PANalytical X'Pert Pro powder diffractometer in θ–θ configuration with an X'Celerator detector and variable divergence- and fixed receiving slits with Fe filtered Co-Kα radiation (λ=1.789Å). The phases were identified using X'Pert Highscore plus software. The relative

phase amounts (weight %) was estimated using the Rietveld method (Autoquan Program). Errors are on the 3 sigma level in the column to the right of the amount.

4.2.1.5 Analysis of chemical composition using XRF technique

The elemental composition of the Al oxide-modified clay soil in the form of their oxides of the 30 min mechanochemically activated aluminosilicate-rich clay soil was done using PANanalytical Axios instrument. The sample preparation involved milling of clay samples to less than 75 μ fraction. The milled sample was then roasted at 1000 °C for at least 3 hours to oxidize iron (Fe^{2+}) and Sulfur (S), and to determine the Loss on Ignition (L.O.I). The analysis of major oxides required that the glass disks are prepared through fusing 1 g roasted sample, 8 g (12-22) flux consisting of 35% alkali borate ($LiBO_2$) and 64.71% lithium tetra borate ($Li_2 B_4 O_7$) at 1050°C. The glass disks were then analysed by XRF instrument equipped with a 4 kW Rhodium (Rh) tube. Trace element analysis was achieved by mixing 12 g milled sample and 3 g Hoechst wax. The mixture was then pressed into a powder briquette by a hydraulic press with the applied pressure of 25 ton.

4.2.1.6 pH at point-of- zero charge

The pH at point-of-zero charge was determined using 0.01, 0.1 and 1 M KCl solutions. The procedure for evaluating the pHpzc of Al-oxide modified mechanochemically activated aluminosilicate clay soil was already discussed in subsection 3.2.3.9.

4.2.2 Synthesis of Al-oxide modified mechanochemically activated aluminosilicate clay soil at optimized conditions

4.2.2.1 Modification of mechanochemically activated aluminosilicate clay using Al oxide

Separate mass of 3 g of mechanochemically activated clay soils were weighed into 20 mL of 1.5 M, 1 M, 0.75 M, 0.5 M and 0.25 M Al^{3+} solutions. The mixtures were agitated at 100 rpm for 20 minutes. After which the pH of each mixture was adjusted to 8.2 by adding 2 M of NaOH by vigorous agitation. The mixtures were shaken for 30 min at 200 rpm and subsequently centrifuged for 5 minutes at 40 rpm. Each solid residue was washed with 100 mL of Milli-Q water and oven-dried at 105 ^{0}C for 12 hours. After cooling, the solid products were milled and passed through 250 μm diameter sieve. The samples were placed in sealed plastic bags for subsequent experiments.

4.2.2.2 Optimization of Al-oxide modified mechanochemically activated aluminosilicate clay soil

Mass of 0.3 g of 1.5 M, 1 M, 0.75 M, 0.5 M and 0.25 M Al-oxide modified mechanochemically activated aluminosilicate clay soil samples were weighed into 100 mL of 10 mg/L fluoride solution in four 250 mL plastic bottles. The initial pH of each mixture was measured and recorded. The mixtures were agitated at 200 rpm for 30 minutes and centrifuged for 5 minutes at 40 rpm. The supernatants were filtered and analysed for residual fluoride. The fluoride in supernatants was analysed using fluoride ion-selective electrode after calibration with four fluoride standards in which TISAB III was added at the volume ratio of 1:10.

4.2.2.3 Preparation of Al-oxide modified mechanochemically activated aluminosilicate clay at optimized conditions

A mass of 75 g of mechanochemically activated clay was weighed into 500 mL of 1.5 M Al^{3+} solution. The mixture was agitated at 100 rpm for 20 minutes, after which the pH of each mixture was adjusted to 8.2 by adding 2 M of NaOH with vigorous stirring. The mixture was agitated for 30 minutes at 200 rpm and centrifuged for 5 minutes at 40 rpm. Each solid residue was washed with 100 mL of Milli-Q water and dried at 105 ^{0}C for 12 hours. After cooling, the residues was milled and sieved through a 250 µm diameter sieve. The samples were stored in plastic bags for subsequent experiments.

4.2.3 Fluoride adsorption experiments

The following experimental parameters were evaluated and optimized:

4.2.3.1 Effect of contact time

Masses of 0.1, 0.3 and 0.4 g of Al-oxide modified mechanochemically activated aluminosilicate clay soil were weighed into 100 mL of 10 mg/L fluoride solution in twenty four 250 mL plastic bottles. The initial pH of each mixture was measured and recorded. The mixtures were shaken at 200 rpm for 1, 5, 10, 20, 30, 50, 70 and 90 minutes at 298 K, followed by the experimental procedures described in subsection 3.2.5.2.

4.2.3.2 Effect of adsorbent dosage

The effect of adsorbent dosage on fluoride removal was evaluated; masses of 0.1, 0.2, 0.5, 0.6, 0.8, 0.9 and 1 g of Al-oxide modified mechanochemically activated aluminosilicate clay soil were weighed into 100 mL of 10 mg/L fluoride solution in seven 250 mL plastic

bottles. The initial pH of each mixture was measured and recorded. The mixtures were shaken at 200 rpm for 30 minutes at 297 K, followed by the experimental procedures described in subsection 3.2.5.3.

The effect of adsorbate concentration was evaluated at temperatures of 298, 309 and 318 K; for each temperature, 0.6 g of the adsorbent was weighed into 100 mL of 5, 10, 20, 40, 50, 60, 80 and 100 mg/L fluoride solution in eight 250 mL plastic bottles. The initial pH of each mixture was measured and recorded. The mixtures were shaken at 200 rpm for 30 minutes, followed by the experimental procedures described in subsection 3.2.5.4.

4.2.3.3 Effect of pH

The effect of pH on fluoride onto Al-oxide modified mechanochemically activated aluminosilicate clay soil was evaluated. A mass of 0.6 g of adsorbent was dispersed into each 90 mL of 10 mg/L fluoride solution contained in seven 250 mL plastic bottles. The pH of the mixture was adjusted using 0.1 M HCl and 0.1 NaOH to the desired acidic and alkaline values. The initial fluoride concentration was 9 mg/L. The bottles were tightly closed and shaken at 200 rpm for 30 minutes, followed by the experimental procedures described in subsection 3.2.5.1.

4.2.3.4 Effect of temperature

The effect of temperature was evaluated at temperatures of 298, 309 and 318 K. For each temperature, 0.6 g of the adsorbent was weighed into each 100 mL of 5, 10, 20, 40, 50, 60, 80 and 100 mg/L fluoride solution in eight 250mL plastic bottles, followed by the experimental procedures described in subsection 3.2.5.5.

4.2.3.5 Effect of medium pH with chemical stability of the adsorbent

The effect of leached metals and pH on fluoride onto Al-oxide modified mechanochemically activated aluminosilicate clay soil was evaluated; a mass of 0.6 g of adsorbent was dispersed into 100 mL of 9 mg/L fluoride solution contained in six 250 mL plastic bottles. The pH of the mixture was adjusted using 0.1 M HCl and 0.1 NaOH to the desired acidic and alkaline values, followed by the experimental procedures described in subsection 3.2.5.6.

4.2.3.6 Effect of co-existing ions

The effect of co-existing ions was evaluated by measuring 1 mL of 1,000 mg/L fluoride and 50 mL of 10 mg/L of the ions such as NO^{-}_{3}, CO_3^{2-}, SO_4^{2}, PO_4^{3-} and Cl^{-} into 100 mL volumetric flask then Milli-Q water was added and made-up to the mark. The resultant solutions which contained 10 mg/L fluoride and 5 mg/L anion were transferred into a 250 mL plastic bottle. A mass of 0.6 g of adsorbent was weighed into the plastic bottles and shaken for 30 minutes at 200 rpm in a water bath shaker, followed by the experimental procedures described in subsection 3.2.5.1.

4.2.3.7 Regeneration and reusability of spent sorbent

The regeneration of the adsorbent was done using 0.1 M K_2SO_4 and 0.1 M Na_3PO_4 solutions. The first process was defluoridation of 100 mL of 10 mg/L fluoride solution using 1 g of Al-oxide modified mechanochemically activated aluminosilicate clay soil. The mixtures were centrifuged and analysis of supernatants for residual fluoride was done as described in subsection 3.2.5.1. The residue was then washed with Milli-Q water, dried in the oven at 110 ^{0}C for 8 h and then cooled in the desiccator. The dry solid was crushed and sieved with a 250 µm test sieve.

The dry, sieved adsorbent was weighed into 100 mL of 0.1 M K_2SO_4 and 0.1 M Na_3PO_4 solutions for 30 minutes to desorb fluoride. The centrifuging, washing of residue, desorbed fluoride measurement and drying of adsorbent were done as described in 3.2.5.1. A known mass of dry, crushed and sieved adsorbent was again weighed into 100 mL of 10 mg/L fluoride solution. Regenerated adsorbent was then re-used for defluoridation for up to five cycles.

4.2.3.8 Defluoridation of field water

The effectiveness of Al-oxide modified mechanochemically activated aluminosilicate clay soil in removal of fluoride from groundwater was evaluated using batch experiments. Dosage of 0.6 g of the sorbent was weighed into 100 mL of groundwater containing initial fluoride of 3.88 mg/L, The mixture was shaken for 30 minutes at a speed of 200 rpm. The initial and equilibrium pH values of mixture were 6.48 and 7.24 respectively. The mixtures were then centrifuged for 5 minutes at 40 rpm and the supernatants obtained were analysed for residual fluoride as described in 3.2.5.1. Complete chemical analysis of the groundwater was carried out before and after defluoridation were analysed Inductively using Coupled Plasma-Mass Spectrometer (ICP-MS) before and after groundwater defluoridation.

4.2.4 Determination of adsorption percentages and capacities

The percentage fluoride removal (adsorption) and desorption capacity were calculated using the following equations:

$$\% \text{ Adsorption} = \frac{C_o - C_e}{C_o} \times 100 \quad (4.1)$$

$$\text{Adsorption capacity } (q_e) = \frac{C_o - C_e}{m} \times V \quad (4.2)$$

Where C_o = initial fluoride concentration (mg/L)

C_e = equilibrium fluoride concentration (mg/L)

m = mass of adsorbent (g)

v = volume of the solution used in the batch (L)

q_e = the amount of adsorbed fluoride at equilibrium (mg/g)

4.3 Results and discussion

4.3.1 Characterization of Al-oxide modified mechanochemically activated aluminosilicate clay soil

4.3.1.1 Morphology of Al-oxide modified mechanochemically activated aluminosilicate clay soil

The SEM images of Al-oxide modified mechanochemically activated aluminosilicate clay soil presented in Figure 4.1.

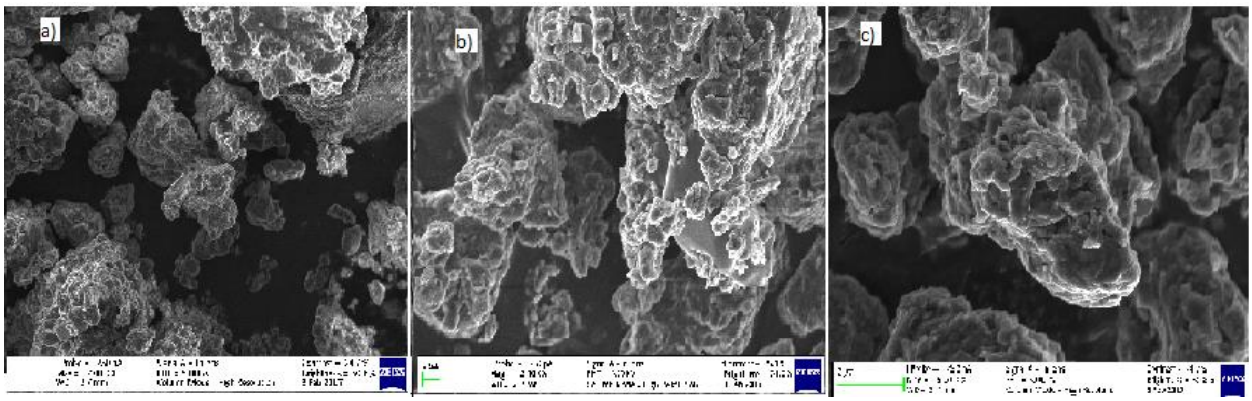

Figure 4.1: SEM image of Al oxide-modified mechanochemically activated aluminosilicate clay soil at magnification of 5000x (a), SEM image at magnification of 10000x (b), SEM image at magnification of20000x(c)

Figure 4.1 showed differences in the pores sizes and appearance of the Al-oxide modified mechanochemically activated aluminosilicate clay soil. The pores of Al-oxide

modified mechanochemically activated aluminosilicate clay soil are not perfectly ordered. The particles appear to be scattered as compared to the raw clay soil. As observed in the previous chapter, raw clay soil appears to be large agglomerates of very fine particles of clay soil. There were many small pores and honey-comb structure on the surface of different images. Therefore, there was a good possibility for fluoride to be adsorbed onto the Al-oxide modified mechanochemically activated aluminosilicate clay soil.

4.3.1.2 Surface area and pore volume of the Al-oxide modified mechanochemically activated aluminosilicate clay soil

The surface area and pore volume of Al-oxide modified mechanochemically activated aluminosilicate clay soil were determined by the Brunauer–Emmett–Teller (BET) method using Micromeritics TriStar II *Surface Area and porosity*. The results are presented in Table 4.1.

Table 4.1: Comparison of the surface area, and pore area and volume of the mechanochemically activated aluminosilicate clay soil and Al-oxide modified mechanochemically activated aluminosilicate clay soil

Form of clay soil	Single point surf. area (m^2/g)	BET surf. area (m^2/g)	BJH adsorption cum. surf. area of pores (m^2/g)	BJH desorption cum. surf. area of pores (m^2/g)	Single point adsorption total pore vol. (cm^3/g)	BJH adsorption cum. vol. of pores (cm^3/g)	BJH desorption cum. vol. of pores (cm^3/g)
Mechanochemically activated clay soil	44.6093	50.5228	38.519	41.1566	0.066401	0.065258	0.06937
Al oxide-modified clay soil	106.1988	108.2727	104.568	94.8389	0.205898	0.205788	0.206872

As shown in Table 4.1 BET surface area and the BDH adsorption cumulative area of the Al-oxide modified mechanochemically activated aluminosilicate clay soil are more than double those for the raw clay soil. This is shows that the mechanochemically activated aluminosilicate clay soil was indeed modified by Al oxide. Increase in surface area of adsorbent implies an increase in active adsorption sites. The results also shown the increase in pore volume of the Al-oxide modified mechanochemically activated aluminosilicate clay soil. The increase in pore surface area and volume is an indication that the percolation of water through the particles of adsorbent during defluoridation would be more readily achieved (Izuagie *et al.*, 2016). Al-oxide modified mechanochemical activated aluminosilicate clay soil showed potential for efficiency in fluoride removal.

4.3.1.3 Fourier Transform-Infra Red (FT-IR) Spectroscopy

FT-IR spectra analysis were carried out to understand the functional groups and surface chemistry of Al-oxide modified mechanochemically activated aluminosilicate clay soils. FT-IR was employed to better understand the adsorption mechanism of the adsorbent. As shown in Figure 4.2, there is increase in the absorbance of the Si-O-H, H-O-H, Al-O-H and Si-O-Al groups stretching vibration at 414 cm^{-1} for the Al-oxide modified mechanochemically activated aluminosilicate clay soil. The absorbance at 1000 cm^{-1} for Si-O-Si stretching vibration for possible replacement of –O-Si group with F^- followed by reduction in absorbance of FT-IR by Si-O-Si was observed.

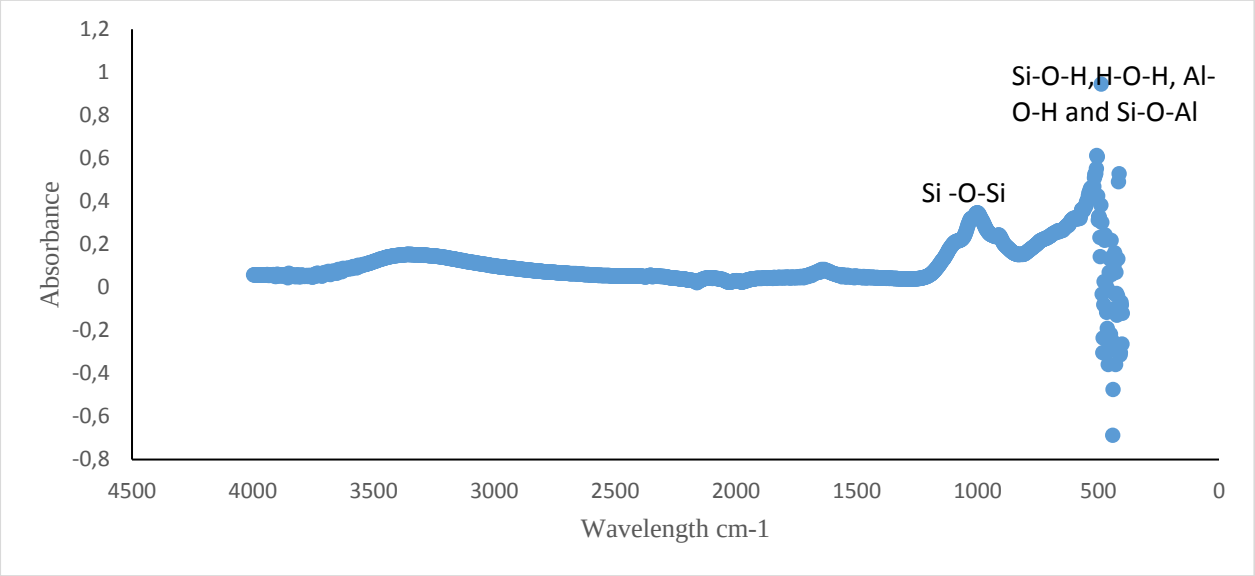

Figure 4.2: FT-IR spectra of Al oxide-modified mechanochemically activated aluminosilicate clay soil.

4.3.1.4 X-ray diffraction of Al-oxide modified mechanochemically activated aluminosilicate clay soil

The results of the X-ray diffraction spectra are shown in Figure 4.3 and the quantitative X-ray diffraction results are indicated in Table 4.2. Figure 4.6 shows the diffraction peaks attributed to crystalline quartz, thenardite, kaolinite, muscovite, hematite and microcline.

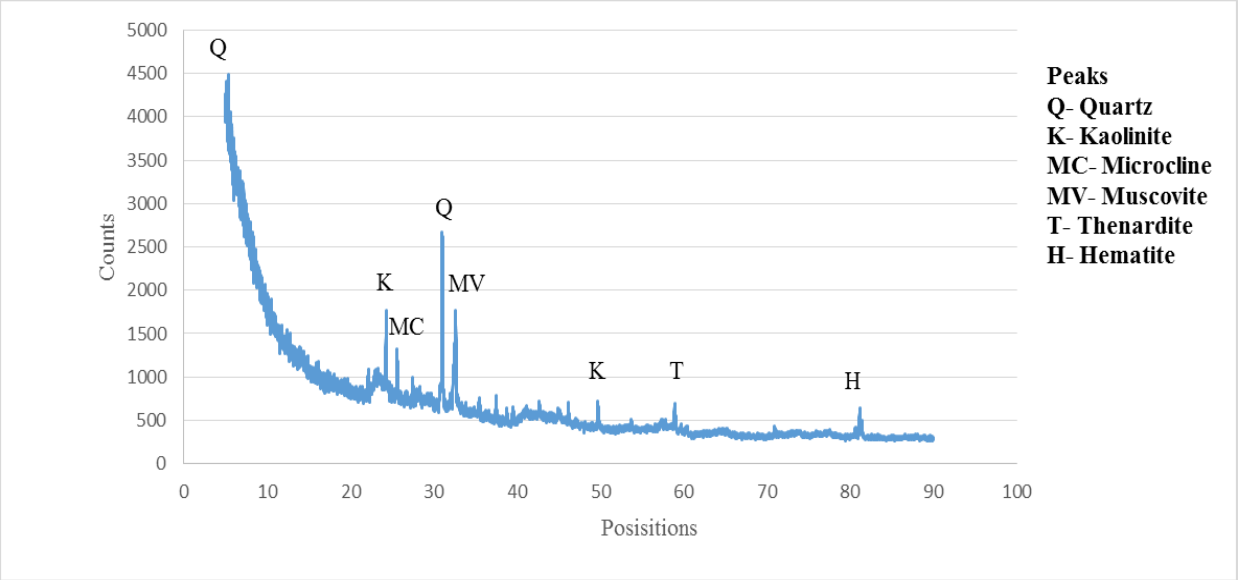

Figure 4.3: Diffraction spectrum with the identified phases

Table 4.2: The results of mineral phases found in Al-oxide modified mechanochemically activated aluminosilicate clay soil

Mineral phases	weight%
Hematite	1.31
Kaolinite	19.99
Microcline	11.07
Muscovite	8.62
Plagioclase	28.73
Quartz	24.36
Thenardite	5.93

Table 4.2 shows the abundance of the mineral phases in the porous ceramic granules. Plagioclase feldspar is the most abundant mineral phase followed by quartz. Similar results were observed for mechanochemically activated clay soil. Other different minerals such as hematite, kaolinite, microcline and thenardite, the difference in mineral composition might be due to modification of clay soil with Al oxide.

4.3.1.5 X-ray fluorescence analysis of Al-oxide modified mechanochemically activated aluminosilicate clay soil

The XRF analysis results of Al-oxide modified mechanochemically activated aluminosilicate clay soil are presented on Table 4.3. The results showed that alumina (Al_2O_3)

has the highest composition followed by silica (SiO_2). The ratio of silicate to alumina was calculated to be 1.18. The presence Al_2O_3 is also due to the modification of aluminosilicate clay soil with Al-oxide modified salt solutions. The minor components are MnO, Cr_2O_3 and P_2O_5. Similar results were also observed for mechanochemically activated aluminosilicate clay soil. This is confirming that the clay is aluminosilicate by composition.

Table 4.3: Physical and chemical parameters of Al-oxide modified mechanochemically activated aluminosilicate clay soil.

Oxide	Composition (wt. %)
SiO_2	23.69
Al_2O_3	31.76
Fe_2O_3	3.78
Na_2O	4.92
K_2O	0.37
MgO	1.18
CaO	0.48
Cr_2O_3	0.04
TiO_2	0.33
MnO	0.02
P_2O_5	0.03
LOI[a]	30.86
Al_2O_3 / SiO_2	1.34
Na_2O/ K_2O	13.30
Fe_2O_3 + MnO + TiO_2	4.13

4.3.1.6 pH at point-of-zero charge (pHpzc)

The pH at point-of-zero charge (pHpzc) of an adsorbent plays an important role in the process of adsorption. When pH of the solution is higher than the pHpzc, the net surface charge of Al-oxide modified mechanochemically activated aluminosilicate clay soil is negative and can adsorb cationic species, on the other hand when pH of the solution is lower than the pHpzc, the surface of Al-oxide modified mechanochemically activated aluminosilicate clay soil is positive and is suitable for the adsorption of anions such as fluoride (Tangsir *et al.*, 2016). Figure 4.3, showed the patterns of the plots for the adsorbent in the solutions of KCl concentrations. The pHpzc of the Al-oxide modified mechanochemically activated aluminosilicate clay soil is 5.1 ± 0.3.

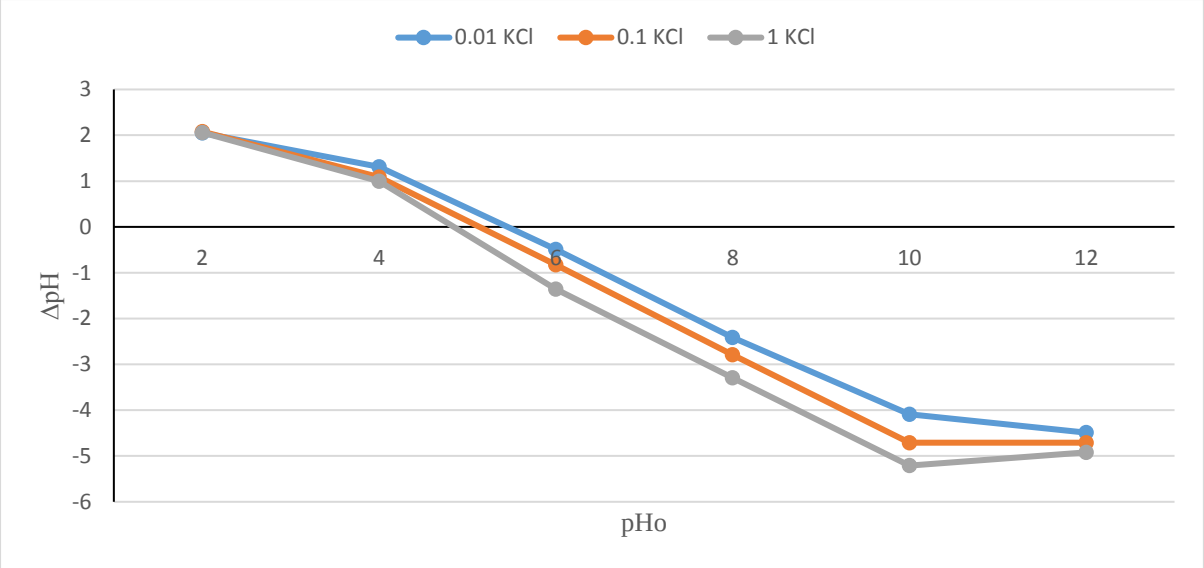

Figure 4.4: Effect of pH at point-of-zero charge of Al oxide-modified mechanochemically activated aluminosilicate clay soil for 0.01, 0.1 and 1 M KCl (volume of solution: 50 mL, adsorbent dosage: 0.6 g, contact time: 24 h and shaking speed: 200 rpm).

4.3.2 Optimizing the Al^{3+} modification of mechanochemically activated aluminosilicate clay

The optimization of Al^{3+} solution for modification of mechanochemically activated aluminosilicate clay soil was conducted using 0.25, 0.50, 0.75, 1.00 and 1.5 M Al^{3+} solutions; represented as AS-A, AS-B, AS-C, AS-D and AS-E respectively. The percentage of fluoride removal increased with a corresponding increase in Al^{3+} concentration. The highest percentage (i.e. 96.5%) removal was obtained at concentration of 1.5 M Al oxide. On the other hand, a corresponding decrease in the C_e and pH_e was observed with increased concentration of Al^{3+}.

Table 4.4. Percent fluoride removal with varying Al^{3+} concentration

Modified clay	C_o (mg/L)	Ce (mg/L)	% F-removal	pHo	pHe
AS- A	10	4.57	54.3	7.75	7.38
AS- B	10	2.00	80.0	7.48	7.23
AS- C	10	0.882	91.2	7.27	6.89
AS- D	10	0.764	92.4	7.30	6.88
AS- E	10	0.355	96.5	7.16	6.86

4.3.3 Fluoride adsorption experiments

4.3.3.1 Effect of contact time

The results of variations of percentage fluoride removal and adsorption capacity with contact time are depicted in Figures 4.4 a, b. It was observed that the adsorption capacity increased with increase in contact time, with fluoride removal at contact time of 1-20 minutes. This might be due to the exchange of fluoride ions with surface hydroxyl ions of the adsorbent (Dayananda *et al*., 2014; Tangsir *et al*., 2016). At 30 minutes of contact time, the fluoride removal was stabilized until 90 minutes. There was no significant change in percentage fluoride removal from 30-90 minutes contact time. Therefore, the optimum fluoride uptake was achieved within an optimum contact time of 30 minutes. The percentage of fluoride removal of 0.1 g absorbent dosage ranged between 60 to 72.5 % with an absorption capacity that vary between 6.06 and 7.25 mg/g. The 0.3 g adsorbent dosage has fluoride removal percentage which vary between 86.1 and 94.4 % and absorption capacity that ranged from 2.87 to 3.08mg/g. The adsorbent dosage of 0.4 g has fluoride removal percentage between 88.4 and 94.9 % and absorption capacity which ranged from 2.21 to 3.09 mg/g (Figure 4.4). Thus, the percentage of fluoride removal increases with the absorbent dosage but the absorption capacity decreases with an increase in the absorbent dosage.

(a)

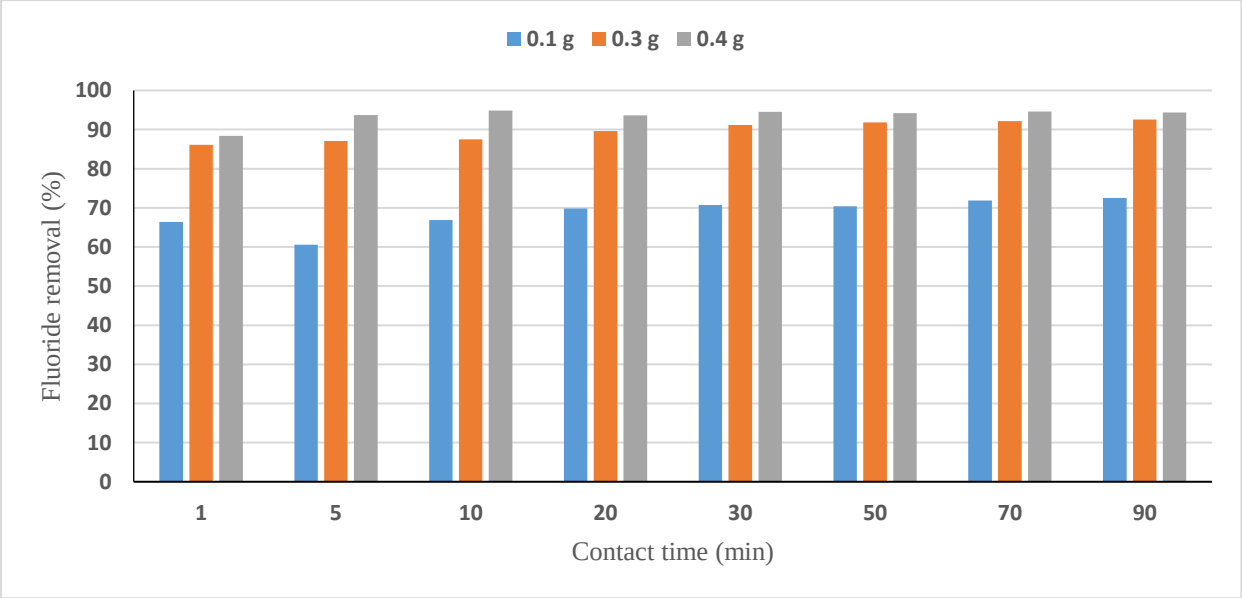

(b)

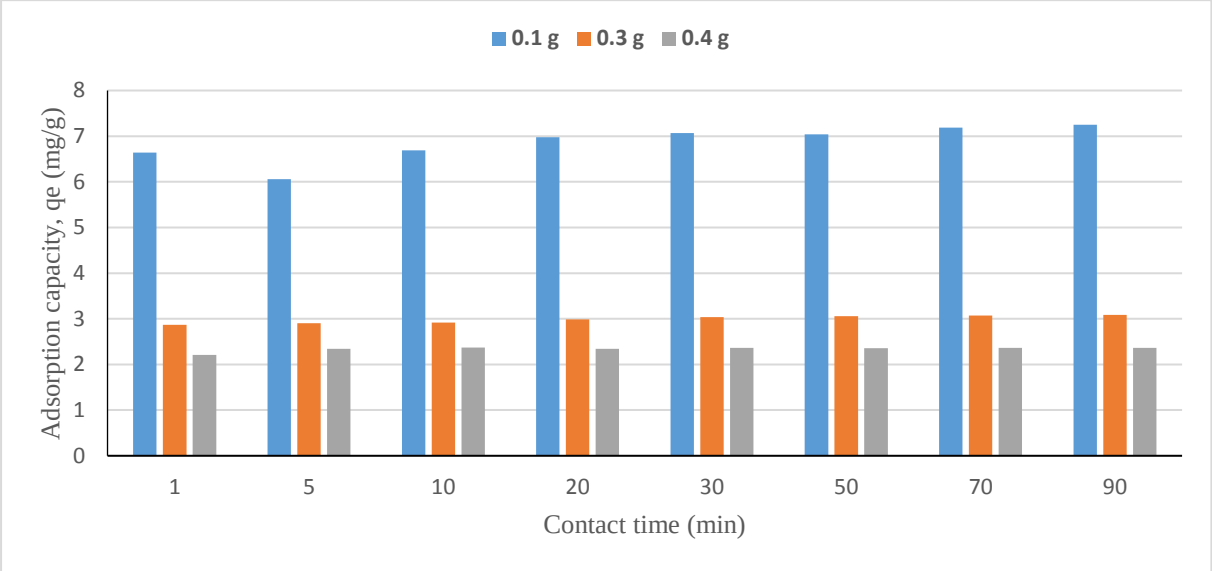

Figure 4.5: Variation of **(a)** % fluoride removal and **(b)** adsorption capacity with contact time at adsorbent doses of 0.1, 0.3 and 0.4 g (initial fluoride concentration: 10 mg/L, solution volume: 100 mL, and temperature: 299 K and shaking speed: 200 rpm).

4.3.3.2 Effect of adsorbent dosage

The effect of adsorbent dosage on fluoride adsorption onto Al-oxide modified mechanochemically activated aluminosilicate clay soil was evaluated. The results of the evaluation of changes in the effect of adsorbent dosage with respect to percentage fluoride removal and adsorption capacity are showed in Table 4.4(refer to appendix B) and Figure 4.5.

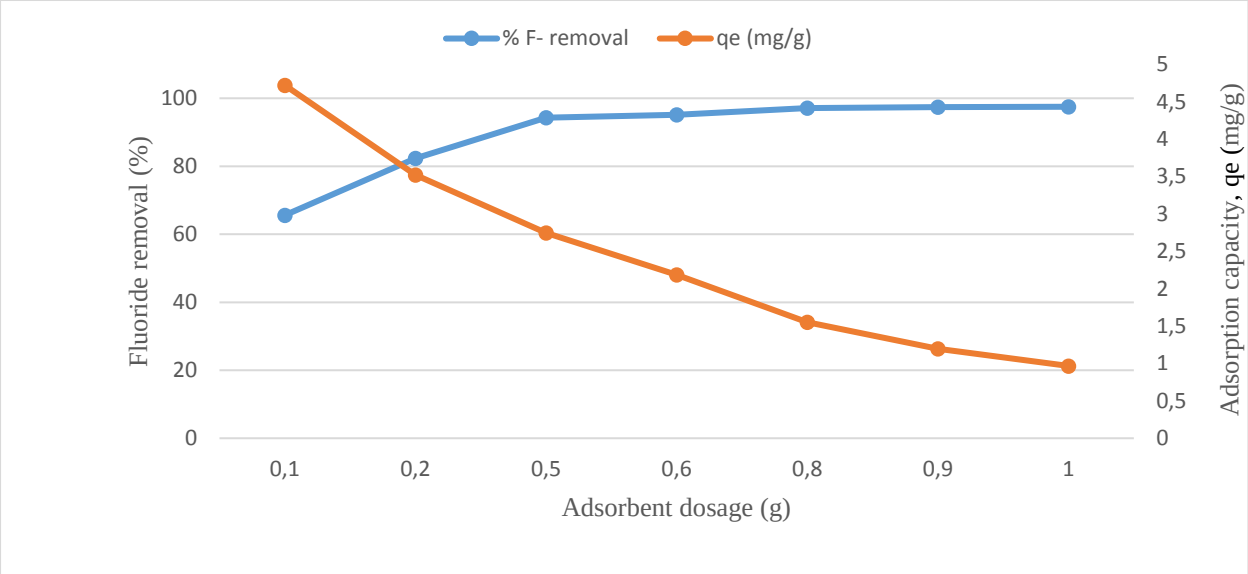

Figure 4.6: Variation of % fluoride removal and adsorption capacity with adsorbent dosage (initial fluoride concentration: 10 mg/L, solution volume: 100 mL, contact time: 30 minutes, shaking speed: 200 rpm and temperature: 297 K).

The percentage fluoride removal increased from 65.6 % to 97.5 %. Therefore it was concluded that the percentage fluoride removal increased with an increase of adsorbent dosage. This is due to the increase in the number of active sites as the dosage increases (Viswanathan *et al*., 2009). There was no significant change in percentage fluoride removal after the adsorbent dosage of 0.6 g, this might be due to too many sites that were available for limited quantity of adsorbate (Kamble *et al*., 2009). The dosage of 0.6 g was adopted as the optimum adsorbent dosage.

4.3.3.3 Effect of adsorbate concentration

The results of the initial fluoride and the percent fluoride removal are reported in Table 4.5(refer to appendix B). The trend in fluoride removal decreased with increasing initial fluoride concentration as shown in Figure 4.6.

(a)

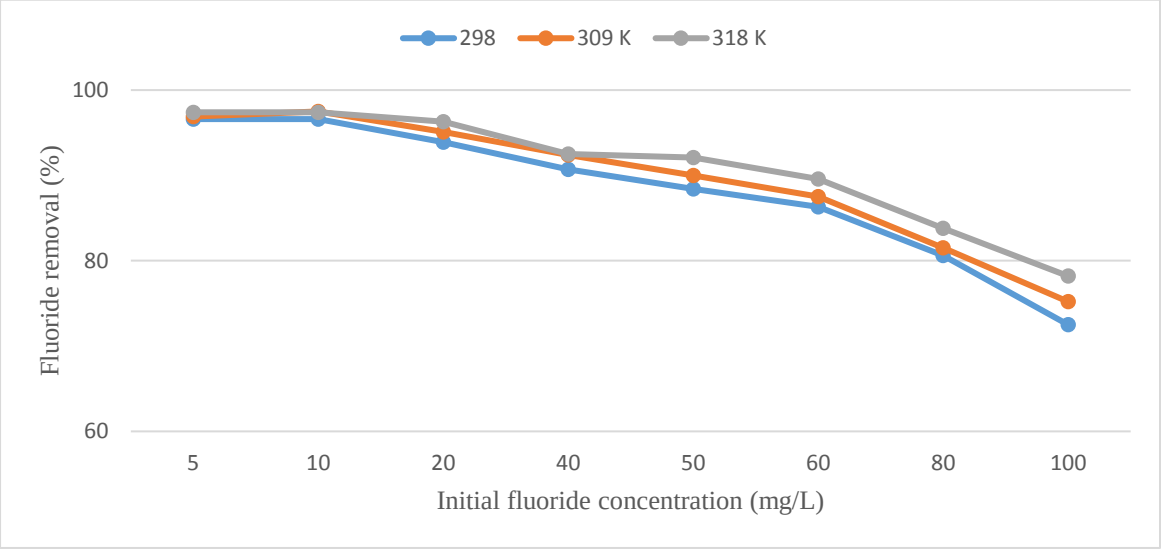

(b)

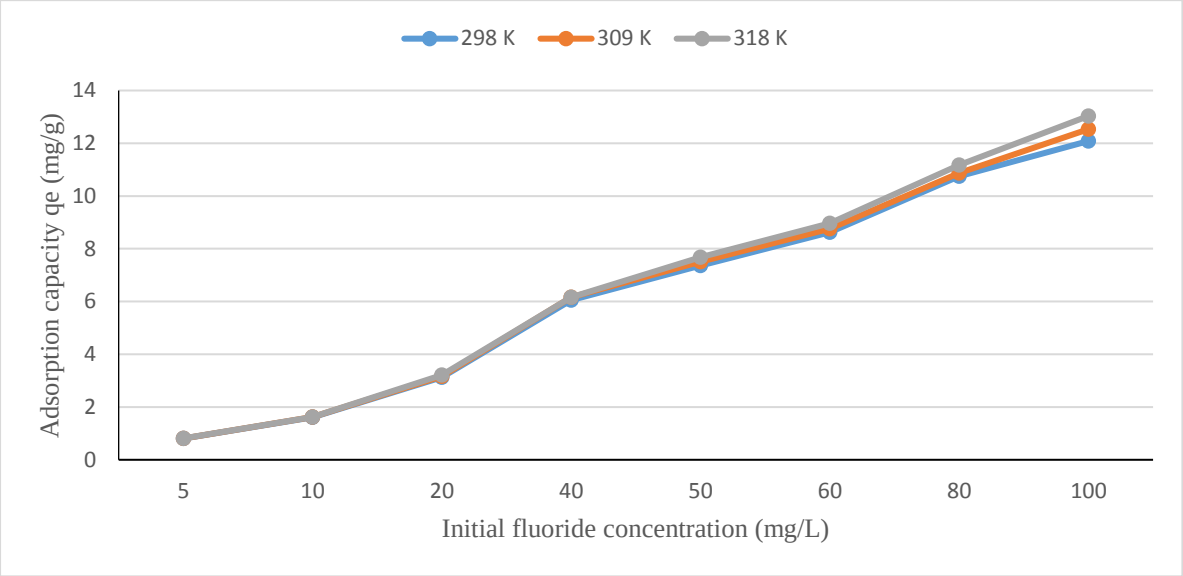

Figure 4.7: Variation of **(a)** % fluoride removal and **(b)** adsorption capacity with adsorbate concentration at 298, 309, and 318 K (contact time: 30 min, solution volume: 100 mL, shaking speed: 200 rpm and dosage: 0.6 g).

The equilibrium fluoride concentration decreased without corresponding increase in dosage. Similar observation were made in the equilibrium fluoride concentration and percentage fluoride removed at different temperatures considered. The increase in adsorbate concentration led to the decrease in percentage fluoride removal. On the other hand the increase in adsorbate concentration led to the increase in adsorption capacity, this is due to the availability of higher number of fluoride ions resulting in higher concentration gradient (Kamble *et al*., 2009).

4.3.3.4 Effect of pH

The results of the equilibrium pH and the percent fluoride removal are reported in Table 4.10 (refer to appendix B) and Figure 4.7.

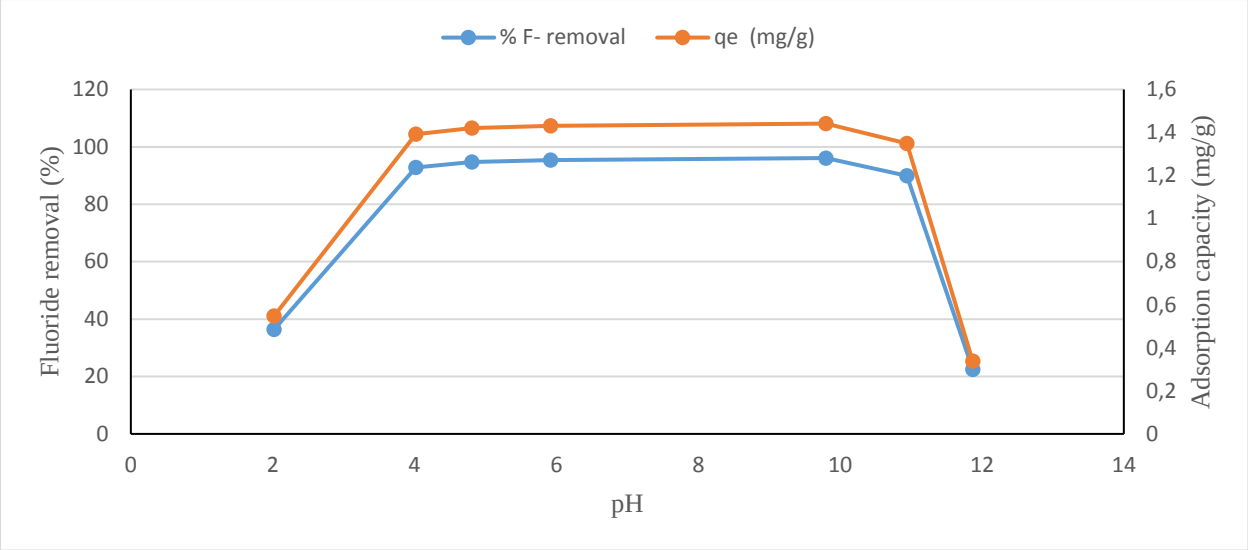

Figure 4.8: Variation of % fluoride removal and adsorption capacity with equilibrium pH (initial fluoride concentration: 9 mg/L, volume of solution: 100 mL, temperature: 298 K, shaking speed: 200 rpm).

It was observed that percentage fluoride adsorption at pH_e of 3.44 was 36.4 %. This might be due to formation of HF, which reduces the coulombic attraction between fluoride and the adsorbent surface (Kumar *et al*., 2011). The increase in pH resulted in an increase of percentage fluoride removal. At pH_e 6.01, the percentage fluoride removal was 96.1 % which may be due to ligand exchange interactions between F^- and OH^- groups (Tomar *et al*., 2013). After pH_e 6.01, the percentage fluoride adsorption decreased due to the hydroxyl ions in the solution which compete with fluoride ions for the possession of active sites on the adsorbent (Christina & Viswanathan, 2015) and also due to the electrostatic repulsion of anionic fluoride by the negatively charged adsorbent's surface (Tangsir *et al*., 2016).

4.3.3.5 Effect of temperature

The results of the effect of temperature in fluoride adsorption is presented in Table 4.7 to 4.9(refer to appendix B). The plot of variations of temperature with percentage fluoride removed by the Al-oxide modified mechanochemically activated aluminosilicate clay is depicted in Figure 4.8. It is evident from this plot that increase in temperature over the range of 298 to 318 K resulted in the increase in fluoride adsorption; showing that the adsorption process is endothermic in nature. Nazari & Hallaj (2014) reported a similar observation from their study and also concluded that adsorption process is endothermic in nature.

(a)

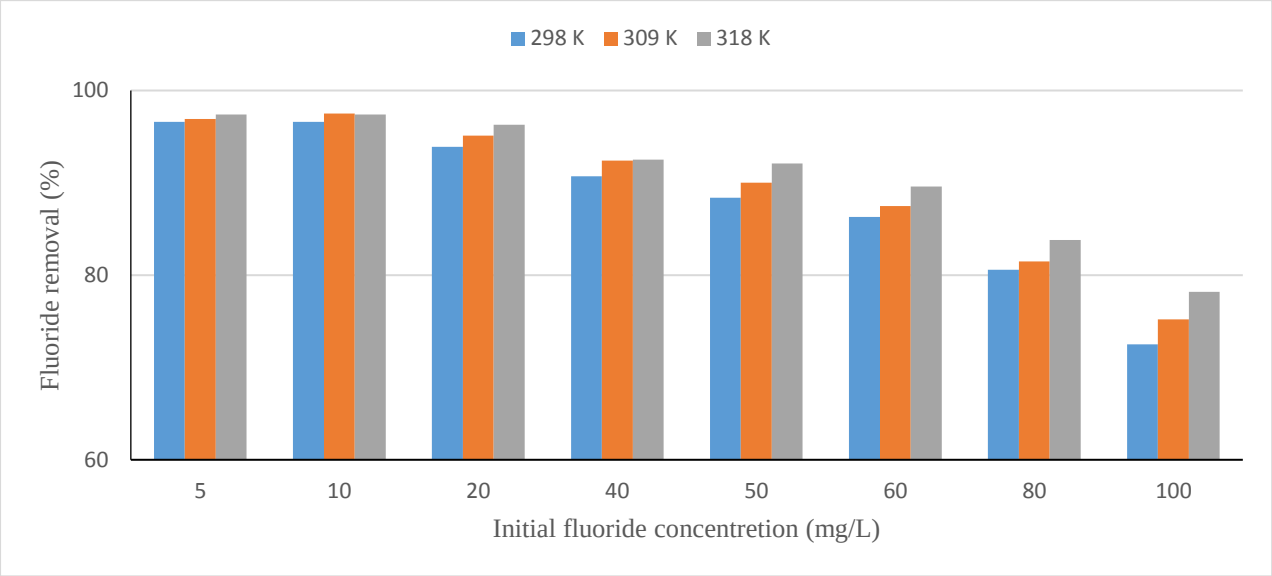

(b)

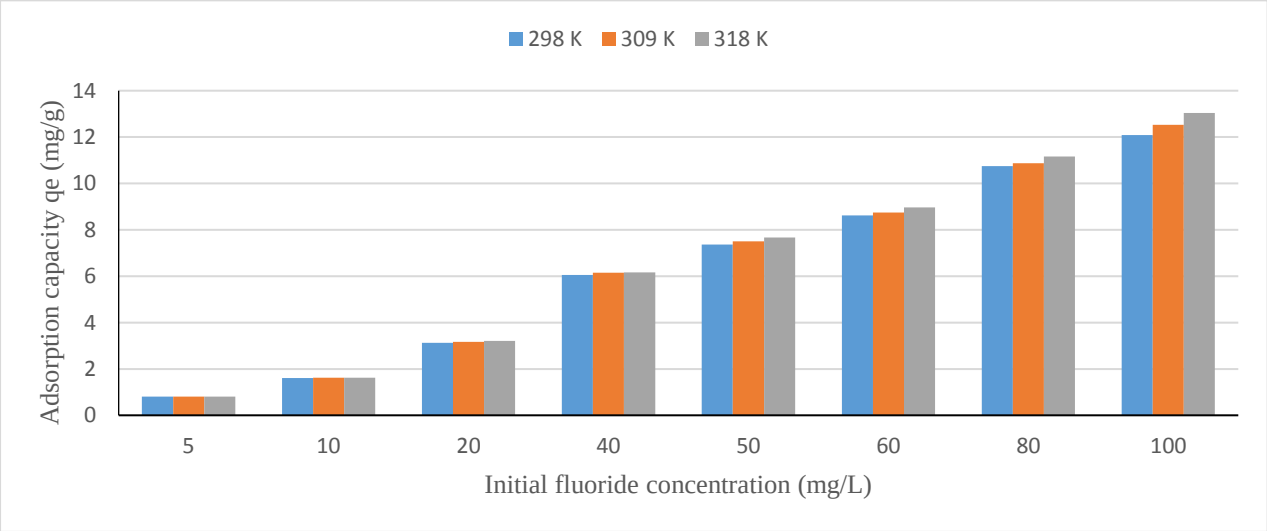

Figure 4.9: Variation of **(a)** % fluoride removal and **(b)** adsorption capacity with temperature at 298, 309, and 318 K (contact time: 30 minutes, solution volume: 100 mL, shaking speed: 200 rpm and dosage: 0.6 g).

4.3.3.6 Effect of medium pH with chemical stability of the adsorbent

The probability of aluminium ions leaching into water at various pH values was evaluated by analysing the supernatants obtained from defluoridation experiments (Figure 4.9). The fluoride removal was low at acidic and alkaline pH solution. The relatively low concentrations of Al ions leached at pH range 4.23 to 10.1 pointed to the fact that if defluoridation experiments is conducted at these pH values would not necessarily pose much

threat resulting from high concentrations of Al ion. The concentration of Na was very high at all pH levels due to the addition of NaOH during pH adjustment while Ca, K, Mg, and Si had low concentrations.

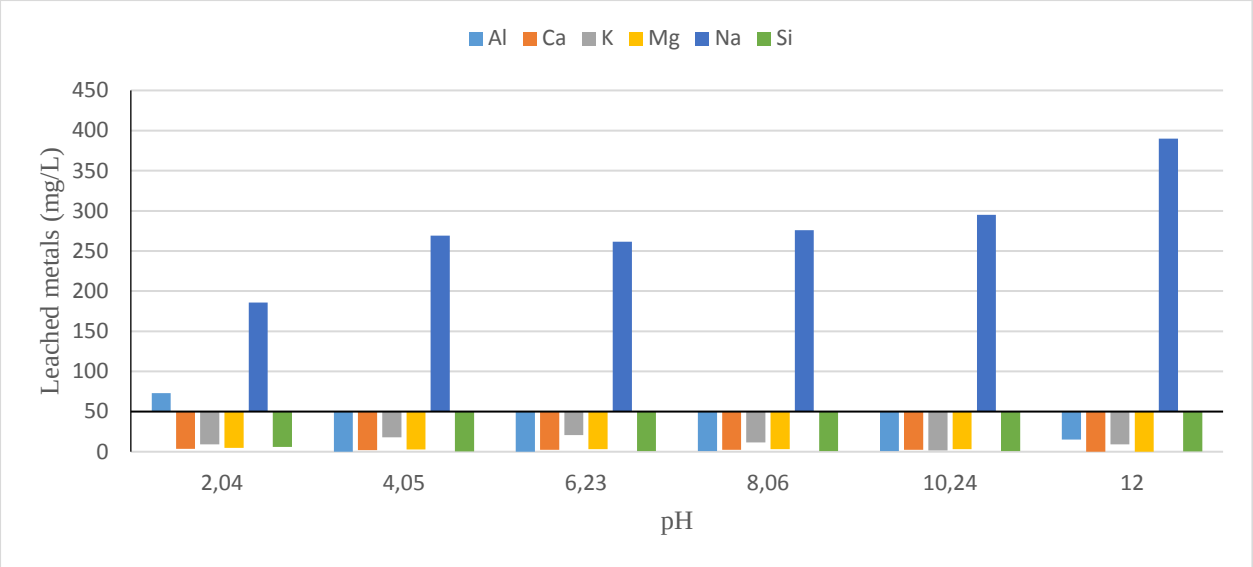

Figure 4.10: Leached metals ions as a function pH (initial fluoride concentration: 9 mg/L, solution volume: 100 mL, temperature: 298 K, shaking speed: 200 rpm).

4.3.3.7 Effect of co-existing ions

The fluoride contaminated water contains several other anions which can equally compete with fluoride during the adsorption process. In order to understand the effect of co-existing ions, the adsorption studies were carried out in the presence of nitrate (NO_3^-) carbonate (CO_3^{2-}), sulphate (SO_4^2), phosphate (PO_4^{3-}) and chloride (Cl^-) on adsorption of fluoride. There was no significant influence of competing anions on fluoride removal capacity (Figure 4.10). In Figure 4.10, PO_4^{3-} competed most with F^- for adsorption than any other anion at the equilibrium pH of 5.69. This could be due to the availability of plenty of exchangeable and sorption sites on this adsorbent. The extent of the competition depends on the relative concentrations of the ions and their affinity for the sorbent (Loganathan *et al.*, 2013). This means that anions with greater charge number are more strongly attracted to cations for bond formation than the univalent anions (Izuagie *et al.*, 2016).

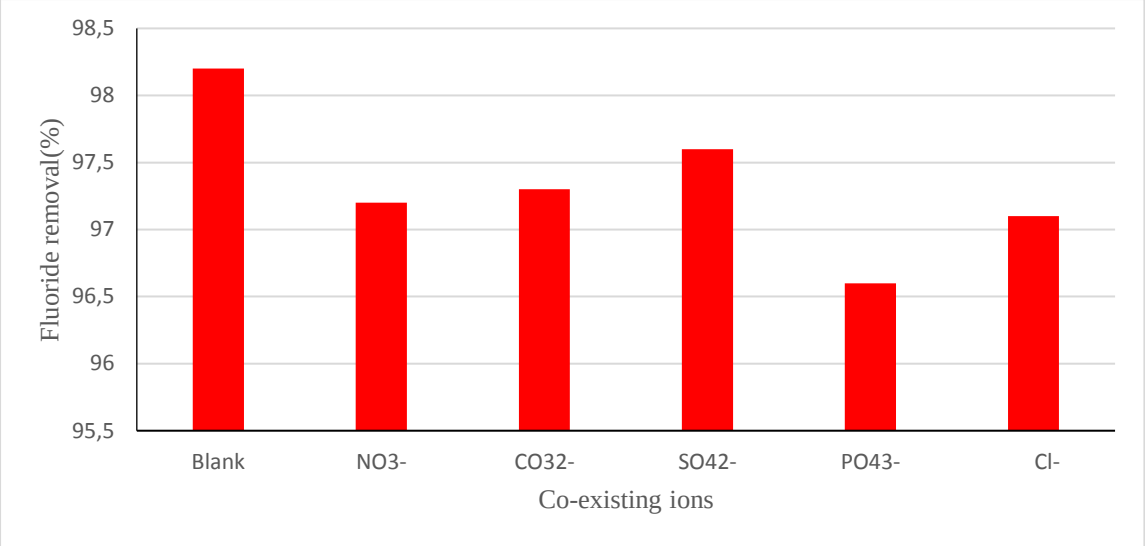

Figure 4.11: Effect of co-existing anions on fluoride removal (initial fluoride concentration: 10 mg/L, initial anion concentration: 5 mg/L, volume of solution: 100 mL, adsorbent dosage: 0.6 g, contact time: 30 minutes, shaking speed: 200 rpm and temperature: 297 K).

4.4 Adsorption models

The equilibrium models are very important for understanding the adsorption systems. It provides essential physiochemical data for assessing the applicability of the adsorption process as a complete unit operation (Aydin & Baysal, 2006).

Two adsorption isotherms Langmuir and Freundlich was applied to fit the equilibrium data of adsorption of fluoride onto Al-oxide modified mechanochemically activated aluminosilicate clay soil.

4.4.1 Langmuir model

The Langmuir adsorption isotherm expression is shown in Equation 3.1 (Langmuir, 1918).

$$q_e = \frac{q_{max} K_L C_e}{1 + K_L C_e} \quad (4.3)$$

The linear form of Langmuir equation is shown below.

$$\frac{C_e}{q_e} = \frac{1}{q_m} C_e + \frac{1}{K_L q_m} \quad (4.4)$$

Where q_e = amount of adsorbed fluoride at equilibrium (mg/g)

q_{max} = measurement of the adsorption capacity (mg/g) based on Langmuir isotherm

K_L = rate of adsorption Langmuir constant (mg/L)

C_e = equilibrium fluoride concentration (mg/L)

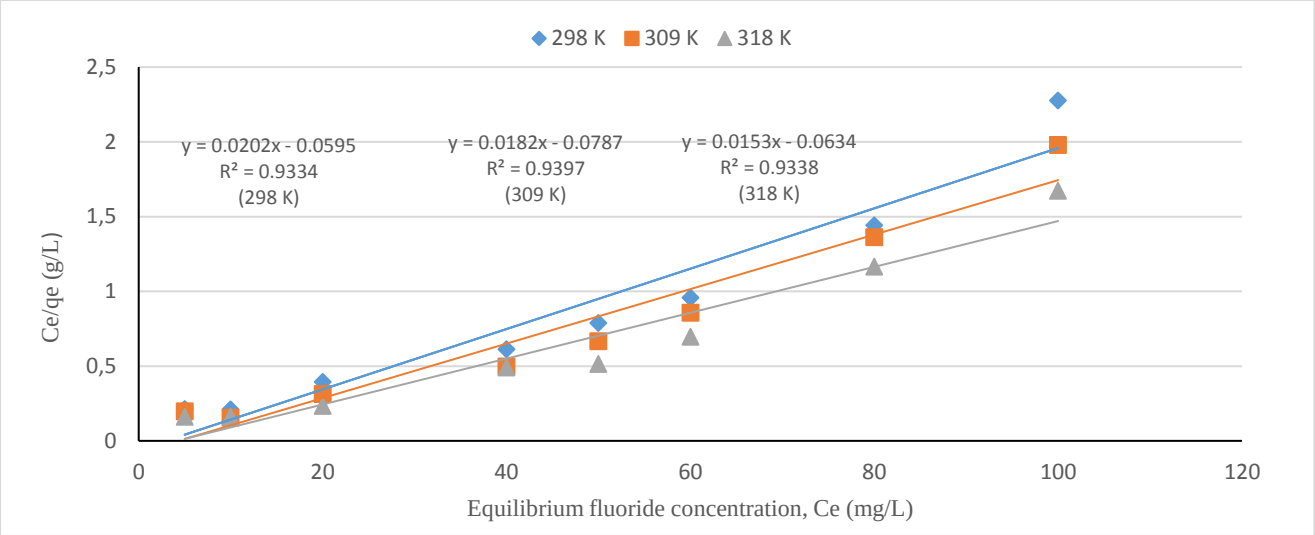

Figure 4.12: Langmuir model graph at temperatures of 298, 309 and 318 K (contact time: 30 minutes, volume: 100 mL, adsorbent dosage: 0.6 g and shaking speed: 200 rpm).

4.4.2 Freundlich model

The Freundlich adsorption model expression is shown in Equation 4.5 (Freundlich, 1906).

$q_e = K_F \ C_e^{1/n}$ (4.5)

The linear form is represented by Equation

$$\log q_e = \log K_F + \frac{1}{n} \log C_e \quad (4.6)$$

Where q_e is amount of adsorbed fluoride at equilibrium (mg/g)

K_F is adsorption capacity of the adsorbent (mg/g (L/mg)$^{1/n}$)

C_e is equilibrium fluoride concentration (mg/L)

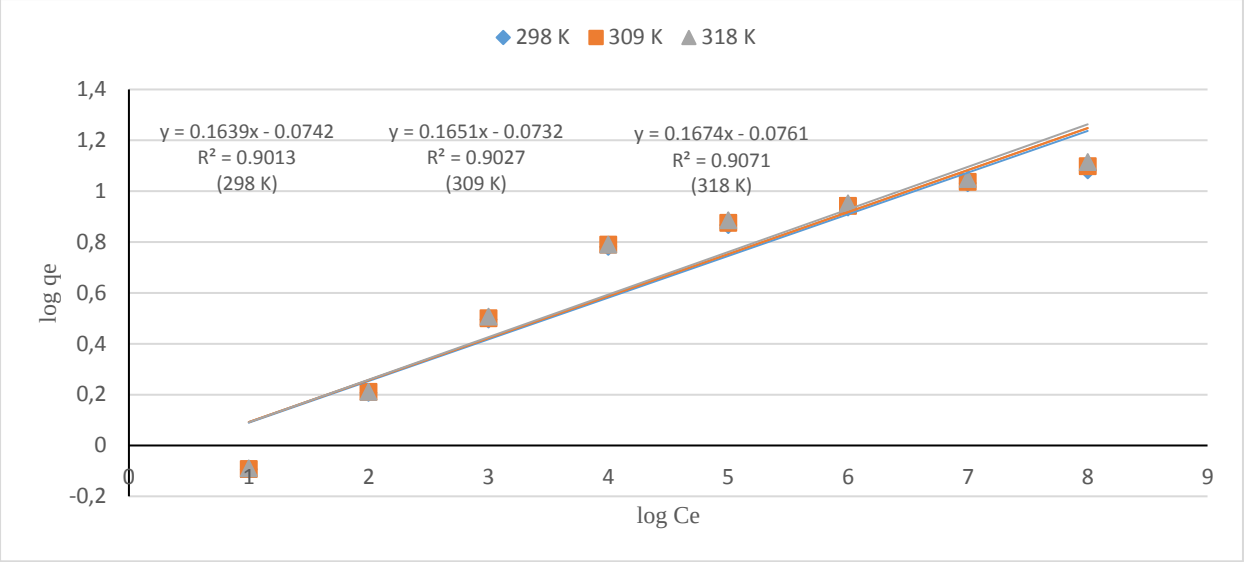

Figure 4.13: Freundlich model graph at temperatures of 298, 309 and 318 K (contact time: 30 minutes, volume: 100 mL, adsorbent dosage: 0.6 g and shaking speed: 200 rpm).

Table 4.14: Calculated Langmuir and Freundlich models parameters

Temperature (K)	Langmuir model constants			Freundlich model constants		
	q_m (mg/g)	K_L (L/mg)	R^2	1/n	K_F	R^2
298	49.505	0.3395	0.933	0.164	1.1863	0.901
309	54.945	0.2313	0.940	0.165	1.1839	0.903
318	65.359	0.2413	0.934	0.167	1.1915	0.907

As indicated in Table 4.14, the R^2 values are closer to 1. Therefore, the experimental data was found to fit well into the Langmuir model. Langmuir model is applicable for monolayer adsorption onto the homogeneous surface of an adsorbent (Langmuir, 1918). Therefore, it is concluded that the adsorbent used in this study is homogeneous. The observed values of 1/n and K_L is less than 1 thus the adsorption was favourable to both Langmuir and Freundlich models. This implies that the material used was homogeneous and partially heterogeneous.

4.5 Adsorption kinetics

Two kinetic models for predicting the order of sorption process were evaluated.

4.5.1. Pseudo-second-order kinetic model

The Lagergren pseudo-first-order model is given as:

$$\frac{dq_t}{dt} = k_1(q_e - q_t) \quad (4.7)$$

q_t(mg/g) is the fluoride concentration at any time *t*,

q_e(mg/g) is the maximum sorption capacity of the pseudo-first-order and

k_1(min^{-1}) is the pseudo-first-order rate constant.

After integration, the Equation (4.8) becomes:

$$\log(q_e - q_t) = -\frac{k_1}{2.303}t + \log q_e \quad (4.8)$$

The pseudo-first-order model was tested by fitting the adsorption data into it as presented in Table 4.15(refer to Appendix B).

The plot of $\log(q_e - q_t)$ values against *t* did not give straight lines. Therefore, the model could not be applied to the sorption process for the batch defluoridation experiments using Al-oxide modified mechanochemically activated aluminosilicate clay (Figure 4.13)

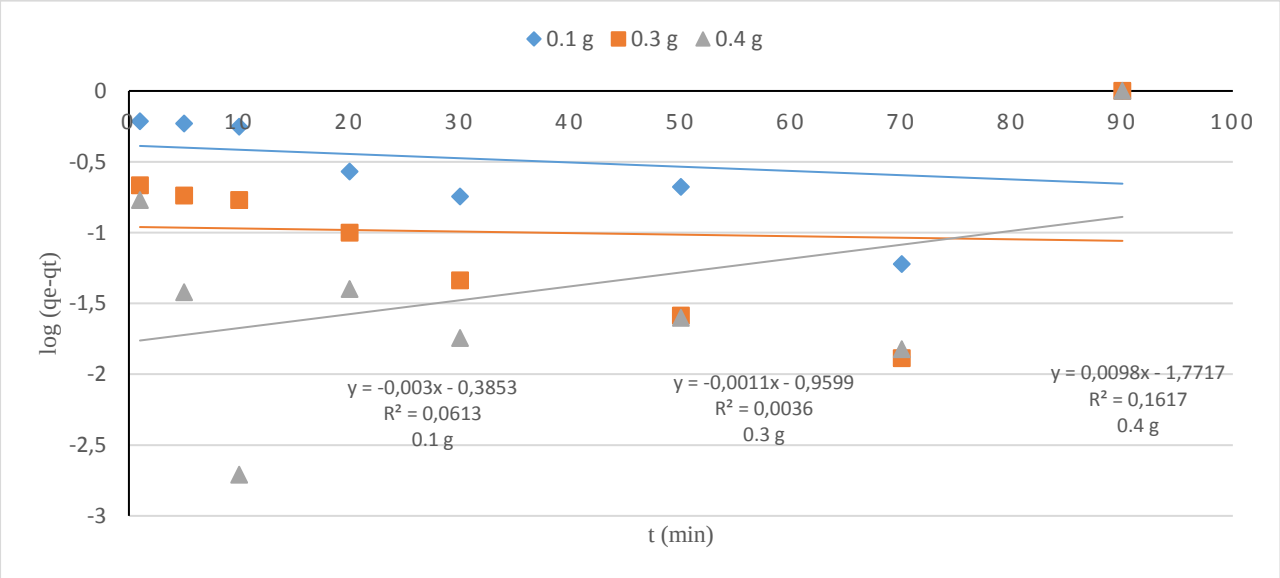

Figure 4.14: Pseudo-first-order plots at different adsorbent dosages of **a.** 0.1 g, **b.** 0.3 g and **c.** 0.4 g of Al oxide-modified aluminosilicate clay soil (initial fluoride concentration: 10 mg/L, solution volume: 100 mL, temperature: 298 K and shaking speed: 200 rpm).

4.5.2. Pseudo-second-order kinetic model

The pseudo-second-order model was also tested on the data. The model is presented in Equation (4.9):

$$\frac{dq_t}{dt} = k_2(q_e - q_t)^2 \quad (4.9)$$

q_t(mg/g) is the fluoride concentration at any time *t*,

q_e (mg/g) is the maximum sorption capacity of the pseudo-second-order and

k_2(g/(mg min)) is the rate constant for the pseudo-second-order process.

After integration, Equation (4.10) gives the linear form of the pseudo-second-order:

$$\frac{t}{q_t} = \frac{1}{k_2\, q_e^2} + \frac{t}{q_e} \quad (4.10)$$

Which is after modification gives the simpler form:

$$\frac{t}{q_t} = \frac{1}{h} + \frac{t}{q_e} \quad (4.11)$$

h (mg/(g min)) is the initial sorption rate defined as:

$$h = k_2 q_e^2 \quad (4.12)$$

The plot of t/q_t values against time *t* for adsorbent dosages of 0.1, 0.3 and 0.4 g gave straight lines as shown in Figure 4.14. Therefore, the data complied with a pseudo-second-order. Fluoride adsorption was therefore by chemisorption.

Table 4.16: Parameters of pseudo-second-order kinetics

Adsorbent dosage (g)	Time (min)	C_t (mg/L) 0.1	C_t (mg/L) 0.3	C_t (mg/L) 0.4	q_t (mg/g) 0.1	q_t (mg/g) 0.3	q_t (mg/g) 0.4	t/q_t (g/L) 0.1	t/q_t (g/L) 0.3	t/q_t (g/L) 0.4
	1	3.36	1.39	1.16	6.640	2.870	2.210	0.1506	0.3484	0.4525
	5	3.94	1.29	0.63	6.660	2.903	2.342	0.7508	1.7224	2.1349
	10	3.31	1.25	0.51	6.690	2.916	2.372	1.4948	3.4294	4.2159
	20	3.02	1.04	0.64	6.980	2.986	2.340	2.8653	6.6979	8.4674
	30	2.93	0.88	0.55	7.070	3.040	2.362	4.2433	9.8684	12.701
	50	2.96	0.82	0.58	7.040	3.060	2.355	7.1023	16.340	21.231
	70	2.81	0.78	0.54	7.190	3.073	2.365	9.7357	22.779	29.598
	90	2.75	0.74	0.56	7.250	3.086	2.380	12.414	29.164	37.815

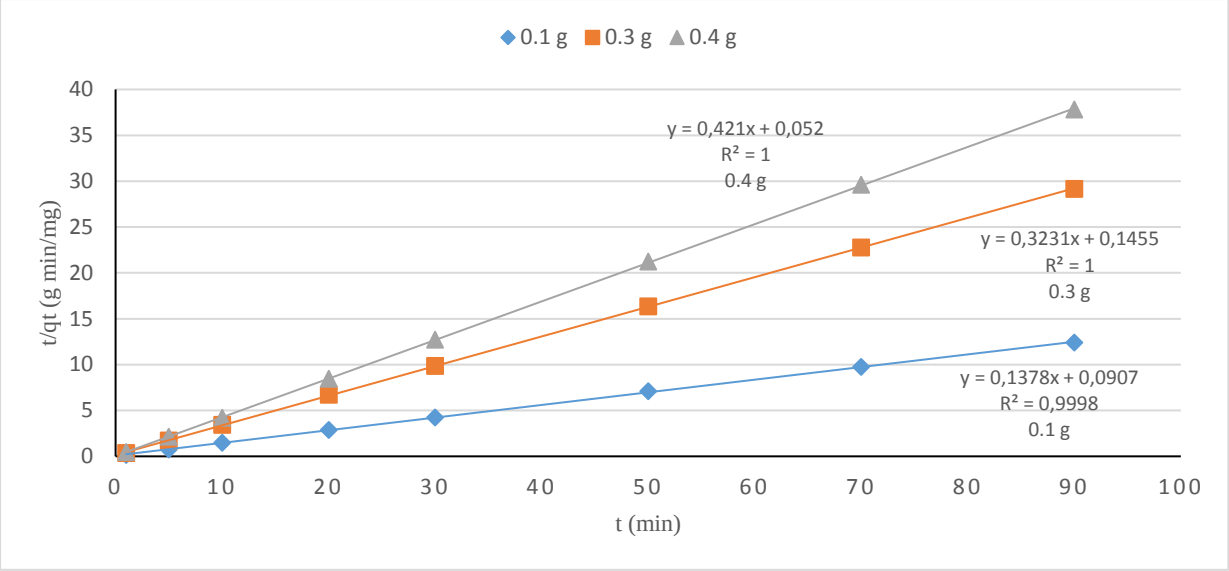

Figure 4.15: Pseudo-second-order profile at different adsorbent dosages (initial fluoride concentration: 10 mg/L, solution volume: 100 mL, temperature: 298 K and shaking speed: 200 rpm).

The calculated q_e and the experimental q_e values were compared. The closeness of the two values as shown in Table 4.17. This indicated that the adsorption data fitted well on pseudo-second-order kinetic model. Similar results were also found in subsection 3.5.2.

Table 4.17: Pseudo-second-order parameters at different adsorbent dosages

Adsorbent dosage (g)	Equation	Experimental q_e (mg/g)	Calculated q_e (mg/g)	k_2 (L mg^{-1} min^{-1})
0.1	y = 0.1378x+ 0.0907	7.257	6.640	0.2094
0.3	y = 0.3231x+ 0.1455	3.095	2.870	0.7175
0.4	y = 0.421x+ 0.052	2.375	2.210	3.4089

4.6 Adsorption mechanism of fluoride onto Al-oxide modified mechanochemically activated aluminosilicate clay soil

The table below (4.18) presented the equilibrium pH and percentage fluoride removal.

Table 4.18 Equilibrium pH and percent fluoride removal

pH_e	5.80	5.85	6.04	6.40	6.61	6.77	7.08	7.35
% F^- removal	96.6	96.6	93.9	90.7	88.4	86.3	80.6	72.5

The pHpzc of the Al-oxide modified mechanochemically activated aluminosilicate clay is 5.1 ± 0.3. The results presented in Table 4.18 revealed that removal of fluoride by Al-oxide modified mechanochemically activated aluminosilicate clay soil occurred above pHpzc; an indication that the surface of the sorbent will be negatively charged. Therefore, adsorption of fluoride onto the surface of the Al-oxide modified mechanochemically activated aluminosilicate clay soil would not have occurred via ion exchange mechanism as represented in equation (4.12).

$$Al(OH)_4^- + 4F^- \rightarrow AlF_4^- + 4OH^- \quad (4.12)$$

The pH at which defluoridation took place ranged between 5.80 and 7.35 which is greater than phpzc. This implies that sorbent surface was negatively charged at all the defluoridation pH values. Hence, there was ion-exchange between F^- in solution and OH^- on the negatively charged sorbent sueface.

4.7 Regeneration and reusability of spent sorbent

The values of the percentage fluoride removal by the regenerated adsorbents in various defluoridation cycles are presented in Table 4.19 (refer to Appendix B). The 0.1 M K_2SO_4 solution was chosen as the suitable solvent to regenerate the spent Al-oxide modified mechanochemically activated aluminosilicate clay soil. After the first regeneration cycle, the adsorbent showed high percentage fluoride removal of 97.2 %. The percentage fluoride removal obtained after the first cycle does not differ much with the blank. Thereafter the percentage fluoride removal decreased with increasing cycle of reuse up to fifth cycle where up to 64.2 % was achieved. A worse trend was observed with the use of Na_3PO_4 because Na_3PO_4 gave a high desorption pH which led to appreciable loss of silica. Izuagie *et al.* (2016) reported similar observation in their study with the use of Na_2CO_3. It is therefore considered inappropriate to use for the regeneration of spent Al-modified mechanochemical activated clay soil.

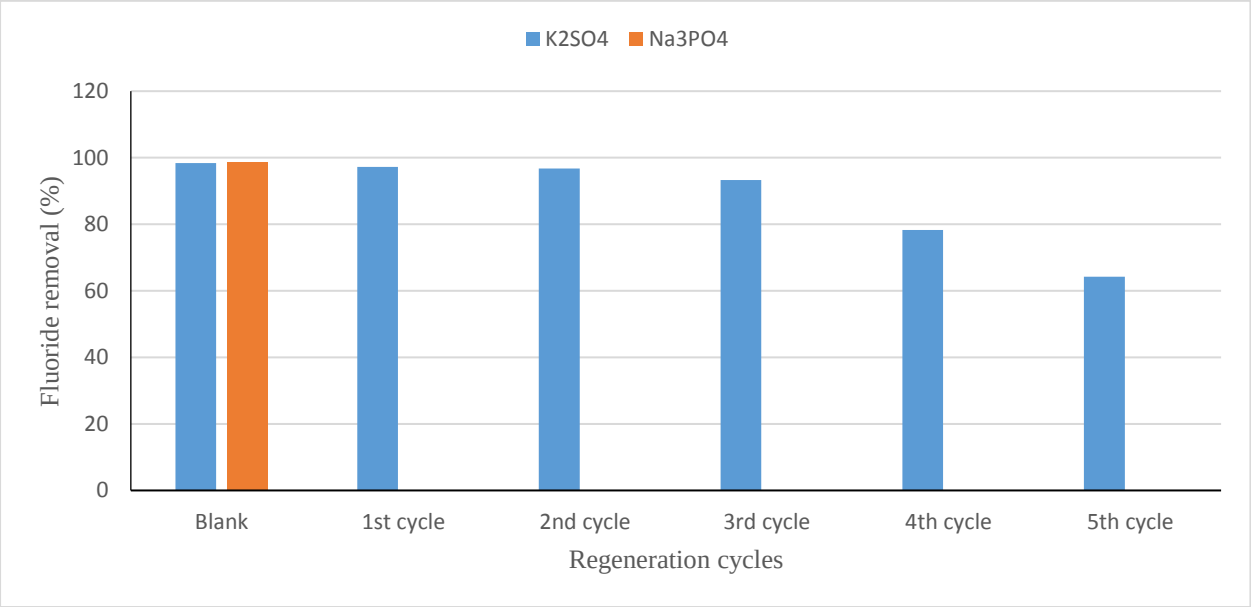

Figure 4.16: Percentage fluoride removal at different defluoridation cycles using 0.1 M K_2SO_4 and 0.1 M Na_3PO_4 (initial concentration of fluoride: 10 mg/L, solution volume: 100 mL and adsorbent dosage: 1 g).

4.8 Defluoridation of field water

The fluoride adsorption efficiency of Al-oxide modified mechanochemically activated aluminosilicate was tested on field water from Siloam community borehole containing 3.88 mg/L fluoride ion concentration. The field water was treated at an optimum contact time of 30 minutes, adsorbent dosage of 0.6 g/100 mL and the shaking speed of 200 rpm. The pH of the water was used was not adjusted (6.46). The results are presented in Table 4.19.

Table 4.19: Concentrations of elements in raw and treated field water in µg/L

Parameters	Before treatment	After treatment
pH	6.46	7.16
Conductivity (µS/cm)	324	400
Total dissolved solids (mg/L)	207	88.4
F^-	3.88	0.134
Li (µg/L)	17,73	1,82
Be (µg/L)	< 0.1	< 0.1
B (µg/L)	33,92	31,19
Al (µg/L)	2,78	29,72
Ti (µg/L)	0,18	0,50
V (µg/L)	0,27	0,24
Cr (µg/L)	0,23	10,04
Mn (µg/L)	4,46	61,61
Fe (µg/L)	525,54	147,93
Co (µg/L)	0,03	0,07
Ni (µg/L)	0,07	0,51
Cu (µg/L)	0,39	< 0.3
Zn (µg/L)	1824,50	153,85
As (µg/L)	0,22	0,05
Se (µg/L)	0,49	0,01
Sr (µg/L)	16,46	22,58
Mo (µg/L)	0,52	0,25
Cd (µg/L)	< 0.005	< 0.005
Sb (µg/L)	0,03	0,06
Ba (µg/L)	12,05	10,12
Hg (µg/L)	0,28	0,11
Pb (µg/L)	0,26	0,12

Comparison of the fluoride removal on spiked and field water shows that there is no significant difference between the fluoride uptake from field water and spiked water. There was an increase in the concentration of aluminium in the treated water as a result of the leaching of the aluminium from the adsorbent. The source could be the Al^{3+} used in modification of mechanochemically activated aluminosilicate clay soil.

4.9 Fluoride adsorption capacity of Al-oxide modified mechanochemically activated clay soil as compared to other adsorbents

Comparison of adsorption capacity of Al-oxide modified mechanochemically activated aluminosilicate clay soil with adsorption capacities of other developed adsorbents is presented in Table 4.20.

Table 4.20: Comparison adsorption capacities of different adsorbents for fluoride removal

Adsorbent	Adsorption capacity (mg/g)	Experimental conditions	Reference
Fe^{3+} bentonite clay	2.91	pH 2; 20 mg/L F^-	Gitari *et al.*, (2013)
Al-coated bauxite clay	12.29	pH 7; 10 mg/L F^-	Salif *et al.*, (2006)
Mg^{2+} bentonite clay	2.25	pH 2-10; 5 mg/L F^-	Thakre *et al.*, (2010)
10%La-bentonite clay	1.4	pH 5; 5mg/L F^-	Meenakshi *et al.*, (2008)
Al oxide-modified aluminosilicate clay	2.18	pH 2.5-10; 10 mg/L F^-	Present study

It was observed that Al-oxide modified mechanochemically activated aluminosilicate clay soil had lower adsorption capacity as compared to Fe^{3+} bentonite clay, Al-coated bauxite clay and Mg^{2+} bentonite clay. It was also observed that Al-oxide modified mechanochemically activated aluminosilicate clay soil had high adsorption capacity as compared to 10%La-bentonite clay.

4.10 Conclusions

The SEM image of Al-oxide modified mechanochemically activated aluminosilicate clay soil showed many small pores and honey-comb structure on the surface of different images. Therefore, there was a good possibility for fluoride to be adsorbed onto the Al-oxide modified mechanochemically activated aluminosilicate clay soil. The BET surface area and the BDH adsorption cumulative area of the Al-oxide modified mechanochemically activated aluminosilicate clay soil are more than double those for the raw clay soil. This is shows that the aluminosilicate clay soil was indeed modified by Al oxide. There was also an increase in pore volume of the Al-oxide modified mechanochemically activated aluminosilicate clay soil.

The FT-IR showed that there is increase in the absorbance of the Si-O-H, H-O-H, Al-O-H and Si-O-Al groups stretching vibration at 414 cm^{-1} for the Al-oxide modified mechanochemically activated aluminosilicate clay soil. In pHpzc, the pH of the solution is higher than the pHpzc, the net surface charge of Al-oxide modified mechanochemically activated aluminosilicate clay is negative and can adsorb cationic species, on the other hand

when pH of the solution is lower than the pHpzc, the surface of Al oxide-modified clay is positive and is suitable for the adsorption of anions such as fluoride.

Al-oxide modified mechanochemically activated aluminosilicate clay soil has a high fluoride removal potential. The study reveals that the fluoride absorption capacity depends on the contact time, absorbent dosage, concentration of fluoride, the pH and temperature. Maximum fluoride uptake was achieved within 30 minutes of agitation for S/L of 0.3 g/100 mL at 200 rpm. At constant agitation time within 30 minutes, the pH was observed to decrease with adsorbent dosage. Maximum adsorption capacity was achieved at 0.6 g absorbent dosage and thereafter there was no significant removal. The percentage of fluoride removal decreased with an increase in initial F^- concentration.

Adsorption capacity of the synthesized material increased with the corresponding decrease in pH. At 5 mg/L co-existing anion concentration, PO_4^{3-} competed most with F^- for adsorption than any other anion. The maximum % fluoride removal (i.e. 96.5%) was obtained at the pH_e of 6.86. The adsorption data fitted well into the Langmuir model when compared to Freundlich model. Sorption process was better modelled using the pseudo-second-order model.

K_2SO_4 solution proved to be the most suitable spent sorbent regenerant as compared to Na_3PO_4. Al oxide modified clay soil was used to remove fluoride in field water and it adsorbed fluoride up to 96.5 %. This shows that Al-oxide modified mechanochemically activated aluminosilicate clay soil is capable of removing fluoride in water. Al-oxide modified mechanochemically activated clay soil is recommended for defluoridation of drinking water even after regeneration. The adsorbent was observed to be efficient for fluoride removal.

References

Aydin, H. & Baysal, G., 2006. Adsorption of acid dyes in aqueous solutions by shells of bittim (pistacia khinjuk stocks). *Desalination*, 196, pp. 248-259.

Christina, E. & Viswanathan, P. 2015. Development of a novel nano-biosorbent for the removal of fluoride from water, *Chin. J. Chem. Eng*. 23, pp. 924-933

Dayananda, D., Sarva, V.R., Prasad, S.V., Arunachalam, J. & Ghosh, N.N. 2014. Preparation of CaO loaded mesoporous Al_2O_3: efficient adsorbent for fluoride removal from water, *Chem. Eng. J*. 248, pp. 430-439

Department of Water Affairs and Forestry (DWAF), South African Water Quality Guidelines for Domestic Use, 1st ed., Department of Water Affairs and Forestry, Pretoria, 1996. Available from: www.dwaf.gov.za

Izuagie, A.A., Gitari, W.M. & Gumbo, J.R. (2016). Synthesis and performance evaluation of Al/Fe oxide coated diatomaceous earth in groundwater defluoridation: towards fluorosis mitigation. *J. Environ. Sci. Health, Part A: Toxic/Hazard. Subs. Environ. Eng.*, pp. 1-15. DOI: 10.1080/10934529.2016.1181445.

Kamble, S.P, Dixit P., Rayalu, S.S. & Labhsetwar, N.K., 2009. Defluoridation of drinking water using chemically modified bentonite clay. *Desalination*, 249, pp. 687-693.

Kumar, E., Bhatnagar, A., Kumar, U. & Sillanpää, M. 2011. Defluoridation from aqueous solutions by nano-alumina: characterization and sorption studies, *J. Hazard. Mater*, 186, pp.1042-1049

Langmuir, I., 1918. The adsorption of gases on plane surfaces of glass, mica and platinum, Journal of *American Chemical Society*, 40, pp. 1361-1368.

Mudzielwana, R. 2016. Synthesis, characterization and performance evaluation of groundwater defluoridation capacity of smectite rich clay soils and Mn-modified bentonite clay composites School of Environmental Sciences, *MSc Thesis*, University of Venda.

Nazari, M. & Halladj, R. 2014. Adsorptive removal of fluoride ions from aqueous solution by using sonochemically synthesized nanomagnesia/alumina adsorbents: an experimental and modeling study, *J. Taiwan Inst. Chem. Eng*., 45, pp. 2518-2525

Salifu, A., Petrusevski, B., Mwamphashi, E.S., Pazi, I. A., Ghebremichael, K., Buamah, R., Aubry, C. & Amy. G.L. 2016. Defluoridation of groundwater using aluminum-coated bauxite: Optimization of synthesis process conditions and equilibrium study, *J Environmental Management*, 181108-117.

Sujana, M.G., Thakur, R.S. Rao & S.B. 1998. Removal of fluoride from aqueous solution by using alum sludge, *J. Colloid Interface Sci*. 206, pp.94-101.

Tangsir, S., Hafshejani, L.D., Lähde, A., Maljanen, M., Hooshmand, A., Naseri, A.A., Moazed, H., Jokiniemi, J. & Bhatnagar, A. 2016. Water defluoridation using Al_2O_3 nanoparticles synthesized by flame spray pyrolysis (FSP) method, *Chem. Eng. J,* 288, pp. 198-206.

Thakre, D., Rayalu, S., Kawade, R,. Meshram, S., Subrt, J. & Labhsetwar, N., 2010. Magnesium incorporated Bentonite clay for defluoridation of drinking water. *Journal of Hazardous Materials*, 180, pp. 122-130.

Viswanathan, N., Sundaram, C.S. & Meenakshi, S. 2009. Sorption behaviour of fluoride on carboxylated cross-linked chitosan beads, *Colloids Surf. B Biointerfaces*, 68, pp. 48-54

CHAPTER 5: Fabrication of porous ceramic granules from Al oxide-modified mechanochemically activated aluminosilicate clay soil and their use in the removal of fluoride

Abstract

Fluoride is frequently present in minerals and it can be leached out due to erosion by rainwater, which leads to contamination of ground and surface water sources. Most rural communities depend on ground water as their source of drinking water. According to World Health Organization, fluoride is considered to be beneficial in drinking water at levels about 0.7 mg/L, but extremely harmful if it exceeds 1.5 mg/L. The objectives of the present study are to: (1) fabricate porous ceramic, (2) physicochemical characterization of porous ceramic granules, (3) to evaluate the efficiency of porous ceramic granules in fluoride removal, and (4) to evaluate the efficiency of fluoride removal from field water. The optimum Al-oxide modified mechanochemically activated aluminosilicate clay soil/ mechanochemically activated clay soil/ corn starch mixing ratio for fabrication of porous ceramic granules was determined by varying ratios and temperature. The optimum ratio found was 20:5:1.The porous ceramic granules were characterised using SEM, BET, FT-IR, XRD and XRF. SEM analysis showed that the porous ceramic granules have the porous structure of the organic foam template. The porous ceramic granule showed an increase in pore surface area and volume as compared to mechanochemically activated aluminosilicate clay soil. The FT-IR showed the presence of a strong broad bending and stretching vibrations band at about 993 cm^{-1} which shows the presence of Si–O–Si bonds. Mineralogical characterisation showed the presence of quartz, albite, horneblende and microcline as the main minerals of the calcined porous ceramic granules. The major oxides of the porous ceramic granules as shown by XRF analysis were SiO_2, Al_2O_3, MnO and Na_2O. The porous ceramic granules reduced the concentrations of fluoride in the water from 10 to 3.31 mg/L. The optimum adsorption capacity was 0.6648 mg/g at a pH_e of 6.32 and the percentage fluoride removal was 66.9 % at an adsorbent dosage of 1.0063 g/100 mL and a temperature of 600 °C. The porous ceramic granules were tested for fluoride removal on field water and the percentage fluoride removal was 45.4 % at the dosage of 1.0009 g/100 mL with the pH_e of 7.87.The study concluded that fabricated porous ceramic granules can be used to remove fluoride in groundwater and it is recommended that further studies should be conducted to in order to evaluate its application future.

Keywords: porous ceramic granules, calcination, characterisation and batch experiments.

5.1 Introduction

Fluoride concentration in surface water is usually less than 1 mg/L, while lower or higher concentration of fluoride in groundwater is observed, depending on the nature of soils or rocks (Chen *et al.*, 2010). Fluoride is essential for human health. High fluoride concentration can pose problems to human health, due to this there is therefore need for defluoridation. The two previous chapters discussed the application of mechanochemically activated and Al-oxide modified mechanochemically activated aluminosilicate clay soil in the defluoridation of groundwater. Both adsorbent showed high fluoride removal efficiency. For mechanochemically activated aluminosilicate clay soils, high fluoride efficiency was obtained at a low pH and for Al-oxide modified mechanochemically activated aluminosilicate clay soil, high fluoride efficiency was observed at neutral pH. Recently, granular ceramic as well as composite adsorbents have been reported to exhibit high fluoride removal capacities with high stability (Chen *et al.*, 2011; Jia *et al.*, 2015; Oladoja *et al.*, 2015, Mudzielwana, 2016).

In this study, the effectiveness of porous ceramic granules for fluoride removal was examined. The characterization studies of the adsorbent by SEM, BET, FTIR, XRD and XRF analyses were carried out to determine the properties of the clay material.

5.2 Materials and methods

5.2.1 Collection and sample preparation

The aluminosilicate-rich clay soil for this study was obtained from Mukondeni Village, Vhembe district in South Africa. Field water was collected from a community borehole in Siloam, Vhembe district in South Africa. All reagents including TISAB-III were obtained from Monitoring and Control Laboratories (Pty) Ltd and Sigma-Aldrich Co. LLC. The preparation of clay soil procedure is explained in subsection 3.2.1.

5.2.2 Physicochemical and mineralogical characterization of aluminosilicate-rich clay

The morphology of the porous ceramic granules sample was determined using a Hitachi X-650 scanning electron micro analyser equipped with CDU lead detector at 25 kV. The surface area was determined by Brunauer–Emmett–Teller (BET) analysis BET surface area and micropore volume was determined using the nitrogen adsorption/desorption isotherms collected at liquid nitrogen temperature (77K). The functional groups of porous ceramic granules were analysed using Bruker Tensor 27 FT-IR & OPUS Data Collection Program.

Mineralogical and chemical composition of the composite adsorbent were determined using X-ray diffraction (XRD) (PANalytical X'Pert pro power) and X-ray fluorescence (XRF) (PANanalytical Axios X-ray fluorescence spectrometer instrument) respectively.

5.2.3 Adsorbent preparation

5.2.3.1 Clay/ Starch mixing ratio

The optimum clay/starch mixing ratio was determined by mixing together Al oxide-modified mechanochemically activated aluminosilicate/mechanochemically activated aluminosilicate clay soil/ corn starch at mass ratios of 20:10:1, 20:5:1, 20:3:2, 40:20:1, 13:6:1 and 10:5:1 were poured into 50 mL glass beaker. Milli-Q water was added until the clay became a lump and the granulation process was done manually. The ceramic granules was heat-treated at 600 ˚C for 2 h, cooled in the open air for about 10 min and then placed in a desiccator to cool at room temperature. The samples were then placed in plastic bags for future experiments. To obtain the optimum clay/starch mixing ratio, defluoridation experiments were conducted as follows: mass of 1 g of the composite were weighed into 100 mL of 10 mg/L fluoride solution in four 250 mL plastic bottles. The initial pH of each mixture was measured and recorded. The mixtures were shaken at 200 rpm for 30 min. They were then centrifuged for 5 min at 40 rpm and the supernatants obtained were analysed for residual fluoride using a four-standard calibrated ORION fluoride ion-selective electrode having added TISAB III to both standards and samples at volume ratio of 1:10.

5.2.3.2 Effect of calcination temperature

To evaluate the effect of calcination temperature, the clay was mixed at ratios determined in the previous section (5.2.3.1). The ceramic granules were air-dried for 2 hours. After drying the granules were placed in an oven for 12 hours at a temperature of 105 ºC. After 12 hours of drying, the granules were calcined at temperatures ranging from 600 to 1000 ºC for 2 hours in a marble furnace. The samples were then placed in plastic bags for subsequent use. The milled ceramic granules were then used for defluoridation experiments. To obtain the optimum temperature, 1 g of the composite prepared at different calcination temperatures were weighed into 100 mL of 10 mg/L fluoride solution in four 250 mL plastic bottles. The initial pH of each mixture was measured and recorded. The mixtures were shaken at 200 rpm for 30 minutes. They were then centrifuged for 5 minutes at 40 rpm and the supernatants obtained were analysed for residual fluoride using a four-standard calibrated ORION fluoride ion-

selective electrode having added TISAB III to both standards and samples at a volume ratio of 1:10.

5.2.4 Defluoridation of field water

The effectiveness of porous ceramic granules in the removal of fluoride in groundwater was evaluated using batch experiments. Dosage of 1.0009 g of the sorbent was weighed into 100 mL of groundwater containing initial fluoride of 3.88 mg/L. The mixture was shaken for 30 minutes at 200 rpm speed. The initial and equilibrium pH values of mixture obtain were 8.85 and 7.87 respectively.

5.3 Results and discussion

5.3.1 Characterization of porous ceramic granules

5.3.1.1 Morphology of porous ceramic granules

Figure 5.1 shows the morphology of porous ceramic granule prepared from Al-oxide modified aluminosilicate clay after calcination at 600 °C for 2 hours.

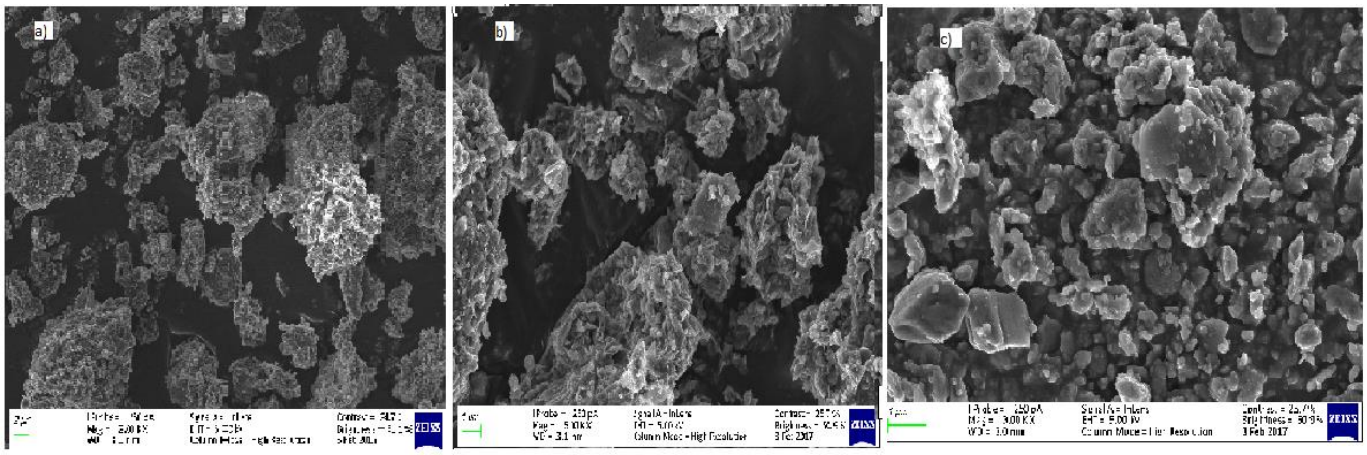

Figure 5.1: SEM image of porous ceramic granules at magnification of 5 000x (a), SEM image at magnification of 10 000x (b), SEM image at magnification of 20 000x (c).

The porous ceramic granules had a morphology that resembled the porous structure of the organic foam template. The granules have high porosity and the pore size was large, ranging between 50 to 100 nm reflecting the pore size in the organic sponge template. Figure 5.1 showed the presence of small pores on the surface of different particles, which ultimately increased the surface area of the porous ceramic granules.

5.3.1.2 Surface area and pore volume of porous ceramic granules

The surface area and pore volume of porous ceramic granules were determined by the Brunauer–Emmett–Teller (BET) method using Micromeritics TriStar II *Surface Area and porosity*. The results are presented in Table 5.1.

Table 5.1: Comparison of the surface area, pore area and volume of the mechanochemically activated aluminosilicate clay soil, Al-oxide modified mechanochemically activated aluminosilicate clay soil and porous ceramic granules.

Form of clay soil	Single point surf. area (m^2/g)	BET surf. area (m^2/g)	BJH adsorption cum. surf. area of pores (m^2/g)	BJH desorption cum. surf. area of pores (m^2/g)	Single point adsorption total pore vol. (cm^3/g)	BJH adsorption cum. vol. of pores (cm^3/g)	BJH desorption cum. vol. of pores (cm^3/g)
Mechanochemically activated aluminosilicate clay soil	47.6093	50.5228	38.519	41.1566	0.089755	0.065258	0.06937
Al-oxide modified mechanochemically activated aluminosilicate clay soil	106.1988	108.2727	104.568	94.8389	0.205898	0.205788	0.206872
Porous ceramic granules	58.0178	58.7541	58.1640	43.5960	0.091353	0.091257	0.096575

Table 5.1 shows the BET surface area and the BDH adsorption cumulative area of the mechanochemically activated aluminosilicate clay soil, Al-oxide modified mechanochemically activated aluminosilicate clay soil and porous ceramic granules. The BET surface area and the BDH adsorption cumulative area of the three adsorbents differs. Al-oxide modified mechanochemically activated aluminosilicate clay soil presented the highest surface area, followed by porous ceramic granules and then the lowest surface area was observed for the mechanochemically activated aluminosilicate clay soil. Increase in surface area of adsorbent implies an increase in active adsorption sites, therefore the increase in percentage fluoride removal. The porous ceramic granule showed an increase in pore surface area and volume as compared to mechanochemically activated aluminosilicate clay soil. This is an indication that the percolation of water through the particles of adsorbent during defluoridation would be more readily achieved for porous ceramic granules (Izuagie *et a*l., 2016).

5.3.1.3 Fourier Transform Infra-red Spectroscopic (FT-IR) Analysis of porous ceramic granules

Figure 5.3 present the FT-IR spectra of the porous ceramic granules.

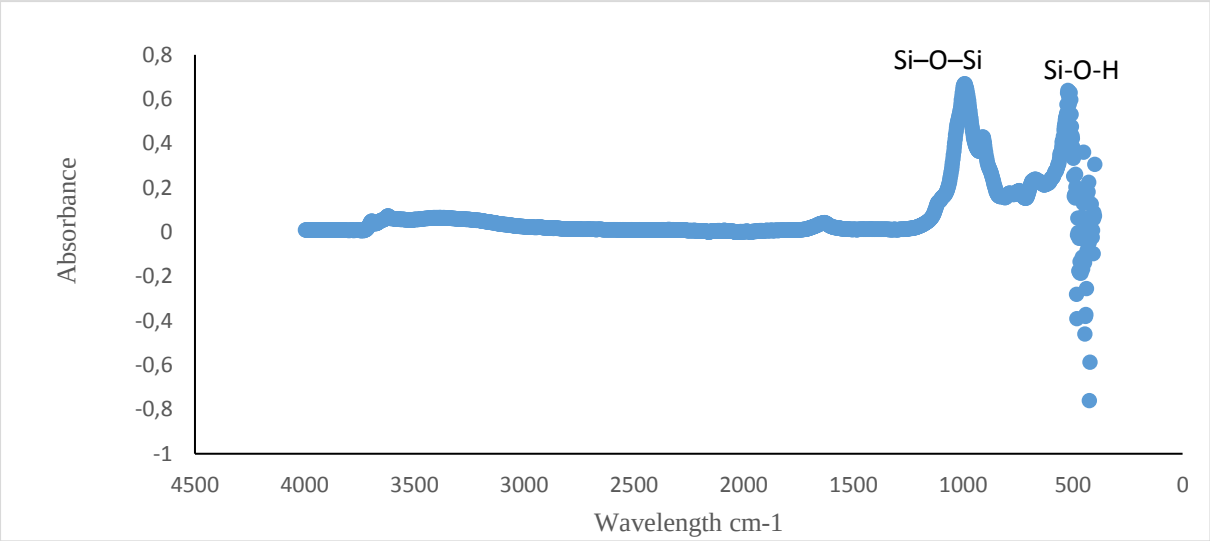

Figure 5.2: FT-IR spectra of porous ceramic granules.

FT-IR spectrum as shown in Figure 5.2 revealed a strong broad bending and stretching vibration band at about 993 cm^{-1} confirming the presence of Si–O–Si bonds. Bending and stretching modes of absorbed water molecules in the porous ceramic granules sample were also observed at 993 and 522 cm^{-1}, respectively.

5.3.1.4 X-ray diffraction of porous ceramic granules

The XRD analysis of the porous ceramic adsorbents confirmed the mineralogical composition of the samples to contain silicon and aluminium oxides. It was observed from Figure 5.3, that diffraction peaks attributed to crystalline quartz, albite, hornblende and microcline (the crystal and amorphous structures of the adsorbent) had significantly changed after the adsorption process (Chen *et al.*, 2010).

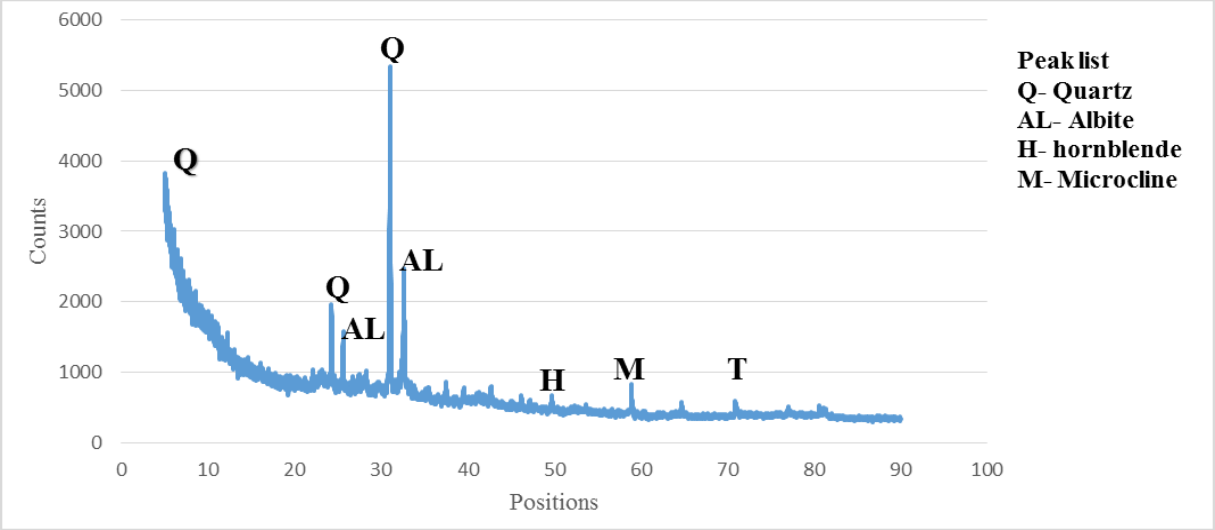

Figure 5.3: Diffraction spectrum with the identified phases

Table 5.2: The results of mineral phases found in porous ceramic granules

Mineral phases	weight%
Hornblende	5.9
Microcline	12.3
Plagioclase	45.3
Quartz	30.9
Thenardite	5.62

Table 5.2 shows the abundance of the mineral phases in the porous ceramic granules. Plagioclase feldspar is the most abundant mineral phase followed by quartz, thenardite had the lowest weight% of 5.62.

5.3.1.5 X-ray fluorescence analysis of porous ceramic granules

The XRF analysis results of major oxides for porous ceramic granules (Table 5.3) showed that alumina (Al_2O_3) has the highest composition followed by silica (SiO_2). The ratio of silicate to alumina was calculated to be 1.01, confirming that the clay is aluminosilicate by composition. The presence of Al_2O_3 is also due to the granular ceramics coated by Al_2O_3 salt solutions. The minor components observed were MnO, Cr_2O_3 and P_2O_5.

Table 5.3: Physical and chemical parameters of porous ceramic granules.

Oxide	Composition (wt. %)
SiO_2	34.92
Al_2O_3	35.40
Fe_2O_3	5.92
Na_2O	4.91
K_2O	0.58
MgO	1.89
CaO	0.71
Cr_2O_3	0.06
TiO_2	0.51
MnO	0.03
P_2O_5	0.04
LOI[a]	12..90
Al_2O_3 / SiO_2	1.01
Na_2O/ K_2O	8.47
Fe_2O_3 + MnO + TiO_2	6.46

5.3.2 Optimization of adsorption conditions

5.3.2.1 Clay/ starch mixing ratio

Figure 5.4 shows the effect of clay/starch mixing ratio on fluoride removal, the results shows that the mixing at ratio of 20:5:1 (Al-oxide modified mechanochemically activated clay soil/ mechanochemically activated aluminosilicate clay soil/ corn starch) achieved the highest percentage F^- removal by 66.9 %.

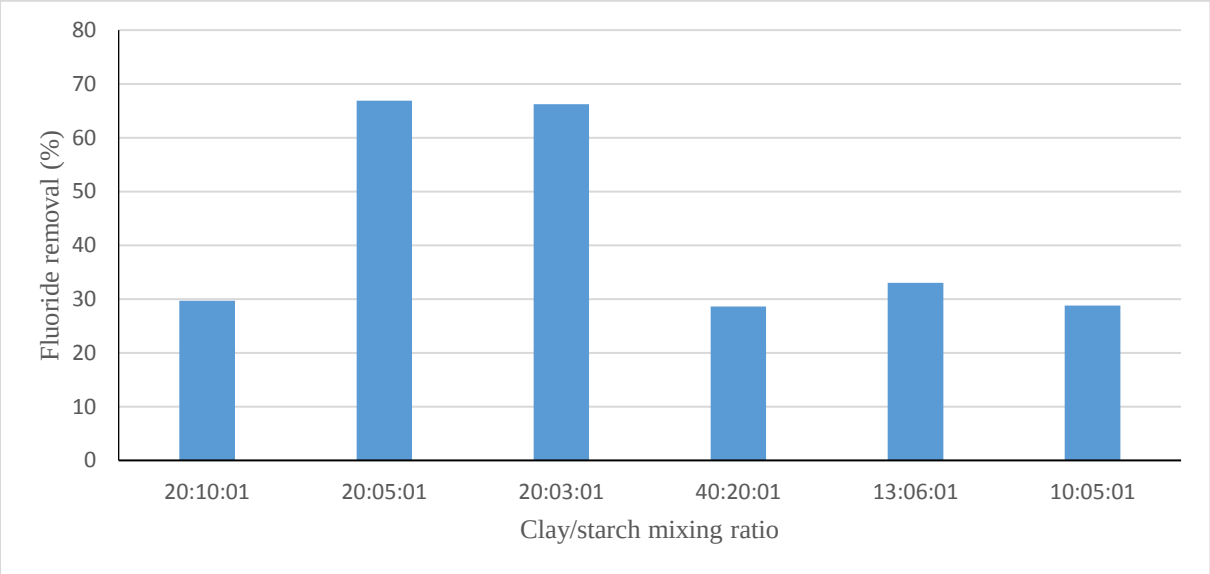

Figure 5.4: Variation of % fluoride removal at different clay/starch mixing ratio (initial fluoride concentration: 10 mg/L, solution volume: 100 mL, contact time: 30 min, shaking speed: 200 rpm and temperature: 297 K).

This ratio was subsequently adopted as the optimum clay mixing ratio for subsequent experiments. In previous experiments before the optimum mixing ratio was obtained, the porous ceramic granules were fabricated without the raw clay soil. Due to this, the Al oxide-modified clay soil lost its plasticity during modification making the porous ceramic granules crumble. In another experiment, the granules burnt to ashes as a result of too much starch which had increased the organic material component of the porous ceramic granule.

5.3.2.2 Effect of calcination temperature

In Figure 5.5, it was observed that the percentage fluoride removal decreased from 59.8 to 6.2 % as the calcination temperature increased from 600 to 1000 ^{0}C.

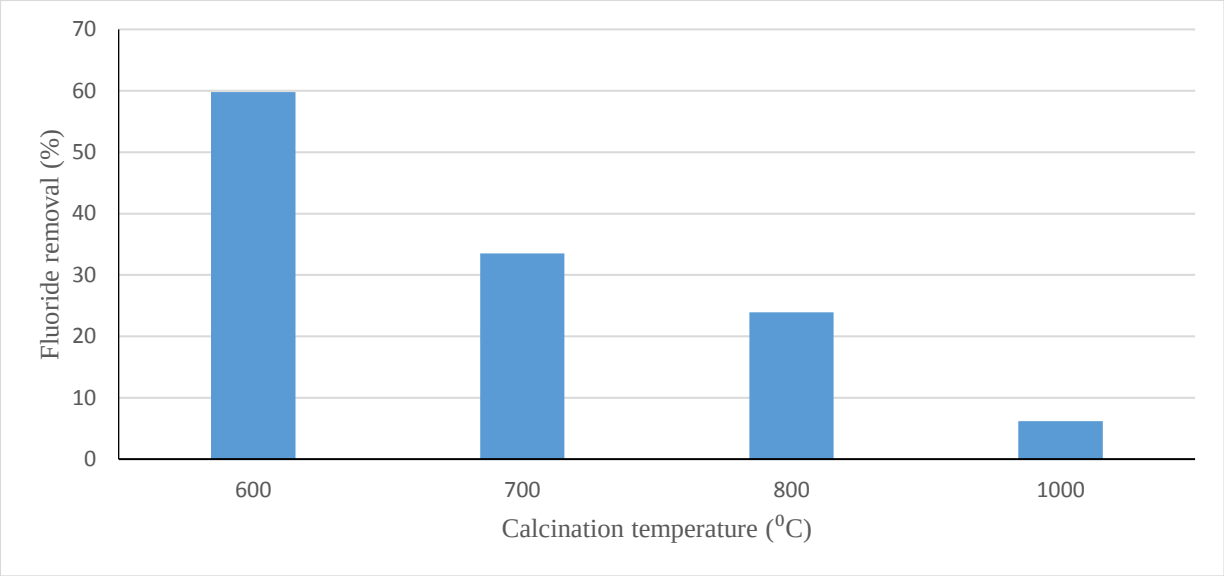

Figure 5.5: Variation of % fluoride removal at different calcination temperature (initial fluoride concentration: 10 mg/L, solution volume: 100 mL, contact time: 30 min, shaking speed: 200 rpm and temperature: 297 K).

The decrease in fluoride removal efficiency due to calcination temperatures above 600 ^{0}C might be caused by the loss of OH^- group as a result of dehydroxylation. The decrease in fluoride removal at temperatures above 600 ^{0}C may be attributed to loss of surface hydroxyl groups from the adsorbent (Mudzielwana, 2016). Figure 5.7 shows the image of porous ceramic granules calcined at different temperatures. The porous ceramic granules appear brown in colour.

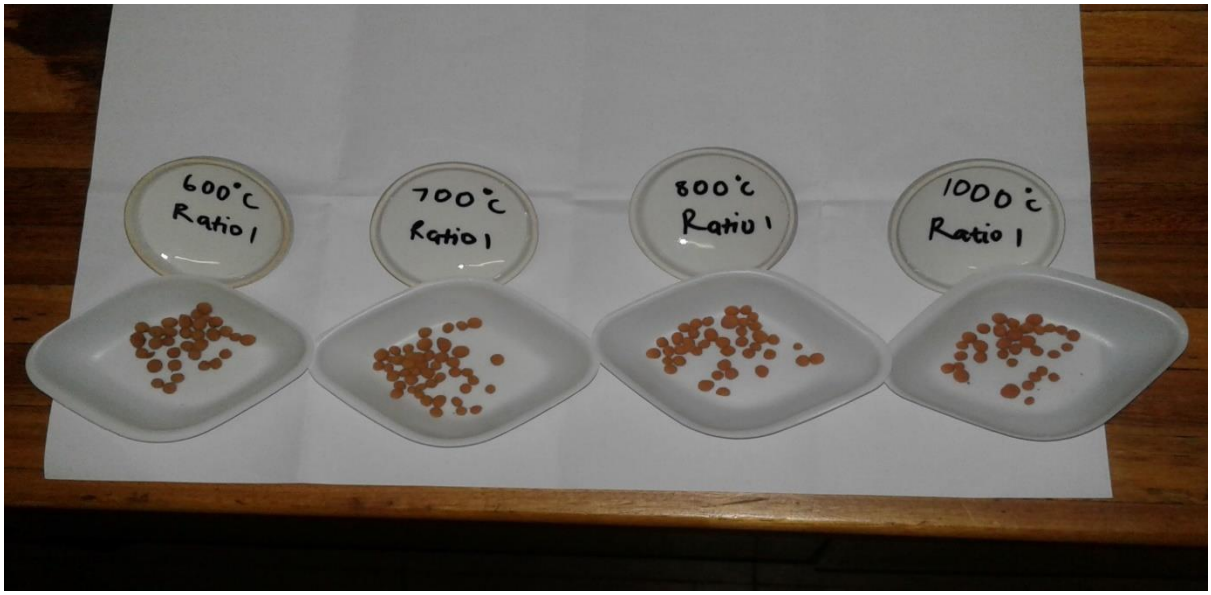

Figure 5.6: Porous ceramic granules calcined at different temperatures (600 ºC, 700 ºC, 800 ºC and 1000 ºC).

It was observed that clay calcined at 600 ^{0}C is most effective for fluoride removal, as the increase in temperature reduced fluoride adsorption.

5.4 Defluoridation of field water

The fluoride adsorption efficiency of porous ceramic granules were tested on field water samples obtained from Siloam community borehole containing 3.88 mg/L fluoride ion concentration. The field water was then treated at an optimum contact time of 30 minutes, adsorbent dosage of 1 g/100 mL and the shaking speed of 200 rpm. The pH value of the water sample was 6.46.

Table 5.6: Concentration of elements in raw and treated field water in µg/L

Parameters	Before treatment	After treatment
pH	7.24	7.75
Conductivity (µS/cm)	328	415
Total dissolved solids (mg/L)	201	82.4
F^-	3.88	2.12
Li (µg/L)	17,73	37,96
Be (µg/L)	< 0.1	< 0.1
B (µg/L)	33,92	29,79
Al (µg/L)	2,78	402,68
Ti (µg/L)	0,18	2,03
V (µg/L)	0,27	4,95
Cr (µg/L)	0,23	91,49
Mn (µg/L)	4,46	20,80
Fe (µg/L)	525,54	581,34
Co (µg/L)	0,03	0,42
Ni (µg/L)	0,07	2,89
Cu (µg/L)	0,39	1,78
Zn (µg/L)	1824,50	1584,61
As (µg/L)	0,22	0,24
Se (µg/L)	0,49	0,46
Sr (µg/L)	16,46	18,02
Mo (µg/L)	0,52	0,68
Cd (µg/L)	< 0.005	0,01
Sb (µg/L)	0,03	0,04
Ba (µg/L)	12,05	6,35
Hg (µg/L)	0,28	0,24
Pb (µg/L)	0,26	0,35

Percentage fluoride removal of 45.4 % was achieved from the field water samples. These percentages were lower than the obtained values from fluoride removal using spiked water (66.9 %). This might be due to the competition for binding sites between co-existing anion and fluoride since field water contain different co-existing ions. The aluminium concentration after before treatment was higher as compared to after treatment, this confirmed the leaching of the aluminium from the adsorbent. The source could be the Al^{3+} used in modification of mechanochemically activated aluminosilicate clay soil before fabrication of the porous ceramic granules.

5.5 Fluoride adsorption capacity of porous ceramic granules as compared to other adsorbents

Comparison of the adsorption capacity of porous ceramic granules with adsorption capacities of other developed adsorbents is presented in Table 5.7.

Table 5.7: Comparison of adsorption capacities of different adsorbents for fluoride removal

Adsorbent	**Adsorption capacity (mg/g)**	**Experimental conditions**	**Reference**
Granular ceramic	0.44	pH 5-8; 10 mg/L F^-	Chen *et al.*, (2010)
Al/Fe granular ceramic	1.79	pH 6; 10 mg/L F^-	Chen *et al* (2010)
LECA	23.86	pH 6; 5-20 mg/L F^-	Sepehr *et al.*, (2014)
Iron-impregnated granular	2.17	pH 7; 10 mg/L F^-	Chen *et al.*, (2010)
Porous ceramic granules	0.66	pH 6; 10 mg/L F^-	Present study

It was observed that porous ceramic granules had lower adsorption capacity as compared to Al/Fe granular ceramic, LECA and Iron-impregnated granular. It was also observed that porous ceramic granules had high adsorption capacity as compared to Granular ceramic.

5.6 Conclusion

Porous ceramic granules synthesized in this study showed improved efficiency in fluoride removal from field water samples obtained from Siloam community borehole. In this study, SEM analysis showed that the porous ceramic granules possess a porous structure as a result of the organic foam template. The porous ceramic granule showed an increase in pore surface area and volume as compared to mechanochemically activated aluminosilicate clay soil. This is an indication that the percolation of water through the particles of adsorbent during defluoridation would be more readily achieved for porous ceramic granules.

The FT-IR showed the presence of a strong broad bending and stretching vibrations at about 993 cm^{-1} confirming the presence of Si–O–Si bonds. Bending and stretching modes of absorbed water molecules in the porous ceramic granules sample were observed at 993 and 522 cm^{-1}, respectively. Mineralogical characterisation showed the presence of quartz, albite, horneblende and microcline as the main minerals of the calcined porous ceramic granules. The major oxides of the porous ceramic granules for XRF analysis showed that SiO_2, Al_2O_3, MnO and Na_2O were prevalent.

The optimum Al-oxide modified mechanochemically activated aluminosilicate clay soil/ mechanochemically activated aluminosilicate clay soil/ corn starch ratio was found to be 20:5:1. The optimum temperature for calcination of porous ceramic granules was found to be 600 ^{0}C. The porous ceramic granules fabricated were able to remove up to 66.9 % fluoride from an initial fluoride concentration of 10 mg/L. There was progressive improvement in the adsorption capacity of the porous ceramic granules due to the activation, modification and granulation of the clay. When comparing the percentage fluoride removal of mechanochemically activated and porous ceramic granules, the porous ceramic granules percentage fluoride removal presented the higher rate at 66.9 % compared to mechanochemically activated aluminosilicate clay soil gave a 41.0 % fluoride removal. Porous ceramic granules were used to remove fluoride from field water. Percentage fluoride removal of 45.4 % was obtained at the dosage of 1.0009 g/100 mL with the pHe of 7.87. This study recommends further studies to evaluate the applicability the material in community based defluoridation of groundwater.

References

Chen, N., Zhang, Z., Feng, C., Li, M., Zhu, D., Chen, R. & Sugiura, N., 2010. An excellent fluoride sorption behavior of ceramic adsorbent. *Journal of Hazardous Materials*, 183, pp.460–465

Chen, N., Zhang, Y.Z., Feng, C.P., Sugiura, N., Li, M. & Chen, R.Z., 2010. Fluoride removal from water by granular ceramic adsorption, *Journal of Colloid Interface Science*, 348, pp. 579-584.

Chen, N., Zhang, Y.Z., Feng, C.P., Li, M., Zhu, D., Chen, R. & Sugiura, N., 2010. Studies on fluoride adsorption of iron-impregnated granular ceramics from aqueous solution. *Material Chemistry and Physics*, 125, pp. 293-295.

Chen, N., Zhang, Z., Feng, C., Zhu, D., Yang, Y. & Sugiura, N., 2011. Preparation and characterization of porous granular ceramic containing dispersed aluminium and iron oxides as adsorbents for fluoride removal from aqueous solution. *Journal of Hazardous Materials*, 186, pp.863-868.

Izuagie, A.A., Gitari, W.M. & Gumbo, J.R. (2016). Synthesis and performance evaluation of Al/Fe oxide coated diatomaceous earth in groundwater defluoridation: towards fluorosis mitigation. *J. Environ. Sci. Health, Part A: Toxic/Hazard. Subs. Environ. Eng.*, pp. 1-15. DOI: 10.1080/10934529.2016.1181445.

Jia Y., Zhu B. S., Zhang K. S., Jin Z., Luo T., Yu X. Y., Kong., L. T., & Liu J. H., 2015. Porous 2-line ferrihydrite/byerite composite (LFBC): Fluoride removal performance and mechanism. *Chemical Engineering Journal*, 268, pp. 325-336.

Mudzielwana, R. 2016. Synthesis, characterization and performance evaluation o fgroundwater defluoridation capacity of smectite rich clay soils and Mn-modified bentonite clay composites School of Environmental Sciences, *MSc Thesis*, University of Venda.

Oladoja, N. A., Liu, Y., Drewes, J. E & Helmreich, B., 2015. Preparation and Characterization of a Reactive Filter for Groundwater Defluoridation. *Chemical Engineering Journal. In press.*

Sepehr, M.N., Kazemian, H., Ghahramani, E., Amrane, A., Sirasankar, V. & Zarrabi, M., 2014. Defluoridation of water via light weight expanded clay aggregate (LECA): adsorbent characterization, competing ions, chemical regeneration, equilibrium and kinetic modeling. *Journal of the Taiwan Institute of Chemical Engineers*, 45, pp. 1821-1834.

CHAPTER 6: Conclusions and recommendations

6.1 Conclusions

This study attempted to answer the following research questions about mechanochemically activated aluminosilicate clay soil, Al-oxide modified mechanochemically activated aluminosilicate clay soil and porous ceramic granules. The questions are as follows:

- What are the physicochemical and mineralogical characteristics of the mechanochemically activated aluminosilicate clay soil, Al-oxide modified mechanochemically activated aluminosilicate clay soils and porous ceramic granules?
- How will mechanochemically activated aluminosilicate clay soil be modified with Al oxide?
- How will the porous ceramic granules be fabricated?
- What is the adsorption capacity of the Al-oxide modified mechanochemically activated aluminosilicate clay soil?
- What is the adsorption capacity of the porous ceramic granules?
- How will the adsorption data be modelled?
- How to regenerate the Al-oxide modified mechanochemically activated aluminosilicate clay soil using alkaline solutions?

6.1.1 Mechanochemical activation, modification and fabrication of porous ceramic granules

The optimum mechanochemical activation time for aluminosilicate clay soil obtained was 30 minutes. The optimum conditions for modification of aluminosilicate clay soil obtained was 30 minutes contact time and 1.5 M Al oxide concentration. The optimum mass ratio of Al-oxide modified mechanochemically activated aluminosilicate clay soil/mechanochemically activated aluminosilicate clay soil/ corn starch for fabrication of porous ceramic granules was 20:5:1. The optimum temperature was obtained 600 ^{0}C.

6.1.2 Physicochemical and mineralogical characterization of mechanochemically activated clay soil, Al-oxide modified mechanochemically activated aluminosilicate clay soil and porous ceramic granules

The physicochemical characterization of the clay adsorbents were evaluated. The surface morphology of the adsorbents were evaluated using SEM, surface area using BET, functional

groups using FT-IR, XRD for mineralogical composition, elemental composition using XRF, CEC using ammonium acetate method and pHpzc using titration method.

Mechanochemically activated aluminosilicate clay soil

The SEM images revealed the effect of milling on the shape of the mechanochemically activated aluminosilicate clay soil. The images also demonstrated that milling tend to breakdown elongated, high aspect ratio particles. The morphological analysis reveals smaller particle sizes at 30 minutes milling time which promoted adsorption of fluoride. The surface area and pore volume of the mechanochemically activated aluminosilicate clay samples increased with a corresponding increase in the milling time. Conversely, the pore size decreased with increase in the milling time. FT-IR of the mechanochemically activated aluminosilicate clay soil showed the stretching vibrations of Si-O-H bands at absorbance 998 cm^{-1} for activation at 5 minutes; 910 cm^{-1}, for activation at 10 minutes while the same absorbance value of 996 $cm^{-1}$was noticed at activation time 15 and 30 minutes. However, changes in the Si-O-H stretching at different activation time may be due to changes in the release of functional groups necessary for interaction with fluoride. The XRD major mineral components include quartz and plagioclase feldspar. Other minerals occurring in minor quantities include vermiculite, talc, muscovite and actinolite. Quartz is the most abundant mineral phase with 31.37 weight %, followed by plagioclase (29.12 weight %); feldspar and actinolite had the lowest weight % of 5.23. The XRF analysis of major oxides showed that silica (SiO_2) has the highest composition followed by alumina (Al_2O_3). The ratio of silicate to alumina was calculated to be 3.87, confirming that the clay is aluminosilicate by composition. The minor components are MnO, Cr_2O_3 and P_2O_5. The pHpzc plots showed the points where the curve crosses the horizontal axis, owing to this the pHpzc is the abscissa for ΔpH equals zero. The trend of CEC concentrations were observed in the following order Mg^{2+}> Ca^{2+}> K^{+} >Na^{+}.

Al-oxide mechanochemically activated aluminosilicate modified clay soil

The SEM image of Al-oxide modified mechanochemically activated aluminosilicate clay soil showed many small pores and honey-comb structure on the surface of different images. Therefore, there was a good possibility for fluoride to be adsorbed onto the Al-oxide modified mechanochemically activated aluminosilicate clay soil. The BET surface area and the BDH adsorption cumulative area of the Al-oxide modified mechanochemically activated aluminosilicate clay soil are more than double those for the raw clay soil. This showed that the

aluminosilicate clay soil was indeed modified by Al^{3+}. There was also an increase in pore volume of the Al-oxide modified mechanochemically activated aluminosilicate clay soil. The FT-IR showed that there was an increase in the absorbance of the Si-O-H, H-O-H, Al-O-H and Si-O-Al groups stretching vibration at 414 cm^{-1} for the Al-oxide modified mechanochemically activated aluminosilicate clay soil. In pHpzc, the pH of the solution was higher than the pHpzc with a negative net surface charge of Al-oxide modified mechanochemically activated aluminosilicate clay that can adsorb cationic species. On the other hand, when pH of the solution is lower than the pHpzc, the surface of Al-oxide modified mechanochemically activated aluminosilicate clay soil is positive, suitable for the adsorption of anions such as fluoride.

Porous ceramic granules

Porous ceramic granules showed efficiency in fluoride removal. In this study, SEM analysis showed the existence of a porous structure of the organic foam template for the porous ceramic granules. The porous ceramic granule showed an increase in pore surface area and volume as compared to mechanochemically activated aluminosilicate clay soil. This gave an indication that the percolation of water through the particles of adsorbent during defluoridation would be more readily achieved for porous ceramic granules. The FT-IR results showed the presence of a strong broad bending and stretching vibrations at about 993 cm^{-1} confirmed the presence of Si–O–Si bonds. Bending and stretching modes of absorbed water molecules in the porous ceramic granules sample were observed at 993 and 522 cm^{-1}, respectively. Mineralogical characterisation showed the presence of quartz, albite, horneblende and microcline as the main minerals of the calcined porous ceramic granules. These major oxides from the porous ceramic granules was reveled by XRF analysis (SiO_2, Al_2O_3, MnO and Na_2O).

6.1.3 Adsorption efficiency, regeneration, isotherms, kinetics and the adsorption mechanisms

Mechanochemically activated aluminosilicate clay soil.

The mechanochemical activation had tremendous impact on the efficiency of adsorption. The study reveals that the fluoride absorption capacity depends on the contact time, absorbent dosage, concentration of fluoride, the pH and temperature. Maximum fluoride uptake was achieved within 30 minutes of agitation for S/L of 0.6 g/100 mL at 200 rpm. At constant agitation time within 30 minutes, the pH was observed to decrease with adsorbent dosage. Maximum adsorption capacity was achieved at 0.6 g absorbent dosage thereafter there was no

significant removal. The percentage of fluoride removal decreased with an increase in initial F^- concentration. Adsorption capacity of the synthesized material increased with the corresponding decrease in pH. The maximum % fluoride removal (i.e. 41.0 %) was obtained at a pH_e of 2.41. The adsorption data fitted well into the Freundlich model when compared to Langmuir model. Pseudo-first-order and pseudo-second-order models were then tested to ascertain that the Pseudo-second-order model was the appropriate kinetic model for the fluoride sorption. The mechanism involved in the fluoride adsorption process using aluminosilicate clay soil was also evaluated. Considering the fact that optimum adsorption was achieved at a pH value of 2.41 as reported, there exists a research gap that could be pursed with regards to the modifications of the mechanochemically activated aluminosilicate clay soil for effectiveness.

Al-oxide modified mechanochemically activated aluminosilicate clay soil

Al-oxide modified mechanochemically activated aluminosilicate clay soil has a high fluoride removal potential. The study reveals that the fluoride absorption capacity depends on the contact time, absorbent dosage, concentration of fluoride, the pH and temperature. Maximum fluoride uptake was achieved within 30 minutes of agitation for S/L of 0.3 g/100 mL at 200 rpm. At constant agitation time within 30 minutes, the pH was observed to decrease with adsorbent dosage. Maximum adsorption capacity was achieved at 0.6 g absorbent dosage thereafter there was no significant removal. The percentage of fluoride removal decreased with an increase in initial F^- concentration. Adsorption capacity of the synthesized material increased with the corresponding decrease in pH. At 5 mg/L co-existing anion concentration, PO_4^{3-} competed most with F^- for adsorption than any other anion. The maximum % fluoride removal (i.e. 96.5%) was obtained at the pH_e of 6.86. The adsorption data fitted well into the Langmuir model when compared to Freundlich model. Sorption process was better modelled using the pseudo-second-order model. K_2SO_4 solution proved to be the most suitable spent sorbent regenerant compared to Na_3PO_4. The limitations of Al-oxide modified mechanochemically activated aluminosilicate soil clay proves to be cost effective and it might not be applied on community based defluoridation. Al-oxide modified mechanochemically activated aluminosilicate clay soil is recommended for defluoridation of drinking water even after regeneration. The adsorbent was observed to be efficient for fluoride removal.

Porous ceramic granules

The optimum Al-oxide modified mechanochemically activated aluminosilicate clay soil/ mechanochemically activated clay soil/ corn starch ratio was determined to be 20:5:1 while the optimum temperature for calcination of porous ceramic granules was found to be 600 ^{0}C. The porous ceramic granules fabricated were able to remove up to 66.9 % fluoride from an initial fluoride concentration of 10 mg/L. There was progressive improvement in the adsorption capacity of the porous ceramic granules due to the activation, modification and granulation of the clay. When comparing the percentage fluoride removal of mechanochemically activated and porous ceramic granules, the porous ceramic granules percentage fluoride removal presented the highest value at 66.9 % while for mechanochemically activated presented a percentage fluoride removal of 41.0 %.

6.2 Recommendations

- Mechanochemically activated aluminosilicate clay soil showed higher adsorption capacity at an acidic pH of 2.41, therefore it is recommended that subsequent study should work on improving adsorption capacity at wider range of pH.
- There is a need to further investigate the modifications of the mechanochemically activated aluminosilicate clay soil with other metal oxide like Fe^{3+} for effectiveness.
- This study recommends further studies to evaluate the field applicability of the Al-oxide modified mechanochemically activated aluminosilicate clay soil in community based defluoridation of groundwater.
- The porous ceramic granules can also be used further in column experiments to appraise their technical feasibility for field application.

CHAPTER 7: Appendices

Appendix A

Table 3.5: Concentrations of exchangeable cations in aluminosilicate-rich clay soil

Metal	Concentration (mg/L)
Ca^{2+}	74.65
K^{+}	33.12
Mg^{2+}	109.8
Na^{+}	2.93

Table 3.6: Effect of equilibrium pH on fluoride adsorption

pH_0	pH_e	C_0 (mg/L)	C_e (mg/L)	% F^- removal	q_e (mg/g)
2.03	2.41	9.00	5.31	41.0	0.6150
4.23	6.39	9.00	6.43	28.6	0.4280
6.37	6.89	9.00	6.33	26.7	0.4450
8.04	6.94	9.00	6.71	25.4	0.3820
10.1	7.33	9.00	7.00	22.2	0.3330
12.0	11.5	9.00	8.39	6.7	0.1020

Table 3.7: Variation of % fluoride removal and with contact time

Adsorbent dose (g)	Time (mi)	Ce (mg/)	Ce (mg/)	Ce (mg/)	% F-removal	% F-removal	% F-removal	qe (mg/g)	qe (mg/g)	Qe (mg/g)
		0.1	0.3	0.4	0.1	0.3	0.4	0.1	0.3	0.4
	0	9.00	9.00	9.00	0	0	0	0	0	0
	1	5.84	5.43	5.42	35.1	39.7	39.6	3.160	1.190	0.895
	5	5.99	5.62	5.62	33.4	37.6	37.6	3.010	1.127	0.845
	10	6.25	5.77	5.74	30.6	35.9	36.2	2.750	1.077	0.815
	20	6.28	5.77	5.77	30.2	35.9	35.9	2.720	1.077	0.808
	30	5.37	6.00	5.66	30.3	33.5	37.1	3.030	1.000	0.835
	50	6.16	5.81	5.78	31.6	35.4	35.8	2.840	1.063	0.805
	70	6.30	5.94	5.78	30.0	34.0	35.8	2.700	1.020	0.805
	90	6.26	5.94	6.00	30.4	34.0	33.5	2.740	1.020	0.750

Table 3.8: Variation of % fluoride removal and adsorption capacity with adsorbent dosage

Adsorbent dosage (g)	C_0 (mg/L)	C_e (mg/L)	% F^- removal	q_e (mg/g)	pH_0	pH_e
0.1	9	5.77	35.9	3.2300	2.08	2.07
0.2	9	5.68	36.9	1.6600	2.05	2.00
0.5	9	5.56	38.2	0.6880	2.05	2.28
0.6	9	5.53	38.5	0.5780	2.13	2.27
0.8	9	5.50	38.9	0.4375	1.95	2.35
0.9	9	5.44	39.6	0.3956	2.03	2.37
1.0	9	5.41	39.9	0.3590	2.10	2.55

Table 3.9: Variation of % fluoride removal with adsorbate concentration at 298 K

C_0 (mg/L)	C_e (mg/L)	% F^- removal	q_e (mg/g)	pH_0	pH_e
4.5	2.07	54.1	0.4050	2.15	2.39
9	5.41	39.9	0.5983	2.17	2.53
18	13.1	27.2	0.8167	2.20	2.41
36	27.8	22.8	1.3667	2.28	2.53
45	34.5	23.3.	1.7500	2.32	2.53
54	41.9	22.4	2.0167	2.35	2.66
72	56.9	20.2	2.5167	2.41	2.72
90	73.0	18.9	2.8330	2.45	3.00

Table 3.10: Variation of % fluoride removal with adsorbate concentration at 309 K

C_0 (mg/L)	C_e (mg/L)	% F^- removal	q_e (mg/g)	pH_0	pH_e
4.5	2.12	52.9	0.3967	2.02	2.27
9	5.47	39.2	0.5883	2.03	2.31
18	13.2	26.7	0.8000	2.07	2.36
36	27.2	24.4	1.4667	2.13	2.44
45	34.9	22.4	1.6000	2.21	2.49
54	42.6	21.1	1.9000	2.19	2.60
72	58.1	19.3	2.3167	2.26	2.71
90	73.5	18.3	2.7500	2.31	2.93

Table 3.11: Variation of % fluoride removal with adsorbate concentration at 318 K

C_0 (mg/L)	C_e (mg/L)	% F^- removal	q_e (mg/g)	pH_0	pH_e
4.5	2.10	53.3	0.4000	2.12	2.28
9	5.32	40.8	0.6133	2.13	2.29
18	13.2	26.7	0.8000	2.05	2.42
36	27.2	24.7	1.4833	2.22	2.48
45	34.6	23.1	1.7333	2.14	2.46
54	41.8	22.6	2.0167	2.26	2.52
72	58.2	19.2	2.3000	2.32	2.71
90	73.3	18.6	2.7833	2.33	2.96

Table 3.12: Concentrations of leached raw clay soil at different pH values

Parameter	Sol. 1	Sol. 2	Sol. 3	Sol. 4	Sol. 5	Sol. 6	DWAF guidelines (mg/L)*
pH_0	2.03	4.23	6.37	8.04	10.01	12	-
pH_e	2.41	6.39	6.89	6.94	7.33	11.48	-
Al (mg/L)	14.20	0.93	0.67	1.25	1.01	70.90	0-0.15
Ca (mg/L)	14.22	1.78	1.08	1.31	1.33	2.19	0- 32
K (mg/L)	5.75	3.47	3.33	3.32	3.35	4.94	0- 50
Mg (mg/L)	22.63	3.35	1.95	2.31	2.48	11.46	0- 30
Na (mg/L)	11.18	103.9	52.68	64.30	111.3	223.0	0- 100
Si (mg/L)	16.50	5.54	4.79	5.95	5.68	162.30	-

*(DWAF, 1996)

Table 3.13: Langmuir isotherm parameters at different temperatures

C_0 (mg/L)	C_e (mg/L) at 298 K	q_e (mg/g) at 298 K	C_e/q_e (g/L) at 298 K	C_e (mg/L) at 309 K	q_e (mg/g) at 309 K	C_e/q_e (g/L) at 309 K	C_e (mg/L) at 318 K	q_e (mg/g) at 318 K	C_e/q_e (g/L) at 318 K
4.5	2.07	0.4050	5.1111	2.12	0.3967	5.3441	2.10	0.4000	5.2500
9	5.41	0.5983	9.0422	5.47	0.5883	9.2979	5.32	0.6133	8.6744
18	13.1	0.8167	16.040	13.2	0.8000	16.500	13.2	0.8000	16.500
36	27.8	1.3667	20.341	27.2	1.4667	18.545	27.2	1.4833	18.338
45	34.5	1.7500	19.714	34.9	1.6000	21.813	34.6	1.7333	19.962
54	41.9	2.0167	20.777	42.6	1.9000	22.421	41.8	2.0167	20.727
72	56.9	2.5167	22.609	58.1	2.3167	25.079	58.2	2.3000	25.304
90	73.0	2.8330	25.768	73.5	2.7500	26.727	73.3	2.7833	26.336

Table 3.14: Freundlich model parameters at different temperatures

C_0 (mg/L)	C_e (mg/L) at 298 K	q_e (mg/g) at 298 K	log C_e at 298 K	log q_e at 298 K	C_e (mg/L) at 309 K	q_e (mg/g) at 309 K	log C_e at 309 K	log q_e At 309 K	C_e (mg/L) at 318 K	q_e (mg/g) at 318 K	log C_e at 318 K	log q_e at 318 K
4.5	2.07	0.4050	0.3159	-0.3925	2.12	0.3967	0.3263	-0.4015	2.10	0.4000	0.3222	-0.3979
9	5.41	0.5983	0.7332	-0.2231	5.47	0.5883	0.7379	-0.2304	5.32	0.6133	0.7259	-0.2123
18	13.1	0.8167	1.1173	-0.0879	13.2	0.8000	1.1205	-0.0969	13.2	0.8000	1.1206	-0.0969
36	27.8	1.3667	1.4440	0.1357	27.2	1.4667	1.4346	0.1663	27.2	1.4833	1.4346	0.1712
45	34.5	1.7500	1.5378	0.2430	34.9	1.6000	1.5428	0.2041	34.6	1.7333	1.5391	0.2389
54	41.9	2.0167	1.6222	0.3046	42.6	1.9000	1.6294	0.2788	41.8	2.0167	1.6212	0.3046
72	56.9	2.5167	1.7551	0.4008	58.1	2.3167	1.7642	0.3649	58.2	2.3000	1.7649	0.3617
90	73.0	2.8330	1.8633	0.4522	73.5	2.7500	1.8663	0.4393	73.3	2.7833	1.8651	0.4446

Appendix B

Table 4.5: Variation of % fluoride removal and adsorption capacity with contact time

Adsorbent dose (g)	Time (min)	Ce (mg/L) 0.1	Ce (mg/L) 0.3	Ce (mg/L) 0.4	% F- removal 0.1	% F- removal 0.3	% F- removal 0.4	qe (mg/g) 0.1	qe (mg/g) 0.3	qe (mg/g) 0.4
	0	10.00	10.00	10.00	0	0	0	0	0	0
	1	3.36	1.39	1.16	66.4	86.1	88.4	6.640	2.870	2.210
	5	3.94	1.29	0.63	60.6	87.1	93.7	6.660	2.903	2.342
	10	3.31	1.25	0.51	66.9	87.5	94.9	6.690	2.916	2.372
	20	3.02	1.04	0.64	69.8	89.6	93.6	6.980	2.986	2.340
	30	2.93	0.88	0.55	70.7	91.2	94.5	7.070	3.040	2.362
	50	2.96	0.82	0.58	70.4	91.8	94.2	7.040	3.060	2.355
	70	2.81	0.78	0.54	71.9	92.2	94.6	7.190	3.073	2.365
	90	2.75	0.74	0.56	72.5	92.6	94.4	7.250	3.086	2.380

Table 4.6: Variation of % fluoride removal and adsorption capacity with adsorbent dosage

Adsorbent dosage (g)	C_0 (mg/L)	C_e (mg/L)	% F^- removal	q_e (mg/g)	pH_0	pH_e
0.1	10	3.44	65.6	4.7200	6.59	6.58
0.2	10	1.77	82.3	3.5200	6.56	6.36
0.5	10	0.57	94.3	2.7433	6.21	6.04
0.6	10	0.49	95.1	2.1825	6.25	5.98
0.8	10	0.29	97.1	1.5512	6.20	5.93
0.9	10	0.26	97.4	1.1961	6.58	5.97
1.0	10	0.25	97.5	0.9668	6.56	5.97

Table 4.7: Variation of % fluoride removal with adsorbate concentration at 298 K

C_0 (mg/L)	C_e (mg/L)	% F^- removal	q_e (mg/g)	pH_0	pH_e
5	0.17	96.6	0.8047	5.95	5.80
10	0.34	96.6	1.6100	6.30	5.85
20	1.23	93.9	3.1283	6.44	6.04
40	3.71	90.7	6.0483	7.06	6.40
50	5.80	88.4	7.3667	7.00	6.61
60	8.25	86.3	8.6250	7.14	6.77
80	15.5	80.6	10.750	7.30	7.08
100	27.5	72.5	12.083	7.42	7.38

Table 4.8: Variation of % fluoride removal with adsorbate concentration at 309 K

C_0 (mg/L)	C_e (mg/L)	% F^- removal	q_e (mg/g)	pH_0	pH_e
5	0.16	96.9	0.8075	5.98	5.52
10	0.25	97.5	1.6250	6.42	5.72
20	0.99	95.1	3.1683	6.57	5.93
40	3.06	92.4	6.1561	6.85	6.50
50	4.99	90.0	7.5017	6.86	6.52
60	7.49	87.5	8.7517	7.31	6.76
80	14.8	81.5	10.867	7.27	7.15
100	24.8	75.2	12.533	7.62	7.43

Table 4.9: Variation of % fluoride removal with adsorbate concentration at 318 K

C_0 (mg/L)	C_e (mg/L)	% F^- removal	q_e (mg/g)	pH_0	pH_e
5	0.13	97.4	0.8118	5.77	5.46
10	0.26	97.4	1.6238	5.90	5.59
20	0.75	96.3	3.2088	6.35	5.80
40	3.02	92.5	6.1633	6.75	6.21
50	3.95	92.1	7.6750	7.02	6.44
60	6.23	89.6	8.9617	7.18	6.80
80	13.0	83.8	11.167	7.26	7.15
100	21.8	78.2	13.033	7.55	7.36

Table 4.10: Effect of equilibrium pH on fluoride adsorption

pH_0	pH_e	C_0 (mg/L)	C_e (mg/L)	% F^- removal	q_e (mg/g)
2.02	3.44	9.00	5.72	36.4	0.5470
4.02	5.55	9.00	0.65	92.8	1.3920
4.81	5.73	9.00	0.48	94.7	1.4200
5.92	5.74	9.00	0.42	95.4	1.4306
9.80	6.01	9.00	0.35	96.1	1.4413
10.94	7.01	9.00	0.91	89.9	1.3488
11.87	10.5	9.00	6.98	22.5	0.3375

Table 4.11: Concentrations of leached Al at different pH concentration.

Parameter	Sol. 1	Sol. 2	Sol. 3	Sol. 4	Sol. 5	Sol. 6	DWAF guidelines (mg/L)*
pH_0	2.04	4.05	6.23	8.06	10.24	11.71	-
pH_e	3.32	5.46	5.79	6.02	6.40	10.15	-
Al (mg/L)	72.78	0.09	0.18	0.64	0.89	15.14	0- 0.15
Ca (mg/L)	3.55	2.09	2.27	2.30	2.50	0.06	0- 32
K (mg/L)	9.18	17.79	20.76	11.64	1.64	9.28	0- 50
Mg (mg/L)	4.80	2.92	3.11	3.11	3.24	-	0- 30
Na (mg/L)	185.9	269.3	261.7	275.7	295.3	389.8	0- 100
Si (mg/L)	6.16	0.56	0.72	0.75	0.80	0.25	-

(DWAF 1996) *

Table 4.12: Langmuir isotherm parameters at different temperatures

C_0 (mg/L)	C_e (mg/L) at 298 K	q_e (mg/g) at 298 K	C_e/q_e (g/L) at 298 K	C_e (mg/L) at 309 K	q_e (mg/g) at 309 K	C_e/q_e (g/L) at 309 K	C_e (mg/L) at 318 K	q_e (mg/g) at 318 K	C_e/q_e (g/L) at 318 K
5	0.17	0.8047	0.2112	0.16	0.8075	0.1981	0.13	0.8118	0.1601
10	0.34	1.6100	0.2111	0.25	1.6250	0.1538	0.26	1.6238	0.1601
20	1.23	3.1283	0.3932	0.99	3.1683	0.3125	0.75	3.2088	0.2337
40	3.71	6.0483	0.6134	3.06	6.1561	0.4971	3.02	6.1633	0.4899
50	5.80	7.3667	0.7873	4.99	7.5017	0.6652	3.95	7.6750	0.5147
60	8.25	8.6250	0.9565	7.49	8.7517	0.8558	6.23	8.9617	0.6952
80	15.5	10.750	1.4419	14.8	10.867	1.3619	13.0	11.167	1.1641
100	27.5	12.083	2.2759	24.8	12.533	1.9788	21.8	13.033	1.6727

Table 4.13: Freundlich model parameters at different temperatures

C_0 (mg/L)	C_e (mg/L) at 298 K	q_e (mg/g) at 298 K	log C_e at 298 K	log q_e at 298 K	C_e (mg/L) at 309 K	q_e (mg/g) at 309 K	log C_e at 309 K	log q_e at 309 K	C_e (mg/L) at 318 K	q_e (mg/g) at 318 K	log C_e at 318 K	log q_e at 318 K
5	0.17	0.805	-0.769	-0.094	0.16	0.807	-0.796	-0.093	0.13	0.812	-0.886	-0.091
10	0.34	1.610	-0.468	0.206	0.25	1.625	-0.602	0.210	0.26	1.624	-0.585	0.211
20	1.23	3.128	0.089	0.495	0.99	3.168	-0.004	0.501	0.75	3.209	-0.125	0.506
40	3.71	6.048	0.569	0.782	3.06	6.156	0.486	0.789	3.02	6.163	0.480	0.789
50	5.8	7.367	0.763	0.867	4.99	7.502	0.698	0.875	3.95	7.675	0.597	0.885
60	8.25	8.625	0.916	0.936	7.49	8.752	0.875	0.942	6.23	8.962	0.795	0.952
80	15.5	10.75	1.190	1.031	14.8	10.87	1.170	1.036	13	11.17	1.114	1.048
100	27.5	12.08	1.439	1.082	24.8	12.53	1.395	1.098	21.8	13.03	1.339	1.115

Table 4.15: Parameters of pseudo-first-order

Adsorbent dosage (g)	Time (min)	log ($q_e - q_t$) 0.1	log ($q_e - q_t$) 0.3	log ($q_e - q_t$) 0.4	q_t (mg/g) 0.1	q_t (mg/g) 0.3	q_t (mg/L) 0.4
	1	-0.2147	-0.6655	-0.7696	6.640	2.870	2.210
	5	-0.2291	-0.7375	-1.4202	6.660	2.903	2.342
	10	-0.2518	-0.7696	-2.7093	6.690	2.916	2.372
	20	-0.5686	-1.0000	-1.3979	6.980	2.986	2.340
	30	-0.7447	-1.3372	-1.7447	7.070	3.040	2.362
	50	-0.6778	-1.5850	-1.6021	7.040	3.060	2.355
	70	-1.2218	-1.8861	-1.8239	7.190	3.073	2.365
	90	-	-	-	7.250	3.086	2.380

Table 4.19: Comparison of the sorbent regeneration potentials of selected reagents

Defluoridation cycle	% F^- removal with K_2SO_4 as regenerant	% F^- removal with Na_3PO_4 as regenerant
Blank	98.4	98.6
1st cycle	97.2	-
2nd cycle	96.8	-
3rd cycle	93.3	-
4th cycle	78.3	-
5th cycle	64.2	-

Appendix C

Table 5.4: Variation of % fluoride removal and at different clay/starch mixing ratio

Mixing ratio (Al^{3+}:Raw: Starch)	Mass (g)	pH_0	pH_e	C_0 (mg/L)	C_e (mg/L)	% F-removal	q_e (mg/g)
20:10:1	1.0020	5.52	5.65	10	7.03	29.7	0.2964
20:5:1	1.0063	6.11	5.40	10	3.31	66.9	0.6648
20:3:1	1.0004	6.06	6.32	10	3.38	66.2	0.6617
40:20:1	1.0062	6.11	6.07	10	7.14	28.6	0.2842
13:6:1	1.0012	6.11	6.36	10	6.70	33.0	0.3296
10:5:1	1.0028	6.13	6.44	10	7.12	28.8	0.2182

Table 5.5: Variation of % fluoride removal and at different calcination temperatures

Temperature (^0C)	Mass (g)	pH_0	pH_e	C_0 (mg/L)	C_e (mg/L)	% F-removal	q_e (mg/g)
600	1.0001	6.32	6.40	10	4.02	59.8	0.5979
700	1.0011	6.50	6.82	10	6.65	33.5	0.3350
800	1.0040	6.36	6.61	10	7.61	23.9	0.2390
1000	1.0023	6.44	6.24	10	9.38	6.2	0.0619